UNIVERSITY OF MILAN

PhD SCHOOL IN
CHEMICAL SCIENCES AND TECHNOLOGIES

COURSE IN INDUSTRIAL CHEMISTRY –XXIII Cycle
CHIM 04

NOVEL BIOACTIVE AND BIODEGRADABLE BIOMATERIALS OF POLY(AMIDOAMINE)S STRUCTURE

Coordinator: *PROF. DOMINIQUE ROBERTO*

Tutor: PROF. ELISABETTA RANUCCI

Co-Tutor: PROF. PAOLO FERRUTI

PhD student: ***FENILI FABIO***

R07830

TABLE OF CONTENT

SUMMARY

Biomaterials are any materials designed to interface with biological system to evaluate, support or replace any tissue, organ or body function. Metals, ceramics, polymers and composites are biomaterials commonly used every day for biomedical applications in the form of sutures, vascular grafts, heart valves, intraocular lenses, dental and orthopaedic implants, pacemakers, biosensors, drug delivery systems, gene carriers, etc.

Compared to the other types of biomaterials, polymeric biomaterials offer the advantages that can be prepared in different compositions with a variety of structures and properties. In particular, in the case of biodegradable polymers, their physical, chemical, and biological features as well as degradation rate can be tuned to meet specific applications.

Among polymeric biomaterials, poly(amidoamine)s (PAA), a family of biodegradable and biocompatible polymers, can be considered as promising materials for different pharmaceuticals and biotechnological applications.

PAAs are synthetic polymers obtained by Michael-type polyaddition of amines to bisacrylamides. Their polymer chain contains tert-amine and amide groups in regular succession. In addition, many reactive functional groups can be introduced as side substituents. Several PAAs exhibit many relevant properties useful for biomedical applications. In fact, they are biodegradable and biocompatible, and owing to their versatility can be tailored to specific applications. In particular, amphoteric PAAs that in extra cellular fluids (pH ≈7.4) are zwitterionic, but predominantly anionic, are highly biocompatible and exhibit a “stealth-like” behaviour, that is, after intravenous injection in test animals are not captured by the reticulo-endothelial system and have a prolonged permanence in the blood circle. In tumour-bearing animals they are passively concentrated in the tumour tissues by the so called EPR (Enhanced Permeation and Retention) effect.

The present PhD project aimed at the design of novel poly(amidoamine)s biomaterials of different architecture for diversified biomedical applications, each representing a distinct research sub-objective.

Poly(amidoamine)-gelonin conjugates as potential anti-cancer drugs.

Therapeutically relevant proteins such as antibodies, cytokines, growth factors, and enzymes are playing an increasing role in the treatment of viral, malignant, and autoimmune diseases. The development and successful application of therapeutic proteins, however, is often hindered by several difficulties, as for instance insufficient stability and shelf-life, costly production, immunogenic and allergic potential, as well as poor bioavailability and sensitivity towards proteases. To overcome these problems, a possible approach is to modify proteins by covalently conjugating them with water-soluble polymers, thus increasing their plasma residence, reducing protein immunogenicity and increasing their therapeutic index. Numerous polymer–protein conjugates with improved stability and pharmacokinetic properties have been developed by different authors, for example, by anchoring enzymes or biologically relevant proteins to polyethylene glycol components (PEGylation). Increasing attention has devoted to the nature of the chemical linkage between the polymer backbone and protein. In this work reductively cleavable disulphide bonds have been used.

Two PAAs bearing pendant 2-ethenyldithiopyridine (ISA1-SSPy and ISA23-SSPy) (Figure 1) were used to investigate their ability to mediate intracellular delivery of the type I ribosome-inactivating gelonin.

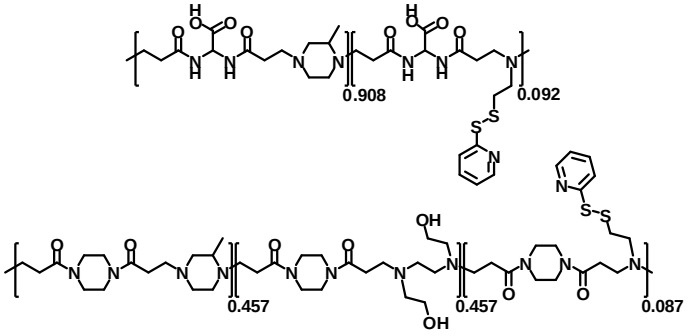

Figure 1: Structures of PAA-SSPy used in this work.

The strategy adopted consists of a three step synthesis. In the first step, a cystamine crosslinked PAA was synthesised generating a hydrophilic tri-dimensional network. In the second step, the hydrogel obtained was de-reticulated by direct disulfide exchange reaction with dipyridyl disulfide. Finally, the linear and soluble PAA-SSPy thus obtained was conjugated via thiol-disulfide exchange reaction to a thiol-containing gelonin, a ribosom inactivating protein (Scheme 1).

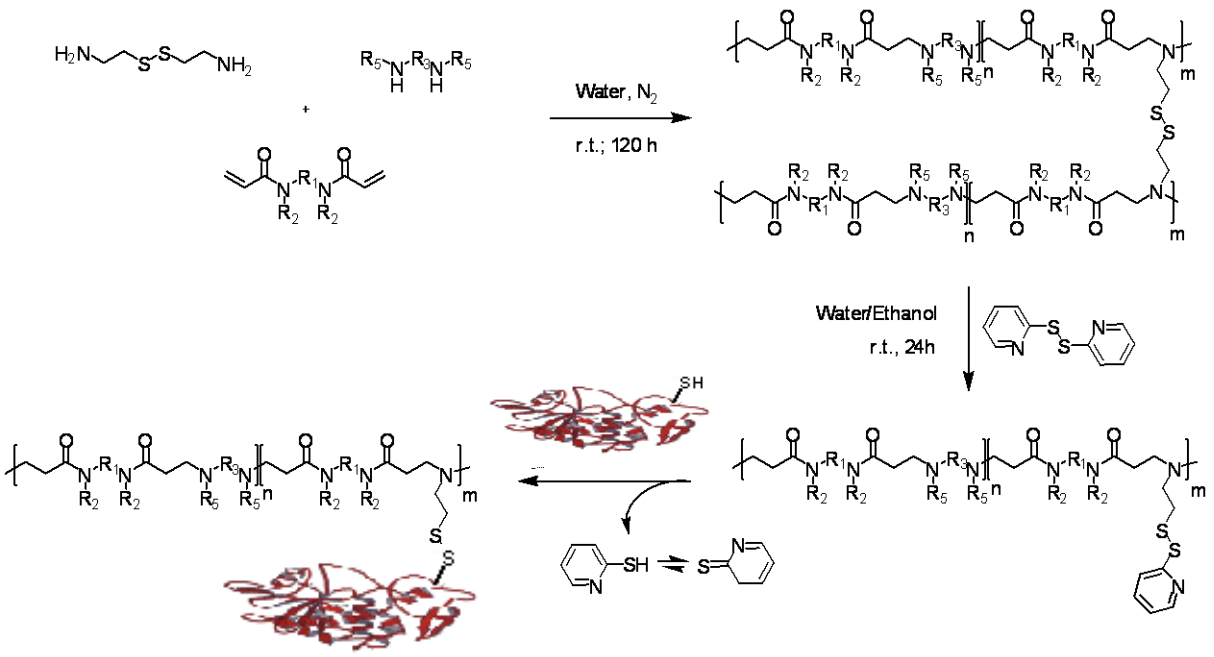

Scheme 1: Synthetic pathway leading to PAA-gelonin conjugates

Two different recombinant proteins, encoding gelonin with an N-terminal 6xHistidine (H or His) and V5 epitope tag (6H-V5 Gelonin) and gelonin encorporating a C-terminal HA and 6xHis tag flanking a cystine residue (Gelonin HA-Cys-6H) were prepared introducing the required tag on a gelonin plasmid by polymerase chain reaction (PCR), isolated and purified from E. Coli.

In vitro experiments were performed on B16F10 cells using non-toxic concentration of gelonin and polymeric samples up to 2 mg/ml. ISA1-SSPy promoted the intracytoplasmic delivery of gelonin more efficiently than the parent non-functionalized ISA1 with IC_{50} values of 100 µg/ml.

The results obtained for ISA1-SSPy-HA-Cys-6H, designed to have a covalent bound between the polymeric vector and the toxin, and ISA1-SSPy-6H-V5 Gelonin were the same, suggesting a non specific conjugation to the thiol-groups in the Gelonin HA-Cys-6H.

This findings could be attributed both to the ability of ISA1-SSPy to react with protein's disulfide groups and to the interactions between the ethenyl-dithiopyridine pendants and the hydrophobic domains of the protein, giving stable complexes. ISA23-SSPy was unable to mediate toxin delivery.

Tricarbonyl-rhenium complexes of a thiol-functionalized amphoteric poly(amidoamine).

Nowadays, there is a high current interest toward radiopharmaceuticals incorporating ^{99m}Tc or $^{186/188}$Re. The γ emitter ^{99m}Tc is commonly used for diagnostic imaging procedures, due to its almost ideal physical properties ($t^{½}$=6.01 h, γ=142.7 keV) and easy production from $Na_2{}^{99}MoO_4$ column generators. The heavier congener rhenium has two radioisotopes of interest for nuclear medicine, both of which have potential for cancer therapy (owing to their β-emission) and diagnosis (owing to their γ emission with energies similar to that of ^{99m}Tc): ^{186}Re ($t^{½}$ =3.7 d, γ= 137 keV, β^-=1.07 MeV), ^{188}Re ($t^{½}$ = 16.94 h, γ=155 keV, β^-=2.12 MeV). Moreover, due to the similar chemistry of Tc and Re, the nonradioactive Re complexes can be used as models of Tc derivatives in preliminary studies aimed at developing novel imaging agents. Therefore, the conjugation of Re to suitable carriers, able to assure transport and cancer targeting, has been the focus of great deal of research. Among the different species that have been tested for bioconjugation, the $[Re(CO)_3(H_2O)_3]^+$ complex has attracted significant attention, due to its fast preparation and versatile chemistry, arising from the presence of three labile water molecules bound to a stable fac-$Re(CO)_3{}^+$ core.

Based on this premise, we decided to investigate the possibility to design new polymeric radiopharmaceuticals using poly(amidoamine)s polymers (PAA)s and $[Re(CO)_3(H_2O)_3]^+$.

An amphoteric thiol-functionalized ISA23 copolymer ($ISA23SH_{10\%}$) has been obtained following a two step pathway: the first was the synthesis of polymers containing cystamine-m-Boc pendants, the second one was the reduction of the disulphide bond in the presence of dithiotreitol (DTT) as reducing agent (Scheme 2).

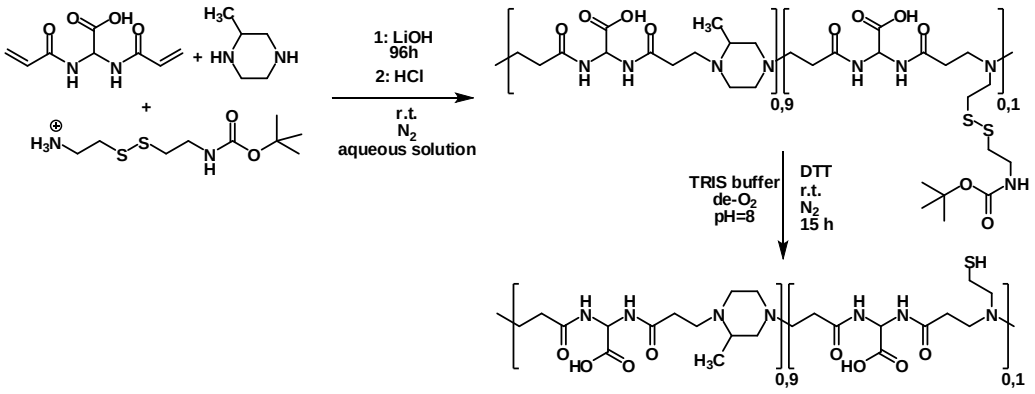

Scheme 2: Synthetic pathway leading to $ISA23_{10\%}$.

The copolymer was able to tightly bind up to 0.8 equivalents of $Re(CO)_3^+$ fragments, with respect to the thiol groups. The polymeric complexes, containing 0.5 or 0.8 equivalents of rhenium, respectively, were easily obtained by reacting $ISA23SH_{10\%}$ with $[Re(CO)_3(H_2O)_3](CF_3SO_3)$, in aqueous solution, at pH 5.5. The complexes maintained the water solubility of the parent polymer and were stable in physiological conditions and also in the presence of cysteine. The coordination of the $Re(CO)_3$ fragment involves the cysteamine-deriving moiety. A detailed ^1H, ^{13}C and ^{15}N NMR characterization of $ISA23SH_{10\%}$ and of complex with 0.8 equivalents of $Re(CO)_3^+$ provided a clear evidence that the binding of rhenium occurs by chelation through the S and N atoms of the β-amino-thiolate fragment. A morphological evaluation by TEM analysis showed that both complexes form nanoparticles with a regular spherical morphology and a narrow size distribution. In vivo toxicological tests showed that $ISA23SH_{10\%}$ is highly biocompatible, with a maximum tolerated dose of 500 mg/kg. Preliminary biological studies in vitro and in vivo have been also performed on both complexes.

No hemolytic activity was observed, up to a concentration of 5 mg/mL, neither citotoxicity effect was observed on Hela cell after 48 h of incubation. No toxic side effects were observed after the intravenous injection in mice of the two complexes in doses up to 20 mg/kg.

Poly(amidoamine)-based hydrogels as scaffold for tissue engineering applications.

Tissue engineering is a rapidly evolving discipline that seeks to repair, replace, or regenerate specific tissues or organs by translating fundamental knowledge in physics, chemistry and biology into practical and effective materials, devices, systems, and clinical strategies. Different polymeric biomaterials have been proposed as scaffold for tissue engineering applications. In recent years, special attention has been given to hydrogels.

Hydrogels are unsoluble and swellable materials that are widely used the biomaterial field due to their biocompatibility, which derives from their high water absorption and surface properties.

Several Agma1-based hydrogels obtained using ethylenediamine as cross-linker have been previously studied as scaffold for tissue engineering applications. They exhibited good results in term of biocompatibility and adhesion properties toward different cell lines. Unfortunately, their mechanical properties were not satisfactory in that their strength was still very low and they were very soft and breakable on handling. To overcome these problem, in this work a new synthetic method has been developed leading to hydrogels with similar composition and exhibiting the same biological properties but with improved mechanical strength. In particular a different two-step pathway has been followed as reported in scheme 3.

In the first step an acryloyl end-capped linear Agma1 oligomer was synthesised using a controlled excess of the selected bisacrylamide; in the second step the oligomer was photopolymerized by UV irradiation producing hydrogels with the required mechanical properties.

Using this new synthetic procedure, Agma1-UV made hydrogels with different form and shape were prepared. In particular, tubular scaffolds with 1 mm inner diameter were tested in vivo as conduit for nerve regeneration in a rat sciatic nerve cut model.

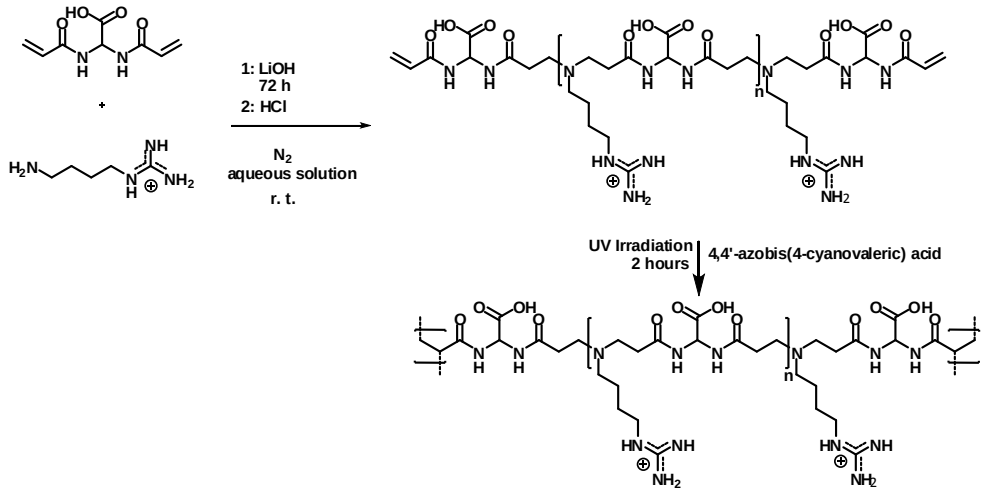

Scheme 3: Synthetic pathway leading to Agma1 hydrogels.

The implant were analyzed at 30, 90 and 180 days post-surgery and resulted particularly promising in many important respects, such as biodegradability, biocompatibility, lack of inflammatory reaction upon degradation and capability of promoting optimum morphological and functional nerve regeneration. The regenerated nerves showed several interesting signs of morphological improvements even at 30 days post-surgery. At 180 day the scaffold was almost completely reabsorbed and the regenerated nerve morphologically comparable to the control animals.

Cationic PAA as non-viral vector for gene therapy.

Gene therapy can be defined as the treatment of human disease by the transfer of genetic material into specific cells of the patient. Different delivery systems, including viral and non-viral carriers, have been developed to promote the insertion of DNA into the cells but the results obtained so far, in vitro and in vivo, are not yet satisfactory.

Viral vectors are biological systems derived from naturally evolved viruses capable of transfering their genetic materials into the host cells. Despite the high efficiency of viral vector in vitro, clinical trials are often limited by several concerns such as toxicity, immunogenicity, and inflammatory responses.

Non-viral vectors, which are mainly of a cationic nature, include cationic peptides, proteins, polymers, and liposomes. In general, polymeric vectors are materials that bind electrostatically to DNA or RNA, condensing the genetic material into nanometer-scale polyplexes that protect the genes and allow them to enter cells. Although cationic polymers have been regarded as promising vectors for non-viral gene delivery for many years, their clinical application is limited by the relatively low transfection efficacy. Moreover, some of them, such as polylysine (PLL), polyethylenimine (PEI), and polyamidoamine dendrimers (PAMAM), are too toxic to be considered for in vivo applications.

Recently, a new linear and amphoteric but prevailing cationic PAA, nicknamed Agma1 (Scheme 4) has been successfully tested as trasfection promoters in vitro without any signs of toxicity is despite its polycationic behavior.

Based on this premise, in this work, three samples of Agma1 having different molecular weights, named AGMA5 ($\overline{M}_w$ =5100), AGMA10 ($\overline{M}_w$ =10100) and AGMA20 ($\overline{M}_w$ =20500) were tested as nucleic acid carriers in order to establish the relationship between the molecular weight of the samples and their gene transfer ability.

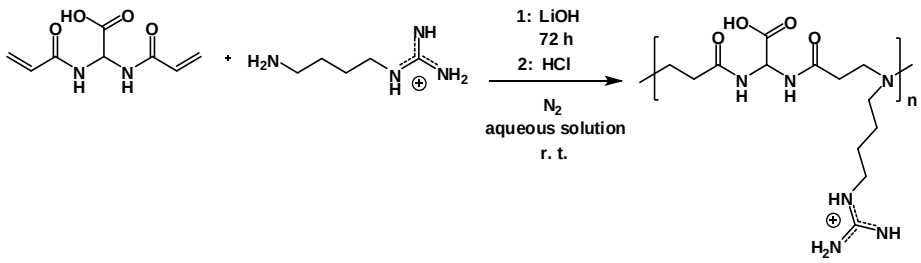

Scheme 4: Synthetic pathway leading to AGMA polymers.

All samples proved able to complex DNA forming stable nanoparticles with positively charged surface and dimensions depending on the weight/weight ratio between polymer and DNA and pH. The molecular weight of the polymeric samples had a significant influence on their efficiency as DNA carrier.

AGMA10 and AGMA20 showed good transfection ability compared to AGMA5 which was almost ineffective even at a 1:100 w/w DNA/polymer ratio. The polyplex nanoparticles proved highly biocompatible and were easily internalized in cells escaping from the endosomal vesicles and mostly localizing in perinuclear region. AGMA10 was chosen for animal experiments and proved effective also in vivo. A 1:30 DNA/AGMA10 polyplex after intravenous administration to mice induced remarkable gene expression in the liver but not in other organs, including lungs without detectable toxic side effects.

LIST OF ABBREVIATIONS

BAC : 2,2-bis(acrylamido)acetic acid acid

BP: N,N'-Bis(acryloyl)piperazine

MP: 2-Methylpiperazine

DHEEDA: bis(2-hydroxyethyl)ethylenediamine

AGR: annual growth rate

p.s.: post-surgery

NOTE: at the beginning of each chapter, in the main title, a list of references to relevant reviews is reported, providing an exhaustive introduction to the specific topic coverd.

CHAPTER 1

BIOMATERIALS [4,7,10,15]

1.1 BIOMATERIALS: DEFINITION AND INTRODUCTION

The use of biomaterials is not new. It has been reported that substitution of part of the body has been done since the pre Christian era. For example, artificial eyes, ears, teeth and noses were found on Egyptian mummies using wood, bronze or copper. Chinese and Indians used waxes, glues and tissues in reconstructing missing or defective parts of the body.

The application of biomaterials has grown rapidly in the late 1800s, particularly after the advent of antiseptic surgical techniques developed by Dr. Joseph Lister in 1860. The first metallic devices to correct bone fractures were introduced in the early 20th century, the first prosthetic replacement of whole hip was implanted in 1983 and between 1950 and 1960 polymers were introduced for the replacement of cornea and blood vessels[1,2].

One of the first definitions described the biomaterials as “any material (other than a drug) or combination of material, synthetic or natural in origin, which can be used for any period of time, as a whole or as a part of a system which treats, augments, or replaces any tissue, organ, or function of the body”[3]. This definition was proposed in 1983 during the Consensus Development Conference on Clinical Application of Biomaterials but didn’t distinguish any difference between a tradition material which may be occasionally used in the biomedical area and a material which positively interacts with a living organism. In this regard the definition of biomaterials was extended during the II° Consensus Conference on Biomaterials in 1991 as a “materials designed to interface with biological system to evaluate, support or replace any tissue, organ or body function”[4].

Medical practice today utilizes a large number of devices and implants made of different kinds of biomaterials such as sutures, bone, plates, joint replacement, ligaments, vascular grafts, heart valves, intraocular lenses, dental implants, pacemakers, biosensors, drug delivery systems, gene carriers, etc.

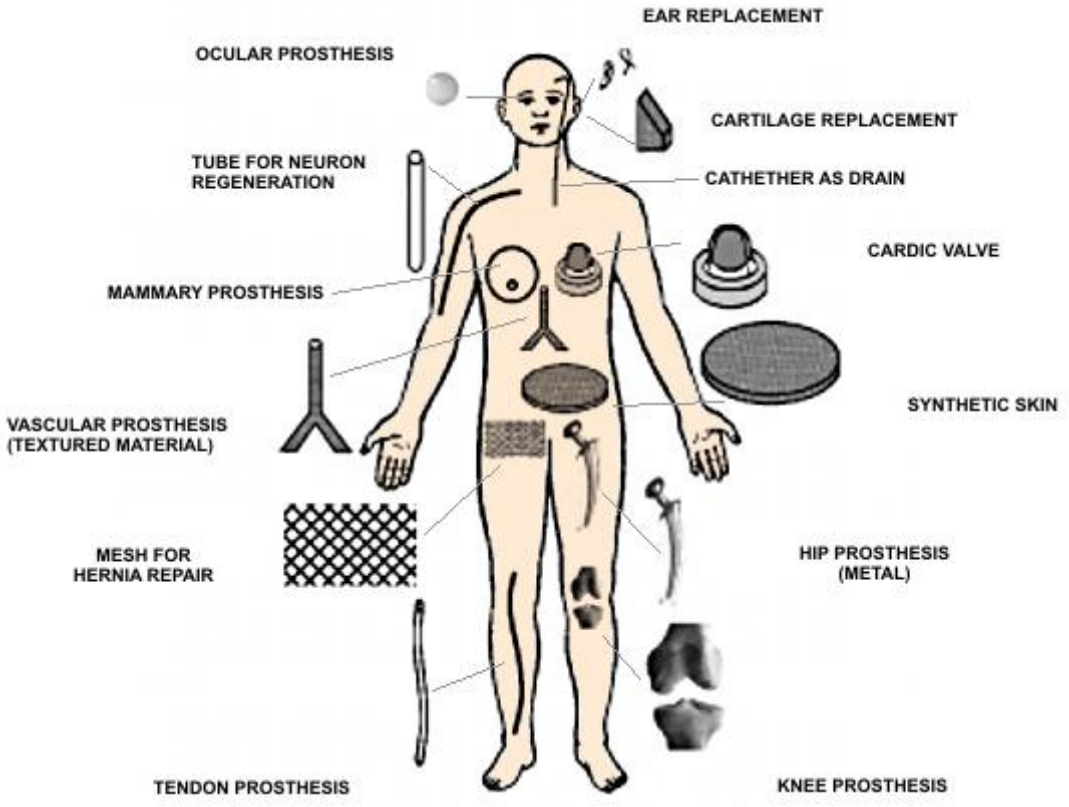

Figure 1.1. Biomedical applications of biomaterials in human body (Image from reference 5).

In order to be successful in biomedical applications, biomaterials must satisfy four requirements: biocompatibility, sterilizability, appropriate physical characteristics, and manufacturability.

Biocompatibility is a descriptive term which indicates the ability of a material to perform with an appropriate host response, in a specific application[6]. In simple terms it implies compatibility or harmony of the biomaterials with the living systems.

According to Barbucci, two processes are observed when a material is implanted in soft tissue or bone: inflammation and/or the foreign body response[7]. Inflammation refers to a well defined series of events that takes place when the body responds to an injury. The foreign body reaction involves parts of this response with particular regard to an implanted solid.

Sterilizability is an essential requirement when a biomaterial is implanted or in contact with a living organism. The physico-chemical and biological properties of the material must not be destroyed or changed by the sterilization techniques, such as autoclaving, dry heat, radiation or ethylene dioxide treatments.

Physical characteristics, such as mechanical properties, must be tuned in order to completely meet those the final applications of the biomaterials require.

The requirement of manufacturability describes the need for the biomaterial to be easily and quickly mass produced for commercial availability.

Other terms describing desirable and relevant properties of biomaterial, depending on the application, include hydrophilicity or hydrophobicity, biodegradability, bioerodibility, bioactivity, bioinertness, and limited immunogenicity.

Biomaterials can be classified depending on their medical applications, biological interactions with a living tissue or physico-chemical properties. There are a lot of books and articles in the scientific literature describing these classifications [8-10].

According to the chemical nature of biomaterials, they are classified in: metals, polymers, ceramics and composites[11].

Metals are used as biomaterials due to their excellent electrical and thermal conductivity and mechanical properties. They are typically used in orthopaedic and dental implants, in the making pacemakers and as components in devices such as heart valves. The main metals in use are: iron (Fe), chromium (Cr), cobalt (Co), nickel (Ni), titanium (Ti), tantalum (Ta), niobium (Nb), molybdenum (Mo), tungsten (W) and their alloys. The biocompatibility of these metallic biomaterials is of considerable concern due to corrosion and ion release problems.

Polymeric biomaterials show good biocompatibility in comparison with metals, and due to their versatility are used in a wide range of applications. Polymers such as poly(ethylene), poly(urethane), poly(tetrafluoroethylene), poly(methylmethacrylate), poly(ethyleneterephthalate), silicone rubber, poly(sulfone), poly(lactic acid) and poly(glycolic acid) are few examples of polymeric biomaterials. Typical applications are in orthopaedic, in cardiovascular prostheses, such as vascular prostheses and grafts to impair damaged or injured arteries, and heart valves as well as in ophthalmology, as biodegradable polymers carriers employed for drug delivery system or as plasma expanders.

Ceramic biomaterials, or bioceramics, are hard, highly bioinert materials, can be bioactive, and possesses high compressive strength. Examples of the ceramics commonly used in orthopaedic and dental implants, or as bone fillers include aluminia, zirconia, bioglass, carbon and hydroxyapatite.

Composite materials are made by the combination of polymers, metals and ceramics. This family of biomaterials fulfils physical or chemical properties that can't be achieved using a single material. Examples of composites include fibre-reinforced polymers, carbon-reinforced polymers and hydroxyapatite reinforced with collagen fibres.

Up to date the FDA regulated 100,000 different products that represent at least 1,700 different types of biomedical devices[12]. The biomaterials market is still in a growing phase, with about 100,000 heart valves, 200,000 pacemakers and 1 million orthopaedic devices implanted worldwide every year. The U.S. market is the largest geographical segment for biomaterials, and is expected to be worth $22.8 billion by 2014 with an annual growth rate (AGR) of 13.6% from 2009 to 2014. Europe is the second largest segment and is expected to reach $17.7 billion by 2014 with an AGR of 14.6% and the Asian market size (China, India, Japan) is estimated to increase at the highest AGR of 18.2% from the year 2009 to 2014. Other emerging economics expected to growth with a high rate are Brazil, Russia, and Romania.

Orthopaedic biomaterials are the dominant segment in global biomaterials market with 38% market share, closely followed by cardiovascular biomaterials with 37%. The market growth for these two segments is driven mainly by the increase in ageing population in developed and developing countries. More than 20% of the global population in 2050 is expected to be over 60 years of age. While the orthopaedic biomaterials market was the biggest segment in 2008 with $9.8 billion, the cardiovascular biomaterial market is estimated to be dominant segment in 2014 with an estimated $20.7 billion. The cardiovascular biomaterial market is expected to grow with an annual growth rate of 14.5% from 2009 to 2014.

The markets for wound care (9% of the global market), plastic surgery (8% market share), and urology (4% market share) applications are also expected to grow at a high rate. Regenerative treatments and biodegradable products hold the key for future investments.

Advances in technology and the emergence of innovative products will enhance the performance and applications of biomaterials. While metals and ceramics currently dominate the biomaterials market, polymers are expected to catalyze the next market growth for biomaterials.

Polymeric biomaterials

Polymers are the most versatile class of biomaterials, being extensively applied in medicine and biotechnology, as well as in food and cosmetics industries.

Natural polymers have been used by ancient civilization as biomaterials whereas the application of synthetic polymers is more or less a recent phenomenon. One of the first attempt was the use of poly(methylmethacrylate) as an artificial corneal substitute during the Second World War. Starting from the 1940s, the use of Nylon suture, Dacron polyester, and poly(vinylchloride) was reported in several medical journals[13,14]. Today polymeric biomaterials are used in surgical devices, implants and supporting materials such as artificial organs, prostheses and suture, drug-delivery systems with different routes of administration and design, biosensors, ocular devices, and materials for orthopaedic applications.

Compared to the other types of biomaterials, polymers offer the advantages that can be prepared in different compositions with a variety of structures and properties. Their physical, chemical, and biological characteristics can be specifically tuned to meet specific applications[15].

Polymers used as biomaterials can be naturally occurring, synthetic or a combination of both. Naturally derived polymers are biocompatible and usually biodegradable by enzymatic mechanism. Their principal disadvantages lies in a strong immunogenic response associated with most of them, their complexity of purification, the risk of viral infection and antigenicity. Additionally, significant batch-to-batch variation occurs because of their preparation in living organism. Synthetic polymers, on the other hand, offer tremendous advantages over natural polymers from the material side. Due to their synthetic flexibility it is possible to develop polymers having a wide spectrum of properties with excellent reproducibility. They can be designed with appropriate degradation rates depending on their applications, processed with various techniques, and consistently supplied in large quantity. One important remaining problem concerning synthetic polymers is an inadequate interaction between polymer and cells, leading to in vivo foreign body reactions, such as inflammation, infections, aseptic loosening, local tissue waste, and implant encapsulations as well as thrombosis and. Approaches to solve these problems include enhancement of specific protein adsorption and modification by immobilization of cell recognition motives, such as the RGD sequence (arginine-glycine-aspartic acid), to obtain controlled interaction between cells and synthetic substrates[16].
Synthetic polymeric biomaterials are also classified in biostable and biodegradable[15,17]. Biostable or non-degradable polymers has been extensively investigated as long term medical implants, such as cardiac pacemakers and vascular graft. For these applications, the main drawback of non-degradable implants is the need of a second surgical procedure to remove the implant to overcome problems such as chronic inflammatory responses.
Biodegradable polymers are those which degrade into products that are normal metabolites of the body or into products that can be completely eliminated with or without further transformations.

If used as implantable devices, they obviate the need for a second surgical procedure as well as eliminate the long-term biocompatibility concern. In addition, the biodegradation offers other advantages in many short-term medical applications such as fine-tuning of drug or bioactive (proteins, growth factors, etc.) release kinetics by varying the degradation rate of the matrix polymer.

According to Lloyd[18], some of important properties of biodegradable polymeric biomaterials can be summarized as follow:

- the material should not evoke a sustained inflammatory or toxic response upon implantation in the body;
- the material should have acceptable shelf life;
- the material should have appropriate mechanical properties for the indicated application and the variation in mechanical properties with degradation should be compatible with the healing or regeneration process;
- the degradation products should be non toxic, and able to get metabolized and cleared from the body;
- the material should have appropriate permeability and processability for the intended application.

Biodegradable polymeric materials are used as temporary prostheses, resorbable sutures, three-dimensional porous structures as scaffolds for tissue engineering and for pharmacological applications, such as drug and gene delivery systems (both localized and targeting systems)[19]. The most promising degradable synthetic polymers used in biomedical applications are: poly(hydroxyacid)s, poly(caprolactone)s, poly(ether-ester), poly(orthoester)s, poly(anhydride)s, poly(phosphazene)s and poly(aminoacid)s.

Polymeric biomaterials are having an enormous effect in medicine[15]. Controlled drug-delivery systems that largely involve polymers are used by tens of millions of people.

In addition, various controlled release systems for proteins, such as the human growth hormone, as well as molecules conjugated to poly(ethyleneglycol), for example the pegylated interferon, have recently been approved by regulatory authorities, and are showing how biomaterials can be used to positively affect the safety, pharmacokinetics and duration release of important new drugs. Another area where polymeric biomaterials have recently had an impact is in tissue engineering. By combining polymers with mammalian cells, it is now possible to make skin for patient who have burns or skin ulcers, and various other polymer/cell combinations are in clinical trials, including corneas, cartilage, bone and liver. Biomaterials have also an important impact as the central components of dental implants, sutures, and numerous medical devices.

References

1. Williams, D. F.; Cunningham J. *Materials in Clinical Dentistry;* Oxford University Press: Oxford, UK, 1979.
2. Park, J. B.; *Biomaterials Science and Engineering, 2nd ed.;* Plenum Press, New York, 1984.
3. Galletti, P. M.; Boretos, J. W. *J. Biomed. Mater. Res.* **1983**, *17,* 539-555.
4. 2nd Consensus Conference on Definitions in Biomaterials *J. Mater. Sci. Mater. Medicine* **1991,** 2 (1), 62.
5. Silver, F. H.; Doillon, C. J. *Biocompatibility. Interaction of Biological and Implantable Materials*; VCH Publisher Inc., New York, 1989.
6. Williams, D. F. *Consensus and definitions in biomaterials. In: de Putter, C.; de Lange, K.; de Groot, K.; Lee, A. J. C. editors, Advanced in Biomaterials;* Elsevier Science, Amsterdam, 1988.
7. Barbican, R.; Busi, E.; Magnani, A.; Ferruti, P.; Ranucci, E.; Taraviras, S. *La Chimica e l'Industria*, **1994**, *76*, 3-9.
8. Hench, L. L.; Polak J. M. *Science,* **2002**, *295* (5557), 1014-1017.
9. Ratner, B. D.; Hoffman, A. S.; Schoen, F. J.; Lemons J. E. *Biomaterials Science, 2nd ed.: An Introduction to Materials in Medicine;* Elsevier Academic Press, New Ypork, 2004.
10. Park, J. B.; Bronzino, J. D. *Biomaterials: Principles and Applications.* Boca Raton, London, New York, Washington, CRC Press, 2003.
11. Black, J.; Hasting, G. W. *Handbook of Biomaterials Properties.* Chapman and Hall, London, UK, 1998.
12. Global Biomaterial Market (2009-2014), published by marketsandmarkets.com, October 2010, Report Code: BT 1026
13. Blaine, J. *Lancet*, **1946**, *2*, 525.
14. Ingraham, F. D.; Alexander, E.; Matson, D. D. *New Engl. J. Med.,* **1947**, *236*, 362-368, 402-407.
15. Dumitriu S. *Polymeric Biomaterials* Marcel Dekker Inc., New York, 2002.
16. Hersel, U.; Dahmen, C.; Kessler, H.; *Biomaterials* **2003***, 24* (24)*,* 4385-4415.
17. Shalaby, S. W.; Burg, K. J. L. *Absorbable and Biodegradable Polymers* Boca Raton, Florida, CRC Press, 2004.
18. Lloyd A.W. *Med. Device Technol.* **2002**, *13*, 18-22.

19. Mallapragada, K.; Narasimhan, B. *Handbook of Biodegradable Polymeric Materials* American Scientific Publishers, Stevenson Ranch, California, 2006

CHAPTER 2

POLY(AMIDOAMINE)S, A FAMILY OF BIOACTIVE AND BIOCOMPATIBLE POLYMERS [1,6,8,13,16]

2.1 POLY(AMIDOAMINE)S PROPERTIES

Poly(amidoamine)s (PAAs) represent a family of biodegradable and biocompatible polymers with a recognized potential in the pharmaceutical field. The first extensive studies on PAA synthesis have been published in 1970 and their chemical properties and biomedical applications reviewed in several instances.

General synthesis and structures

PAAs are obtained by stepwise Michael type polyaddition reaction of primary or bis-secondary amines to bisacrylamides. The polymer obtained presents tert-amino and amido groups regularly arranged along the main chain (Scheme 2.1).

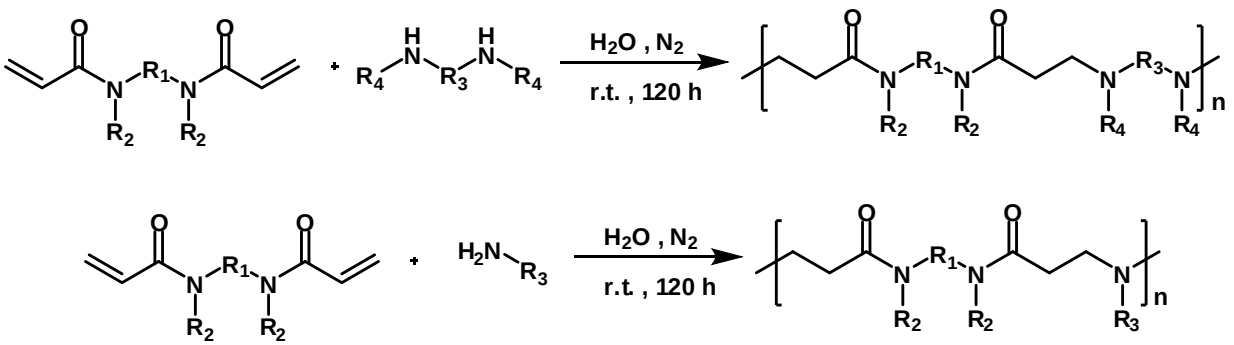

Scheme 2.1. Synthesis of linear PAAs. R_1, R_2, R_3 and R_4 can be any alkyl residues eventually containing carboxyl, amide, ester, ether groups.

Polymerization reaction takes place in solvents carrying mobile protons, such as water or alcohols, without added catalysts (Scheme 2.2)[1-3]. The number-average and weight-average molecular weights of the PAAs usually range between 5,000 – 40,000 and 10,000 – 70,000 respectively, with a polydispersity index around 1.5-2 depending on the isolation method.

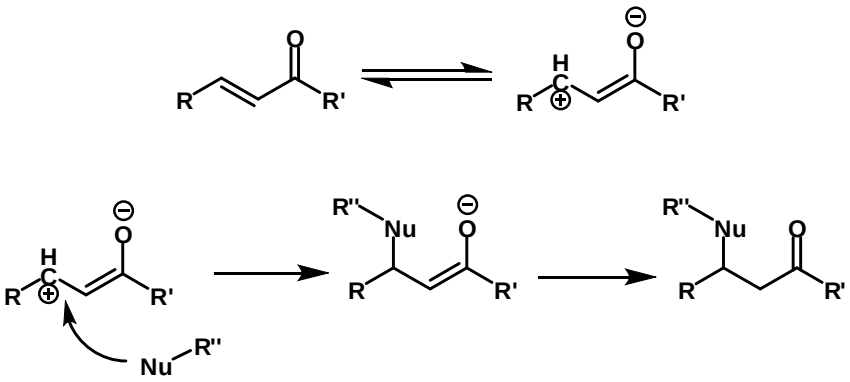

Scheme 2.2. Michael type addition mechanism.

The reaction is considerably influenced by the temperature. High temperatures accelerate the polyaddition reaction rate but the resulting polymers showed lower molecular weights because of the increase of hydrolysis reaction rate[4]. Pioneering studies previously performed showed that high molecular weight polymers can only be obtained in organic solvents bearing mobile hydrogens, such as alcohols; indeed aprotic solvents give always poor results irrespective of their polarity[1]. Recently, further study showed that mobile hydrogens play a key role in the reaction mechanism of Michael addition, and hydrogen mobility strongly influences reaction kinetics[5].

It is possible to obtain amphoteric PAAs using carboxyl containing starting monomers, carboxyl groups in fact, do not influence the polyaddition reaction. In this case, a stoichiometric amount of base (inorganic such as lithium or sodium hydroxide, or organic, such as triethylamine) must be added to the monomers mixture in order to prevent amine protonation by the acid groups. Amphoteric PAAs show remarkable biological properties as will reported later in this chapter.

Non amphoteric PAAs are soluble in water as well as in chloroform, lower alcohols, dimethyl sulfoxide and other polar solvents. However, amphoteric PAAs dissolve only in water[6].

The intrinsic viscosities of PAAs in organic solvents or aqueous media usually range from about 0.15 to 1 dl/g. As a rule, PAAs exhibit relatively large hydrodynamic volumes in solution if compared with vinyl polymers of similar molecular weight, indicating a tendency to assume an extended chain conformation in solution.

Functionalisation of poly(amidoamine)s

PAAs are inherently highly functional polymers, however, further functionalisation of PAAs may be useful for special purposes. Functional groups not capable of undergoing Michael addition under the conditions of PAA synthesis, for instance hydroxy, tert-amino, allyl, amido and ether groups, do not compete with the polimerisation reaction. Therefore, the introduction of these additional functions in PAAs as side substituents can be simply achieved by using monomers properly functionalised. Chemical groups capable of reacting with activated double bonds under the conditions of PAA synthesis such as -SH, $-NH_2$, -NHR and $-PH_2$, if unprotected, cannot as a rule be introduced directly as side substituents in PAAs. However, it is possible to obtain these types of functional groups by functionalization of purposely pre-synthesised polymers.

Degradation of poly(amidoamine)s

All PAAs containing in their main chain tertiary amine in β to amidic bonds, are degradable in aqueous solution. The degradation of several PAAs has been extensively studied in physiological conditions by means of viscometric and chromatographic techniques (37°C and phosphate buffer pH=7.4)[7,8]. It has been demonstrated that the degradation rate of PAAs in aqueous media is strongly influenced by basic pH and increasing temperatures (40-60°C), as well as by the structure of both the amine and amide moieties. The mechanism of PAAs degradation seems to be purely hydrolytic as no vinyl groups, such as those which would have derived from a β-elimination reaction, could be determined[9]. Furthermore, degradation seems not to be affected by the presence of isolated lysosomal enzymes at pH 5.5[10].

Acid-base properties of poly(amidoamine)s

All PAAs contain tert-amino groups in their main chain and therefore can be classified as polyelectrolytes[11,12]. Normally, the values of the protonation constants (log K) of polyelectrolytes depend on the degree of protonation of the whole macromolecule. They follow the modified Henderson-Hasselbach equation:

$$logK_i = logK_i^o + (n-1)\log\left[\frac{(1-a)}{a}\right] \qquad \text{(Eq. 2.1)}$$

where $logK^0_i$ is the protonation constant of a group present in a completely unionized polymer and α = degree of protonation. The protonation constants of polyelecrolites are usually referred to as "apparent" constants, as opposed to the "real" constants of non macromolecular acids and bases. However, in most PAAs the results of the potentiometric titrations are consistent with n values very close to 1. This means that in PAAs the tendency of the amine nitrogen atoms of each repeating unit to assume a proton in practice does not depend on the degree of protonation of the whole macromolecule. Therefore, real or "quasi real" basicity constants can be determined[13]. As a consequence, non ampohoteric PAAs behave as polycations and show the same number of basicity constant than the amino groups present in their repeating unit.

Differently from normal PAAs, amphoteric PAAs deriving from amino acids, and therefore carrying both carboxyl and amino groups attached to the same monomer tend to exhibit a typical polyelectolite behaviour. In solution, they change their net average charge as a function of pH.

By a proper choice of the starting monomers, the acid and basic strength of the amino and the carboxyl groups can be controlled in such a way that the polymer passes from a prevailingly anionic to a prevailingly cationic state as a consequence of relatively modest pH changes.

Table 2.1. Acid-base properties of same PAA polymers.

PAA name and structure	pK_a	Isoelectric point	Percentage of Charged Units	
			pH= 5.5	pH=7.4
ISA23 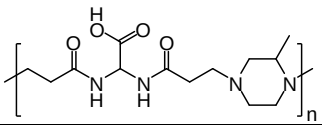	pK_{a1}=2.1 pK_{a2}=3.25 pK_{a3}=7.5	5.5	40% (-)	5% (+)
ISA1 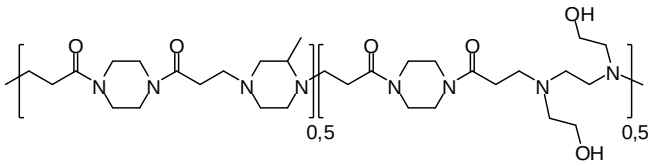	pK_{a1}=8.1 pK_{a2}=6.9 pK_{a3}=3.8 pK_{a4}=2.8	>10	95% (+)	55% (+)
Agma1 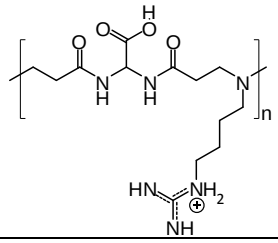	pK_{a1}=2.25 pK_{a2}=7.45 pK_{a3}=12.1	10.0	55% (+)	90% (+)

Biological properties of poly(amidoamine)s

PAAs are endowed with many interesting properties for using in biological and biomedical applications. Cationic PAAs are usually one or two order or magnitude less cytotoxic (IC_{50} between 0.5 and 3 mg/ml) than other commonly used polycations such as poly-L-lysine (IC_{50} 0.012 mg/ml) and poly(ethyleneimine) (IC_{50} 0.01 mg/ml) and exhibit good DNA complexing ability. For this reason they can be regarded as potential transfection promoters[14-16]. Moreover, amphoteric PAAs are often non-cytotoxic (IC_{50} above 5 mg/ml, similar to dextran) and stealth-like: when parenterally administered to living animals, mice or rats, they don't accumulate in liver or kidneys but can circulate for prolonged time in the bloodstream[16]. This property is very important in designing polymer therapeutics for cancer therapy.

To study biodistribution analogues of the PAAs ISA 1 and ISA23 were synthesised to contain approximately 3% tyramin[16]. These polymers were named ISA 4 and ISA22, respectively. After intravenous injection to rats ^{125}I-labelled ISA4 was immediately taken up by the liver (>80% recovered dose at 1 hour) whereas ^{125}I-labelled ISA22 was not (liver uptake was <10% recovered dose at 5 hours) (Table 2.2).

Table 2.2. Body distribution of ^{125}I-labelled PAAs after intravenous injection in rats.

Body district	Percent Localization			
	ISA22		ISA4	
	after 1 h	after 5 h	after 1 h	after 5 h
Blood	≈70	≈20	≈1.5	≈0
Kidney	≈2	≈1	≈7	≈4
Liver	10	8	83	85
Lungs	≈2	≈4	≈4	≈3
Urine	≈13	≈65	≈0	≈15

The longer circulation time of ISA22 relative to other cationic polymers provides opportunity for use in tissue targeting either by the incorporation of receptor targeting ligands or by passive accumulation such as the enhanced permeability and retention effect (EPR)[17,18]. Tumour targeting by the EPR effect occurs due to the fact that circulating macromolecules (proteins or synthetic polymers) are unable to cross the walls of normal capillary vessels but are able to extravasate into tumour tissue due to their leaky angiogenic vasculature. Biodistribution studies in mice bearing subcutaneous B16F10 melanoma showed that ^{125}I-labelled ISA22 was still accumulating in tumour tissue after 5 hours (2.5% dose/g).

Uptake and intracellular trafficking of fluorescent labelled-PAA conjugates were performed in B16F10 cells in vitro using endocytosed and immunological markers to define specific intracellular compartments. PAAs are internalized by cells via the endocytic pathway.

In intracellular compartments, where the pH is first lowered to first 6.5 (endosomes) then to 5.0 (lysosomes), they become prevailingly cationic and display endosomolytic properties[14-16]. Fluorescence microscopy revealed co-localization of ISA1 and ISA23 with lysotracker (marker for lysosome and late endocytic structures). ISA1 also co-localized with EEA-1, the early endosomal antigen 1 that accumulates in early endocytic structures[15].

The degradability of the PAAs is very important as well, in order to allow renal clearance once the polymer has completed his function in the body. The hydrolysis degradation mechanism, completely non-enzimatic, allows a fine tuning of the polymer life in the body. The cytotoxicity of different PAAs degradation products has been also tested, always leading to IC_{50} values similar or larger than the native polymers[10].

Agmatine containing poly(amidoamine)s

Recently a peptidomimetic PAA, labeled AGMA1, has been obtained by polyaddition reaction of bis(acrylamido)acetic acid and agmatine (4-aminobutylguanidine)[19-21].

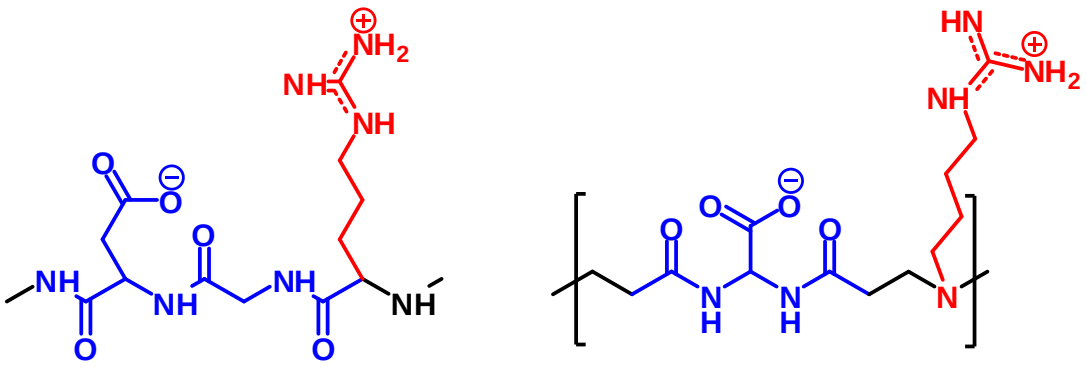

Figure 2.3. Structure of agmatine containinig amphoteric poly(amidoamine) (right part) compared to the RGD tripeptide sequence.

As reported in Figure 2.3, AGMA1 carries guanidine and carboxyl groups and shows a strong structural resemblance to the tripetide arginine-glycine-aspartic acid (RGD sequence).

RGD interacts with $\alpha_v\beta_3$ integrins, and it is involved in cell proliferation and adhesion mechanisms[22].

The repeating unit of AGMA1 contains three ionisable groups, a strong acid (pK_a=2.3), a medium-strength base (pK_a=7.4), and a strong base ($pK_a \geq 12.1$). At pH 7.4 the average excess positive charge is 0.55 per unit. In spite of that, this amphoteric polymer showed a very low toxicity (IC_{50}>5 mg/ml on HT29 cells).

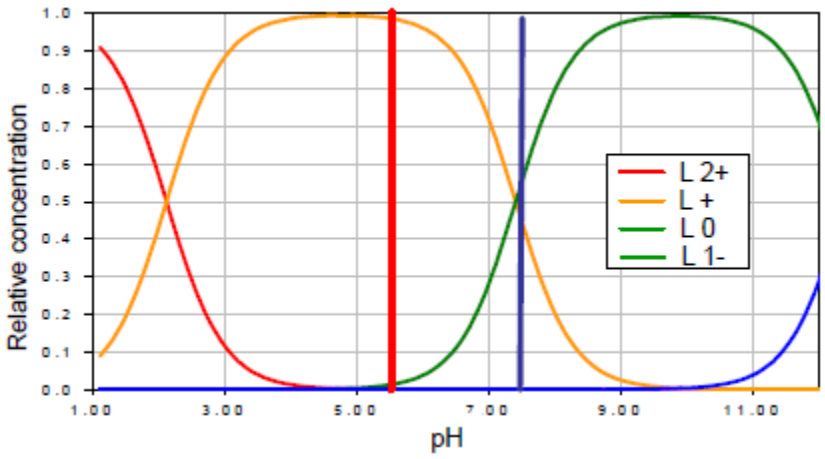

Figure 2.4. Protonation profiles of Agma1, in which each curve represent relative abundance of different profiles of the repeating units.

Agmatine containing amphoteric polymers have been tested as carriers for drug delivery and as transfection promoters. In vitro assays demonstrated the polymer ability to interact with cell membranes in a non disruptive way and to effectively protect DNA by enzymatic degradation in biological environment and to promote stable gene transfection in living cells[19].

In vivo assays demonstrated a stealth like behavior with passive accumulation in tumour by EPR effect[20].

2.2 POLY(AMIDOAMINE)S AS POLYMER THERAPEUTICS

The term "polymer therapeutics" encompasses several families of constructs all using water-soluble polymers as components for design polymeric drugs, polymer-drug conjugates, polymer-protein conjugates, polymeric micelles to which a drug is covalently bound, and those multi-component polyplexes being developed as non-viral vectors[23,24].

Early in the 1970's several PAAs were shown to display inherent antitumour activity[1]. More recently PAAs have systematically been developed as carriers for known anticancer and antiviral and as intracytoplasmic delivery systems of macromolecular proteins and genes.

Poly(amidoamine)-drug conjugates

PAA-mitomycin C (MMC) adducts were synthesised from ISA4[25]. After in vitro studies, preliminary experiments were carried out to investigate the efficacy and toxicity of these PAA-MMC conjugates in vivo. The PAA-MMC conjugates were equi-active compared to MMC given intra-peritoneally and indeed in this pilot experiment a long term survivor was observed in each group treated with conjugate. It was found that PAA-MMC conjugates were less toxic than free MMC when administered at a MMC equivalent dose of 5 mg/kg, that is, the maximum tolerated dose of free MMC that can be given to animals.

ISA23 and two co-polymers of ISA23 and ISA1 containing pendant β-cyclodextrins (β-CD) were used to synthesize PAA platinates by reaction with cisplatin[26]. These polymers were reacted with cisplatin to give products containing between 8–70 % w/w platinum. The amount of platinum released from the conjugates during incubation at pH 5.5 and pH 7.4 varied between 0–20%/72 hours. The PAA-platinates were generally less toxic towards cisplatin in lung tumour cell lines in vitro, the IC_{50} for cisplatin being 2–5 μg/mL and for the PAA-platinates 1–130 μg/mL. These results can be attributed only to their very different cellular pharmacokinetics.

In vivo experiments showed that the ISA23-Pt and ISA23-β-CD-Pt were equi-active compared with cisplatin against an L1210 leukaemia model, confirming their ability to liberate biologically active platinum species. Whereas ISA23-Pt was significantly less toxic than cisplatin, ISA23-β-CD-Pt showed toxicity on repeated dosing.

Poly(amidoamine) nanoparticles

Different PAA-cholesterol conjugates have been synthesised, in which the cholesterol pendants were linked to the polymer backbone through redox-sensitive disulphide bonds[27]. These cholesterol-PAAs were able to self assemble in aqueous media into hydrophilic/hydrophobic nanoaggregates. These nanoparticles were characterized by a strong hydration of the outer shell due to the highly hydrophilic nature of the PAA portion and endowed with a significant loading capability of lipophilic drugs in the hydrophobic domains. They also retained the same behaviour of the parent polymers in the biological environment. The linkage between cholesterol and PAA chain was obtained by means of redox sensitive disulfide bonds[28].

Hyperbranched β-CD/PAA copolymers were obtained as cross-linked nanoparticles and in this form proved capable to "solubilise" paclitaxel up to approximately 5% of their own dry weight. The resultant formulations were injectable and remarkably stable, with a shelf-stability of more than 3 years. They can be freeze-dried and regenerated. Preliminary biological evaluations, including in vitro MCF-7 cell viability tests and in vivo haemolytic activity (human RBC), have confirmed the biocompatibility of the polymer. Paclitaxel even complexed by the polymeric system, maintains its efficiency in the inhibition of cancer cell growth (in vitro MCF-7 cell cultures). The performances, in this respect, of linear or branched, but soluble β-CD/PAA conjugates of similar composition proved to be vastly inferior. This strongly suggested that in the β-CD-PAA nanoparticulated hydrogels the close spatial proximity of the cyclodextrin moieties allows them to cooperate in the formation of Paclitaxel complexes of unique stability.

Poly(amidoamine)-protein conjugates

Plant and bacterial toxins have been widely explored as anticancer agents, particularly in the form of immunotoxins. PAAs ability to mediate intracellular delivery of ribosome-inactivating toxins, in particular ricin and gelonin has been proved[11]. Ricin, derived from Ricinus communis beans, is a highly cytotoxic protein in the native dimeric form, consisting of an A-chain (RTA) and a B-chain (RTB) linked by a disulphide bridge[29]. RTB is the cell binding moiety which acts to promote binding and endocytosis of RTA. Once in the cytosol, RTA refolds and exhibits pharmacological activity by cleavage of the N-glycosidic bond of adenosine nucleoside leading to inhibition of protein synthesis[30]. RTA alone shows some inherent toxicity towards cells but this is a very inefficient process.

Gelonin toxin does not contain the cell-binding subunit of ricin and is non able to across the cell membrane. If delivered inside the cytosol, it is as toxic as ricin toxin.

Cationic membranes interacting PAAs were chosen to investigate their ability to promote intracytoplasmic delivery. They were tested in in vitro experiments using B16F10 with two non permeant toxins: either ricin A-chain (RTA) or gelonin. The relatively non toxic PAAs (IC_{50} 1.8 mg/mL) restored activity to the inherently inert toxins. The addition of small quantity of tyramine in the synthesis of PAA (ISA4) to allow radiolabeling had no effect on their pKa values. Ricin and RTA displayed IC_{50} values of 0.3 and 1.4 μg/mL, respectively, and gelonin was non-toxic over the range studied. In all further experiments, non-toxic concentrations of RTA (250 ng/mL) and gelonin (1.4 μg/mL) were used. When B16F10 cells were incubated with a combination of RTA-PAA conjugates (250 ng/mL), the observed IC_{50} fell to 0.65±0.05 mg/mL. Similar results were obtained with gelonin. Cytotoxicity assays were again performed using B16F10 cells but in this case a fixed concentration of ISA4 was combined with increasing concentrations of RTA (0-10 μg/mL). As the PAA concentration increased, less RTA was required to achieve the IC_{50} level. It can be clearly seen that a mixture of this PAA and RTA can be used to promote cytotoxicity to a greater level than the observed one for the holotoxin at a polymer concentration of 1.5 mg/mL.

Mellitin (MLT) is a peptide with α-helical conformation and it is the main constituent of the venom of the European honey bee (Apis mellifera). It is cationic and it spontaneously associates with natural and artificial membranes. The peptide has a molecular weight of 2,860 and it is a typical representative of biologically active peptide drugs with high therapeutic potential. Bee venom has been found to have a marked effect on the immune system, cardiovascular system and it also exhibits anti-tumour activity. Melittin is commonly used in the treatment of arthritic disorders, such as rheumatoid arthritis and osteoarthritis, but it has been used as an endosomolytic agent too[31].

ISA1- and ISA23-like MLT conjugates have been prepared[32]. The melittin content of the conjugates was 6–19 % w/w. Although ISA1–MLT improved gelonin delivery compared to the parent polymer ISA1 (13-fold increase) and showed pH-dependent haemolytic activity at a polymer concentration of 0.05 mg/mL, this conjugate also displayed high haemolytic activity at pH 7.4. In contrast, ISA23–MLT did not deliver gelonin like the parent compound ISA23. However, this conjugate could have potential as a novel polymeric anticancer conjugate due to its lack of haemolytic activity at pH 7.4 and retention of cytotoxicity.

Bovine serum albumin and human serum albumin have been modified by grafting poly(amidoamine) chains via a hydrogen-transfer addition reaction involving the available amino groups of the protein, in which the amine character of the latter is preserved[33]. The structure of BSA is characterized by a single, carbohydrate-free polypeptide chain consisting of 580–585 amino acid residues stabilized by seventeen S-S bridges. It was chosen as protein model for other proteins and toxins. BSA contains 60 Lysine units and therefore has 60 free - NH_2 groups. The PAA used were ISA 23 and ISA 1. Tests on different ratios of BSA compared to total amount of monomers have shown that a 20 % w/w ratio of protein and a 15% dilution give the best results as regards yield and chemical properties. The grafting reaction required very mild conditions. It took place in water at room temperature and without an added catalyst. The grafting reactions were controlled on the crude product by SEC.

The chemical processes involved are probably of general application for grafting multifunctional polymeric chains on to proteins under very mild, non-denaturing conditions.

Poly(amidoamine) as transfection promoters

Owing to their pH-dependant membrane activity, PAAs have a definite potential to act as fusagenic polymers[34,35]. Fusagenic polymers are able to form complexes with the DNA chains (polyplexes) retarding their degradation and are used to introduce esogenus nucleic acid into cells. Amphoteric PAAs, even those that at pH 7.4 have a negative net average charge, form complexes with DNA, probably because positively and negatively charged sites are located in different positions along the polymer chain. PAAs, for instance ISA 1 and ISA 23, when studied in this respect did in fact exhibit remarkable efficiency as transfection promoters, the latter being as active as polyethylenimine and LipofectIN, and more active than LipofectACE.

Recently, the prevailingly cationic Agmatine-based amphoteric poly(amidoamine) named AGMA1 has been extensively studied as transfection promoters[20]. Compared to the other PAAs, Agma1 behaves unusually in regard to hemolysis, since it is not appreciably hemolytic both at pH 7.4 and at pH 4.0, where the excess average positive charges are, respectively, 0.55 and 1.1 per unit.

Direct observation by TEM revealed that the DNA-AGMA1 complexes were obtained in the form of discrete nanospheres, whose average size and polydispersity depended on the DNA:AGMA1 ratio. In vitro studies confirmed that AGMA1 significantly protects DNA from degradation by DNase I. The ability of AGMA1 to transduce DNA into cells was evaluated with the expression of the green fluorescent protein (GFP) gene in Hela cells. The high number of fluorescent cells, observed by fluorescence microscopy and flow cytometric analysis, indicated a good in vitro transfection efficiency for AGMA1. Best results were obtained with a DNA:polymer ratio of 1:15 w/w. In this experimental condition we observed by cytofluorimetric analysis 60% GFP expressing cells.

The transfection ability of AGMA1 is comparable to that of other commercial polymeric transfection agents such as the JetPEI (63% GFP expressing cells).

By comparing AGMA1 with other PAAs studied as transfection agents, AGMA1 is apparently capable of transporting in the cytosol a DNA payload, without exerting any measurable membranolytic activity in a pH interval including the pH values of both extracellular and intracellular liquids.

Subsequently, other PAAs have been considered as transfection promoters[36-39].

PAAs with pendant primary amines were synthesized by Michael polyaddition of different diamine to N,N-methylenebisacrylamide and proved able to condense plasmid DNA in nanosized polyplexes by electrostatic interactions. The trasnfection efficiency of some of this polymers was comparable to that of commercial branched PEI 25,000[40].

Disulfide-containing cystamine was employed as a co-monomer yielding PAAs with variable amounts of bioreducible disulfide linkages in the main chain. Transfection experiments with COS-7 cells showed that polyplexes from PAAs with disulfide linkages gave significant higher transfection than those from PAAs lacking the disulfide linkage. Variation of the disulfide content revealed that polyplexes of PAA copolymers with appropriate disulfide content have largely improved biophysical properties, yielding enhanced levels of gene expression along with low toxicity[41].

Pendant thiol moieties have been incorporated into PAA homopolymer and a PEG-PAA-PEG copolymer as a self-assembling system. When mixed with DNA, small monodisperse sterically stabilized particles were formed in quantitative yields. This cross-linked formulation has been successfully tested in both freshwater and estuarine field trials as a water tracer[42].

2.3 POLY(AMIDOAMINE)-BASED HYDROGELS

General synthesis and structures

Crosslinked PAAs can be easily obtained by different methods.

So far, the most often employed method to achieve this is to introduce into the polymerization mixture primary diamines as crosslinking agents[43]. Primary diamines carry four different mobile hydrogens and hence behave as tetrafunctional monomers in PAA synthesis (Scheme 2.3). Cross-linked PAAs are typical hydrogels, absorbing large amounts of water if their cross-linking degree is not too high.

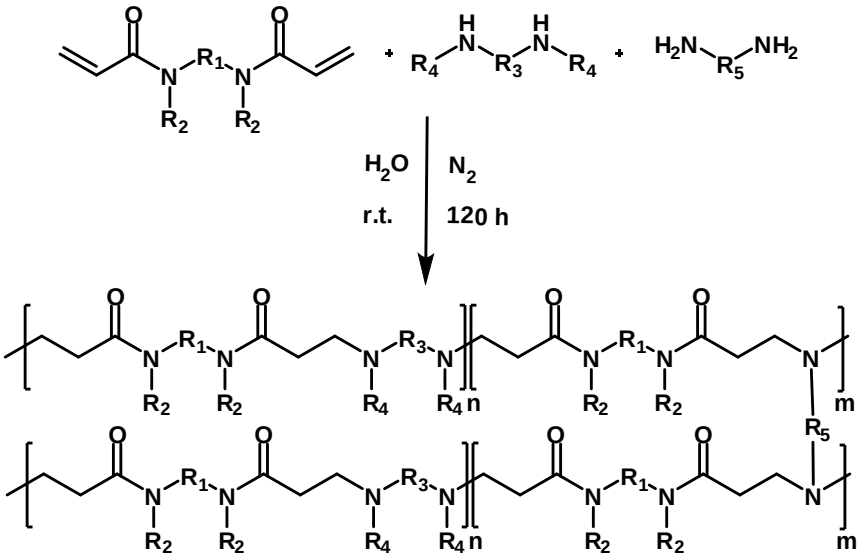

Scheme 2.3. General synthesis of PAA-based hydrogels.

Another synthetic procedure leading to PAA-hydrogels involves the preparation of a linear amphoteric PAA carrying primary amino pendants (NH_2–BAC) by the polyaddition of monoprotonated ethylenediamine (EDA) to 2,2-bis(acrylamido)acetic acid (BAC)[44]. This PAA can be used in the place of diamines as a multifunctional crosslinking agent for preparing PAA hydrogels; in fact, it gives rise to intersegmented networks with PAAs of different structures[45].

PAA hydrogels proved to be cytobiocompatible both as free bases and as salts with different strong or mediumstrong acids. Their biological performance was independent of the counterion's nature. Degradation tests carried out with selected PAA hydrogels under conditions mimicking the body fluids (pH 7.4 and 37 °C) revealed that they degrade fast, since they completely dissolved within ten day from the start of the experiments. Their degradation products proved to be completely non-toxic.

The water content in a hydrogel is a very important property that seems to be connected with biocompatibility. It is defined as:

$$\frac{weight\,(swollen) - weight\,(dry)}{weight\,(dry)}\ x\ 100 \qquad \text{(Eq. 2.2)}$$

If the water content is higher than 90% the hydrogel is defined "super absorbant." Different factors influence the water content of hydrogels such as the osmotic potential, strong interactions with water, a high free volume, a high chain flexibility, and a low density of the crosslinking points. Swelling tests demonstrated that all hydrogels had a high swelling capability. This property, not unexpected considering the hydrophilic and ionic nature of all investigated PAA-hydrogels, ensures an efficient diffusion of low molecular weight substances, thus facilitating purification processes that consisted in extensive extraction with water. However, the mechanical strength of the hydrogels in the swollen form was scarce and the materials appeared relatively fragile. The swelling behaviour of PAA-hydrogels protonated with different acids is still very high and not significantly different from that of the corresponding free bases, with the exception of the sulfates, that were slightly less swollen.

Agmatine containing PAAs-based hydrogels, easily obtained using 4-aminobutyl guanidine as monomer, were fully cytocompatible and showed also remarkable adhesion and proliferation properties towards several cell lines[46].

Agmatine contains a primary amino group and a guanidine group carrying five potentially mobile hydrogens that could participate in the polyaddition reaction. It is, therefore, a potential cross-linking agent in PAA synthesis like primary diamines as, for instance, EDA. Nevertheless, a large difference in basic properties exists between the amine and the guanidine groups of agmatine. The latter has a p*K*a of 12.5, much higher that of any aliphatic amine, and remains protonated under the conditions employed in PAA synthesis.

Biological properties of poly(amidoamine) hydrogels

According to literature[47] a material can be considered non-cytotoxic when the cell viability and proliferation reaches around 70% of the control.

Different test performed on PAA-based hydrogels by direct contact assay with different cell lines (MDCK, fibroblast) proved to be non cytotoxic and bioactive in terms of allowing cell adhesion and further proliferation. The morphology of cells grown onto the surface of the hydrogels was comparable with that of cells grown on the tissue culture polystyrene plates used as control.

A systematic comparative study of the response of an epithelial cell line was performed on hydrogels with agmatine and on non-functionalized amphoteric poly(amidoamine) hydrogels and tissue culture plastic substrates[48,49]. The cell adhesion on the agmatine containing substrates was comparable to that on plastic substrates and significantly enhanced with respect to the non functionalized controls.

All the above considerations point to the general conclusion that amphoteric PAA hydrogels have a definite potential as biomimetic materials and deserve to be further considered for different biotechnological applications such as substrates for cell culture.

However, their mechanical properties are not yet satisfactory in view of a use as scaffolds for tissue engineering, in that their strength is still very low and they are very soft and breakable on handling.

2.4 POLY(AMIDOAMINE)S AND COMMERCIAL AVAILABLE POLY(AMINE)S: DIFFERENCES AND SIMILARITY

To understand the uniqueness of PAAs' behaviour, one should compare them, as regards the biomaterials field, with the behaviour of different poly(amine)s proposed for similar applications, such as for instance poly(ethyleneimine) (PEI), poly(L-lysine) (PLL) and poly(amidoamine) PAMAM dendrimers.

As previously reported, PAAs are obtained by stepwise Michael-type polyaddition of primary or secondary amines to bis-acrylamides, and should not be confused with PAMAM, which are dendrimer-like polymers prepared by self-polyaddition of amino-substituted acrylamides and were described considerably later.

Dendrimers are spherical, highly branched polymers. Dendrimers[50] are specific in that they have a hierarchical, three-dimensional structure. The heart of the molecule provides a central point from which monomers will ramify in a well-ordered and symmetrical manner. The tree-like construction is made by the repetition of the same sequence of reactions until the formation, at the end of every reaction cycle, of a new generation with an increased number of identical branches. The most currently used dendrimers are polyamines, polyamides or polyesters, but the most commonly encountered is polyamidoamine (PAMAM)[51-53]. Dendrimers bear primary amine groups on their surface and, similar to PAAs, tertiary amine and amide groups inside. By regulating dendrimer synthesis, it is possible to precisely manipulate both their molecular weight and chemical composition, thereby allowing predictable tuning of their biocompatibility and pharmacokinetics. These branched polymers are studied as anti-viral drugs, tissue repair scaffolds, targeted carriers of anticancer drugs and gene-delivery systems[54]. Despite these promising premises, PAMAM dendrimers face against some important drawbacks.

Cationic PAMAM generally display concentration-dependent toxicity (PAMAM gen 1 tested up to 100 μg/mL using B16F10 did not show toxicity, PAMAM gen>1 displayed IC_{50} values similar to those seen for PLL) and haemolysis (above 1 mg/mL, excepted PAMAM gen 1 that is non-haemolytic), whereas dendrimers containing only neutral or anionic components have been shown to be much less toxic and less haemolytic[55,56]. They also face the extra obstacles of multistep synthesis and associated higher costs of dendrimer preparation.

PEI and PLL are two of the most effective gene-delivery studied to date. They are designed in a variety of macromolecular architectures and co-polymers but their extensive use is often hindered by their relatively high cytotoxicity[57].

PLL polymers are one of the first cationic polymers employed for gene transfer[58]. They are linear polypeptides with the amino acid lysine as the repeat unit; thus, they possess a biodegradable nature. Many PLL polymers with different molecular weights were tested and evaluated for gene transfer[59-61]. It has been shown that DNA condensation and transfection efficiency increased with high molecular weight PLL, which was also associated with undesirable high toxicity[62].

PEI can be synthesized in different lengths, be branched or linear, and undergo functionalized group substitution or addition. It is a versatile polymer which has a privileged place in the components of non-viral gene delivery, due to its superior transfection efficiency in a broad range of cell types compared to other systems. Non-protonated amines with different pKa values gave to PEI a buffering effect in a wide range of pH levels. This buffering property enabled the PEI to escape from the endosome due to the mechanism known as the 'proton-sponge' effect[63]. However, the high amount of positive charges and their non-biodegradability resulted in fairly high toxicity of PEI polymers in vivo[64,65].

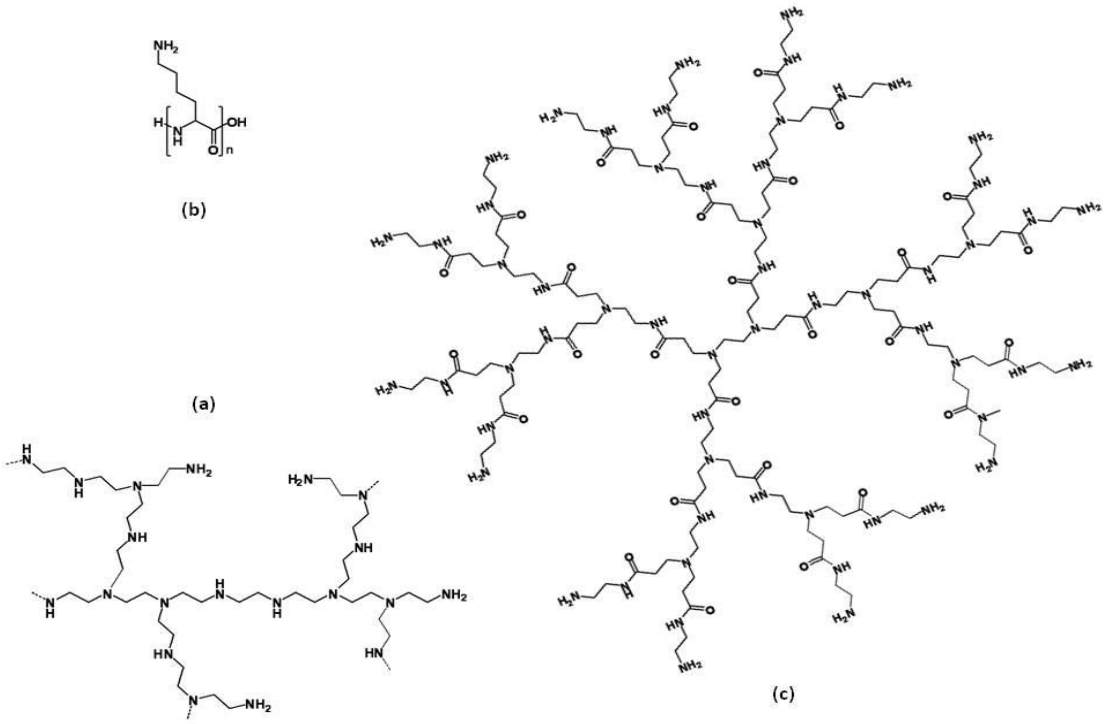

Figure 2.5. Structures of branched PEI (a), PLL (b) and PAMAM dendrimers.

PAAs show interesting biological properties as well as all the poly(amine)s reported above. Furthermore, PAAs can be easily designed as complex purpose-tailored molecular architectures by relatively simple synthetic procedures, with improved biocompatibility and low cost production.

References:

1. Danusso, F.; Ferruti, P. *Polymer* **1970**, *11*, 88.
2. Ferruti, P.; Marchisio, M.A.; Barbucci, R. *Polymer* **1985**, *26*, 1336.
3. Ferruti, P *Ion-chelating Polymers (Medical Applications)., In: Polymeric Materials Encyclopedia*, J. C. Salamone, CRC Press Inc, Boca Raton, Florida, 1996.
4. Ferruti, P.; Ranucci, E.; Bignotti, F.; Sartore, L.; Bianciardi, P.; Marchisio, M.A. *J. Biomater. Sci. Polym. Ed.* **1994**, *6*, 833-844.
5. Manfredi, A., Suardi, M.A.; Ranucci, E.; Ferruti, P. *Journal of Bioactive and Compatible Polymers* **2007**, *22* (2), 219-231.
6. Ferruti, P.; Marchisio, M.A.; Duncan, R *Macromol. Rapid Commun.* **2002**, *23*, 332.
7. Ranucci, E.; Sartore, L.; Bignotti, F.; Marchisio, M.A.; Bianciardi, P.; Veronese, F.M. *Biomaterials* **1994**, *15,* 1235-1241.
8. Franchini, J.; Ferruti, F. *Chapter 16 in Polymeric gene delivery: Principles and Applications.,* Mansoor M. Amiji, CRC Press, 2005.
9. Bignotti, F.; Sozzani, P.; Ranucci, E.; Ferruti, P. *Macromolecules* **1994,** *27*, 7171-7178.
10. Ranucci, E.; Spagnoli, G.; Ferruti, P.; Sgouras, D.; Duncan, R. *J. Biomat. Sci. Polym. Ed*. **1991**, *2*, 303-315.
11. Pattrick, N.G.; Richardson, S.C.W.; Casolaro, M.; Ferruti, P.; Duncan, R. *J. Contr. Rel.* **2001**, *77*, 225-232.
12. Ferruti, P.; Manzoni, S.; Richardson, S.C.W.; Duncan, R.; Pattrick, N.G.; Mendichi, R.; Casolaro, M. *Macromolecules* **2000**, *33*, 7793-7800.
13. Ranucci, E.; Ferruti, P.; Lattanzio, E., Manfredi, M.; Rossi, M.; Mussini, P.R.; Chiellini, F.; Bartoli C. *Journal of Polymer Science: Part A: Polymer Chemistry* **2009**, *4*, 6977.
14. Lavignac, N.; Lazenby, M.; Foka, P.; Malgesini, B.; Verpilio, I.; Ferruti, P.; Duncan, R. *Macromol Biosci.* **2004**, *4*, 922-929.
15. Richardson, S.C.W.; Pattrick, N.G.; Lavignac, N.; Ferruti, P.; Duncan, R. *J. Contr. Rel.* **2009**, *142* (1), 78-88.
16. Richardson, S.C.W.; Ferruti, P.; Duncan, R. *J. of Drug Targeting* **1999**, *6*, 391-404.

17. H. Maeda *Polymer conjugated macromolecular drugs for tumour-specific targeting, in: Polymeric Site Specific Pharmacotherapy.* A. J. Doumb, Ed., John Wiley and Sons Ltd., New York, 1994.
18. R. Duncan *Pharm. Sci. Technol. Today* **1999**, *2*, 441.
19. Franchini, J.; Ranucci, E.; Ferruti, P.; Rossi, M.; Cavalli, R. *Biomacromolecules* **2006**, *7* (4), 1215-1222.
20. Ferruti, P.; Franchini, J.; Bencini, M.; Ranucci, E.; Zara, G.P.; Serpe, L.; Primo, L.; Cavalli, R. *Biomacromolecules* **2007**, *8* (5), 1498-1504.
21. Annunziata, R.; Franchini, J.; Ranucci, E.; Ferruti, P. *Magn. Res. Chem.* **2007**, *45*, 51-58.
22. Ruoslahti, E. *Matrix Biol.* **2003**, *22*, 459.
23. Duncan R. *Nature Review/Drug Discovery* **2003**, *2*, 347-360.
24. Duncan R. *Nature Review/Cancer* **2006**, *6*, 688-701.
25. Schacht, E.; Ferruti, P.; Duncan, R. *PCT Internat. Pat. Appln. No. PCT/IB94/00259 to the Commission of the European Communities.* 1994.
26. Ferruti, P.; Ranucci, E.; Trotta, F.; Gianasi, E.; Evagorou, E.; Wasil, M.; Wilson, G.; Duncan, R. *Macromol. Chem.* **1999**, *200*, 1644-1654.
27. Ranucci, E.; Suardi, M.A.; Annunziata, R.; Ferruti, P.; Chiellini, F.; Bartoli, C. *Biomacromolecules* **2008**, *9*, 2693-2704.
28. Ranucci, E.; Ferruti, P.; Suardi, M.A.; Manfredi, A. *Macromol. Rapid Commun.* **2007**, *28*, 1243-1250
29. Endo, Y.; Mitsui, K.; Motizuki, M.; Tsurugi, K. *J. Biol. Chem.* **1987**, *262* (12), 5908-5912.
30. Lord, M.; Roberts, L.; Robertus, J. *FASEB J.* **1994**, *8*, 201-208.
31. Dempsey, C.E. *Biochim. Biophys. Acta* **1990**, *1031*, 143–161.
32. Lavignac, N.; Lazenby, M.; Franchini, J.; Ferruti, P.; Duncan, R. *Int. J. Pharm.* **2005**, *300*, 101-112.
33. Ranucci, E.; Bignotti, F.; Paderno, L.; Ferruti, P. *Polymer* **1995**, *36* (15), 2989-2994.
34. Richardson, S.C.W.; Pattrick, N.G.; Stella Man, Y.K.; Ferruti, P.; Duncan, R. *Biomacromolecules* **2001**, *2* (3), 1023-1028.
35. Duncan, R.; Ferruti, P.; Sgouras, D.; Toboku-Metzger, A.; Ranucci, E.; Bignotti, F. *J. Drug Target.* **1994**, *2* (4), 341-347.
36. Hill, I.R.; Garnett, M.C.; Bignotti, F.; Davis, S.S. *Biochim. Biophys. Acta vol.* **1999**, *1427*, 161-174.

37. Jones, N.A.; Hill, I.R.; Stolnik, S.; Bignotti, F.; Davis, S.S.; Garnett, M.C. *Biochim. Biophys. Acta* **2000**, *1517*, 1-18.
38. Hill, I.R.; Garnett, M.C.; Bignotti, F.; Davis, S.S. *Anal. Biochem.* **2001**, *291* (1), 62-68
39. Rackstraw, B.J.; Stolnik, S.; Bignotti, F.; Garnett, M.C. *Biochim. Biophys. Acta* **2002**, *1576*, 269-286.
40. Christensen, V.; Chang, C.W.; Kim, W.J.; Kim, S.W.; Zhong, Z.; Lin, C.; Engbersen, J.; Feijen J. *Bioconjugate Chem.* **2006**, *17* (5), 1233-1240.
41. Garnett, M.C.; Ferruti, P.; Ranucci, E.; Suardi, M.; Heyde, M.; Sleat, R. *Biochem. Soc. Trans.* **2009**, *37*, 713-716.
42. Min, L.; Chen, J.; Cheng, Y.P.; Xue, Y.N.; Zhuo, R.X.; Huang, S.W. *Macromol. Biosci.* **2010**, *10*.
43. Ferruti, P.; Bianchi, S.; Ranucci, E.; Chiellini, F.; Caruso, V. *Macromol. Biosci.* **2005**, *5* (7), 613-622.
44. Malgesini, B.; Verpilio, I.; Duncan, R.; Ferruti, P. *Macromol. Biosci.* **2003**, *3*, 59-66.
45. Ferruti, P.; Ranucci, E.; Bianchi, S.; Falciola, L.; Mussini, P.R.; Rossi, M. *Journal of Polymer Science: Part A: Polymer Chemistry*, **2006**, *44*, 2316-2327.
46. Ferruti, P.; Bianchi, S.; Ranucci, E.; Chiellini, F.; Piras, A.M. *Biomacromolecules* **2005**, *6* (4), 2229-2235.
47. Montanaro, L.; *Biomaterials* **2001**, *22*, 1607-1611.
48. Jacchetti, E.; Emilitri, E.; Rodighiero, S.; Indrieri, M.; Gianfelice, A.; Lenardi, C.; Podestà, A.; Ranucci, E.; Ferruti, P.; Milani, P. *Journal of Nanobiotechnology* **2008**, *6*, 14.
49. Emilitri, E.; Guizzardi, F.; Lenardi, C.; Suardi, M.; Ranucci, E.; Ferruti, P. *Macromol. Symp.* **2008**, *266*, 41-47.
50. Dykes, G.M.; Brierley, L.I.; McGrail P.T.; Seeley, G.J. *Chemistry* **2001**, 7, 4730-4739.
51. Li, F.; Liu, W.G.; Yao, K.D. *Biomaterials* **2002**, *23* (2), 343-347.
52. Kim, Y.H.; Gihm, S.H.; Park, C.R.; Lee, K.Y.; Kim, T.W.; Kwon, I.C. *Bioconjugate Chem*, **2001**, *12*, 932-938.
53. Sato, T.; Ishii, T.; Okahata, Y. *Biomaterials* **2001**, *22* (15), 2075-2080.
54. Esfand, R.; Tomalia, D.A. *Drug Discovery Today* **2001**, *6* (8), 427-436.
55. Lee, C.C.; MacKay, J.C.; Frechet, J.M.J.; Szoka, F.C. *Nature Biotechnology* **2005**, *23*, 1517-1523.

56. Malik, N.; Wiwattanapatapee, R.; Klopsch, R.; Lorenz, K.; Frey, H.; Weenerc, J.W.; Meijerc, E.W.; Paulusd, W.; Duncan, R. *J. Contr. Rel.* **2000**, *65*, 253-259.

57. Pack, D.W.; Hoffman, A.S.; Pun, S.; Stayton, P.S. *Nature Review/Drug Discovery* **2005**, *4*, 581-593.

58. Chien, P.Y.; Wang, J.; Carbonaro, D.; Lei, S.; Miller, B.; Sheikh, S.; Ali, S.M.; Ahmad, M.U.; Ahmad, I. *Cancer Gene Ther* **2005**, *12*, 321-328.

59. Landen, C.N.; Chavez-Reyes, A.; Bucana, C.; Schmandt, R.; Deavers, M.T.; Lopez-Berestein, G.; Sood, A.K. *Cancer Res.* **2005**, *65* (15), 6910-6918.

60. Dow, S.; Elmslie, R.; Kurzman, I.; MacEwen, G.; Pericle, F.; Liggitt, D. *Hum. Gene Ther*. **2005**, *16* (8), 937-946.

61. Zuber, G.; Dauty, E.; Nothisen, M.; Belguise, P.; Behr, J.P. *Adv. Drug. Deliv. Rev.* **2001**, 52, 245-253.

62. Luo, D.; Saltzman, W.M. *Nat. Biotechnol*. **2000**, *18*, 33-37.

63. Boussif, O.; Lezoualch, F.; Zanta, M.A.; Mergny, M.D.; Scherman, D.; Demeneix, B.; Behr J.P. *Proc. Natl. Acad. Sci. USA* **1995**, *92*, 7299-7301.

64. Fischer, D.; Bieber, T.; Li, Y.; Elsasser, H.P.; Kissel, T. *Pharm. Res.* **1999**, *16* (8), 1273-1279.

65. Gosselin, M.A.; Guo, W.; Lee, R.J. *Bioconjugate Chem.* **2001**, *12* (6), 989-994.

CHAPTER 3

POLY(AMIDOAMINE)-GELONIN CONJUGATES AS POTENTIAL ANTI-CANCER DRUGS [6,18,19,20,22]

3.1 INTRODUCTION

The use of polymers in medicine is not new. Natural polymers have been used as components of herbal remedies for millennia. The use of synthetic, water-soluble polymers as macromolecular drugs or components of injectable drug delivery systems has, in contrast, a relatively short history. During the second world war synthetic polymeric plasma expanders were widely adopted (e.g. poly(vinylpyrrolidone)[1] and in 1955 the first polymer-drug conjugates appeared (e.g. mescaline-N-vinylpyrrolidine conjugates)[2]. Biologically active polymeric drugs also started to gain popularity, and divinylether-maleic anhydride copolymer (pyran copolymer) was tested clinically as an anticancer agent in the 1960s. From that moment on, a wide range of polymers - modified polysaccharides, synthetic polypeptides and synthetic polymers - have been successfully transferred into the market as polymeric drugs, giving rise in 1970s to more clearly defined chemical and biological rationale for the design of polymeric drugs, polymer-protein conjugates[3] and polymer-drug conjugates[4], the so called “polymer therapeutics” family[5,6].

As reported in literature by Duncan[5,6], a large number of advantages that can be achieved through a polymer conjugation. Some noteworthy benefits are as follow:

- stabilization of labile active molecules from chemical and biological degradation;

- protection from proteolytic degradation;
- increased plasma half life;
- modification of organ disposition;
- drug penetration into selected cell compartments through endocytosis;
- enhanced possibilities of drug targeting.

Conjugation to polymeric carriers may impart several other potential advantages such as reduction of immunogenicity and decreased antibody recognition.

Cancer therapy represents one of the fields in which polymer-drug conjugation could bring major advantages[7]. In fact, the opportunity to exploit passive tumour-targeting phenomenon called the "enhanced permeability and retention" (EPR) effect constitutes another important development, since consequent passive tumour targeting leads to enhanced efficacy of drugs with reduced side effects[8].

Another important field of research is that of polymer-protein conjugation. Therapeutically relevant proteins such as antibodies, cytokines, growth factors, and enzymes (collectively referred to as “biologics”) are playing an increasing role in the treatment of viral, malignant, and autoimmune diseases. The development and successful application of therapeutic proteins, however, is often impeded by several difficulties, for example, insufficient stability and shelf-life, costly production, immunogenic and allergic potential, as well as poor bioavailability and sensitivity towards proteases. Consequently, frequent administration at an excessively high dose is required to reveal their therapeutic effects in vivo. As a result, unexpected side effects occur. Therefore, there has been a continuing search for improved alternatives. Bioconjugation with water-soluble polymers improves the plasma clearance time and body distribution, resulting in increased therapeutic effects and decreased side effects[5,6].

The first practical use of polymer therapeutics as anticancer agent was in the form of polymer-protein conjugates.

Although several water-soluble polymers have been successfully used for protein conjugation, polyethyleneglicole (PEG) is particularly attractive because is already used as a pharmaceutical, is non-toxic and non-immunogenic and posses stealth-like properties. The design of PEG-protein conjugates is now well established and is called PEG-ylation. PEG-ylation increases protein solubility and stability and hence prolongs plasma half-life and can reduce protein immunogenicity. The first PEG-ylated proteins were approved by regulatory authorities for routine clinical use in the early 1990s: PEG-adenosine deaminase[9] used to treat acute immunodeficiency syndrome and PEG-L-asparaginase[10] to treat acute lymphoblastic leukaemia. At the same time in Japan, a styrene-co-maleic anhydride conjugate of the anticancer protein neocarzinstatin called SMANCS[8,11], developed by Maeda and colleagues, was successfully used as a treatment of patients with primary liver cancer and this led to market approval for the treatment of this disease. Other PEGylated proteins in clinical use or under development are reported in Table 3.1[12-17].

Table 3.1. Polymer-protein conjugates in clinical use or development.

Compound	Name	Status	Indication
SMANCS	Zimostatin Stimalmer	Market	Hepatocellular carcinioma
PEG-L-asparaginase	Oncaspar	Market	Acute lymphoblastic leukaemia
PEG-GCSF	Neulasta	Market	Prevention of neurotropaenia associated with cancer chemotherapy
PEG-IFNα 2a	PEG-asys	Market Phase I/II	Hepatitits B and C Melanoma, chronic myeloid leukaemia and renal-cell carcinoma
PEG-IFNα 2b	PEG-Intron	Market Phase I/II	Hepatitits C Melanoma, chronic myeloid leukaemia and renal-cell carcinoma
PEG-arginine deiminase	ADI-PEG20	Phase I	Hepatocellular carcinioma
PEG-glutaminase combined with a glutamine anti-metabolite 6-diazo-5-oxo-L-norleucine (DON)	PEG-PGA and DON	Phase I/II	Various cancers
PEG-D-amino acid oxidase (DAO) combined with the substrate DAO, D-proline	PEG-DAO and DAO,D-proline	Preclinicical	

GCSF: granulocyte colony-stimulating factor; IFNα: interferon-α.

Although there are other available polymers for protein conjugation such as N-(2-hydroxypropyl)methacrylate copolymers, poly(ethyleneimine), linear poly(amidoamine)s, poly(vinylpyrrolidone), poly(acrylamide), poly(dimethylacrylamide), poly(vinylalcohol), chitosan, dextrin and dextran, PEG is still the most popular option since the clinical value of PEGylation is now well established.

Several poly(amidoamine)s (PAAs) have been studied in the past in the field of polymer therapeutics as water-soluble carriers for known anticancer and antiviral drugs and as intracytoplasmic delivery systems of proteins and genes.

In a previous work, it was found that linear ISA1 and ISA23 polymers displayed membrane disruptive properties in response to a decrease in pH[18,19]. This attribute confers PAAs with endosomolytic properties in vitro and the ability to promote the endosomal escape of two ribosome-inactivating proteins (RIPs): either ricin A-chain or gelonin[20]. RIPs are a group of naturally occurring plant and bacterial proteins that have been widely studied for several potential applications as therapeutics, especially as anticancer agents[21]. Examples of plant RIPs include abrin, ricin, gelonin, momordin, mistletoe lectin, etc. Type I RIPs are made up of the toxic subunit alone, while type II RIPs consist of a toxic subunit (A-chain) and a lectin like subunit (B-chain) linked together. One commonly found linker is the disulfide bond, though other strategies have been employed and are evident within some type II RIPs. The role of the B-chain is to help in the transport of RIPs into the cells by binding to specific sugar residues associated with glycoproteins or glycolipids, or directly to membrane lipids on the plasma membrane which are then internalized by endocytosis. The toxicity of specific RIPs such as ricin toxin is due to its RNA-N-glycosidase activity, by which it brings about the depurination of adenine residue at position 4324 in the 28 S rRNA leading to inhibition of protein synthesis.

Recently, novel linear PAAs bearing 2-ethenyldithiopyridine pendant (PAA-SSPy) have been synthesized as intermediates for new bioactive macromolecular conjugates sensitive to electric stimuli by exchange reaction with thiol-containing molecules[22,23]. Disulfide bonds play a key role within biological systems. A very wide range of metabolic processes involve disulfide bond formation or reduction, from sugar and lipid metabolism and oxidative phosphorilation, to protein folding and stabilisation, cell signalling, aging and apoptosis[24]. Moreover, many diseases have been recently associated with redox imbalances, such as AIDS and other immune diseases, Parkinson and Alzheimer syndromes, cancer and many others[25-27].

Cytoplasmic fluids are quite strongly reducing compared to extracellular fluids, such as plasma and other body fluids due to the presence of relatively high concentrations of reduced glutathione[28]. As a consequence, disulfide bonds are stable in bloodstream but undergo reduction inside cells and therefore can be regarded as “smart” stimuli-responsive linkages in polymer therapeutic design for intravenous administration[29-32]. Several publications reports the use of disulfides as cleavable linkers in drug or gene delivery systems[33,34].

In this work two PAAs bearing pendant 2-ethenyldithiopyridine (ISA1-SSPy and ISA23-SSPy) were used to investigate their ability to mediate intracellular delivery of the type I ribosome-inactivating gelonin. The strategy adopted consists of a three synthetic step as reported in Scheme 3.1. In the first step an hydrophilic tri-dimensional PAA network was synthesised using cystamine as cross-linking agent. In the second step, the hydrogel obtained was solubilized by direct disulfide exchange reaction with dipyridyl disulfide. Finally, in the third step, the linear and soluble PAA-SSPy obtained was conjugated to a thiol-containing gelonin via thiol-disulfide exchange reaction. A covalent disulfide bond between the polymer and the protein, which is stable in blood stream and stimuli-responsive to intracellular environment, makes these conjugates potential candidates for the development of novel injectable therapeutics.

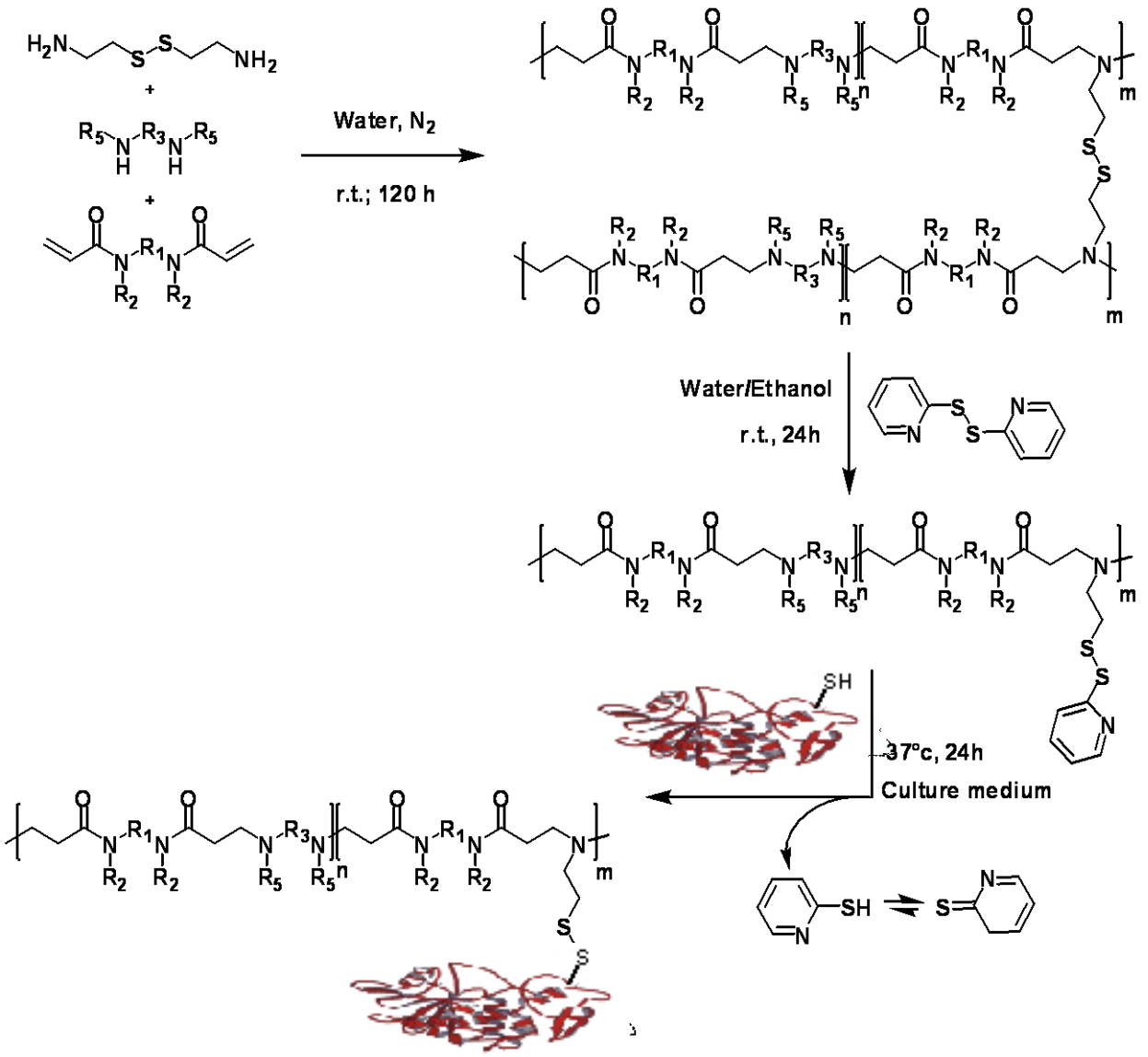

Scheme 3.1. Synthetic pathway leading to PAA-gelonin conjugates

Two different recombinant proteins, encoding gelonin with an N-terminal 6xHistidine (H or His) and V5 epitope tag (6H-V5 Gelonin) and gelonin encorporating a C-terminal HA and 6xHis tag flanking a cystine residue (Gelonin HA-Cys-6H) were prepared introducing the required tag on a gelonin plasmid by polymerase chain reaction (PCR), isolated and purified from E. Coli. Preliminarily in vitro biological tests are reported.

3.2 EXPERIMENTAL PART

Instruments

^{1}H and ^{13}C NMR spectra were run on a Brüker Advance 400 spectrometer operating at 400.132 (^{1}H) and 100.623 (^{13}C) MHz.

Size exclusion chromatography traces were obtained with a Knauer Pump 1000 equipped with a Knauer Autosampler 3800, TSKgel G4000 PW and G3000 PW TosoHaas columns connected in series, Light Scattering Viscotek 270 Dual Detector and a refractive index detector Waters model 2410. The mobile phase was a 0.1 M Tris buffer pH 8.00 ± 0.05 with 0.2 M sodium chloride.

Amplification of DNA fragments by polymerase chain reactions were performed using a BIO-RAD MJ Mini Gradient thermal Cycler.

Materials and methods

Plasmid DNA was purified with Qiagen Miniprep Kit. Agarose was purchased from BIO-RAD Laboratories. All chemicals used in the biological tests were purchased from Sigma-Aldrich unless stated otherwise.

Gelonin template (BBI inc. pUC19 containing an E.coli codon-optimised ORF encoding gelonin) was from GenBank, accession number L12243.

Oligonucleotide primers were synthesized by Invitrogene.

2,2-Bis(acrylamido)acetic acid (BAC) was synthesized as previously described and its purity (99,5%) determined titrimetrically[35]. N,N'-Bis(acryloyl)piperazine (BP) was synthesized as reported in literature and its purity determined by NMR spectroscopy[36]. 2-Methylpiperazine was purchased from Fluka and used after sublimation. Its final purity (98%) was determined with acidimetric titration. Where not otherwise specified all materials and analytic grade solvents were purchased from Fluka and used as received.

Synthesis of cystamine crosslinked ISA23 hydrogel (HG-ISA23)[23]*.* Cystamine di-hydrochloride (0.260 g; 1.129 mmol) and lithium hydroxide monohydrate (95.70 mg; 2.258 mmol) were dissolved into a solution of BAC (3 g; 15.05 mmol) and lithium hydroxide monohydrate (0.638 g; 15.05 mmol) in distilled water (5 mL) under nitrogen atmosphere. Then 2-methylpiperazine (1.31 g; 12.79 mmmol) was added under stirring. The homogeneous solution settled into a hydrogel. After 120 hours the hydrogel was finely ground, extensively extracted with water and ethanol and dried at 37 °C and 0.1 Torr. Yield: 4 g (87.53%).

Synthesis of cystamine crosslinked ISA1 hydrogel (HG-ISA1)[23]*.* Cystamine di-hydrochloride (0.264 g; 1.158 mmol) and lithium hydroxide monohydrate (98.16 mg; 2.316 mmol) were added to a solution of BP (3 g; 15.446 mmol) in distilled water (5.2 mL) and 2-methylpiperazine (0.692 g; 6.564 mmol) and bis(hydroxyethyl)ethylenediamine (1 g; 6.564 mmol) were added under stirring. The homogeneous solution settled into a hydrogel. After 120 hours the hydrogel was finely ground, extensively extracted with water and acetone and dried at 37 °C and 0.1 Torr. Yield: 4.36 (88 %).

Synthesis of ISA23-SSPy. HG-ISA23 (4.0 g; 1.129 mmol disulfide) was soaked in a 2:1 v/v water/ethanol mixture (30 mL) and 2,2'-dipyridyldisulfide (0.508 g; 2.258 mmol) and a catalytic amount of 2-mercaptopyridine were added. The gel dissolved in a few hours. The resultant solution was stirred for further 24 hours at room temperature and then diluted to 100 mL with water. Excess 2,2'-dipyridildisulfide precipitated out. The mixture was then filtered through a HPLC filter (0.45 μm) and then ultrafiltered through a membrane with a nominal molecular weight cut-off 3000 after adjusting the pH to 2.5 with hydrochloric acid. The product was recovered by freeze drying. Yield: 3.65 g (81.11 %). Molecular weight values: $\overline{M}_n$ =12700, $\overline{M}_w$ =23600, PD=1.86. ^{13}C NMR (D_2O): δ= 173.5 (CH-***C***OOH); 171.3 (NH-***C***O); 149.6 (N-***C***H pyridine); 139.3 (CH-***C***H=CH- pyridine); 122.3 (CH-CH=***C***H- pyridine); 122.2 (***C***H-CH=CH- pyridine); 58.248.4 (-***C***H_2N polymer backbone); 31.6-28.8 (-NCH_2***C***H_2- polymer backbone); 13.9 (***C***H_3- piperazine).

^{1}H NMR (D_2O): δ= 8.5 (m, 1H, N=C***H***-C- pyridine); 7.80-7.70 (m, 2H, =C***H***-C***H***= pyridine); 7.30 (m, 1H, C=C***H***-C pyridine); 5.55 (s, 1H, COOH-C***H***); 3.44-2.85 (br, 2H, NHCOC***H$_2$*** polymer backbone); 2.79-2.70 (br, 2H, $NHCOCH_2C$***H$_2$*** polymer backbone); 1.38 (br, 3H, -C***H$_3$*** piperazine). Loading of –SSPy by ^{1}H NMR: 9.2%.

ISA1-SSPy was prepared using the same procedure adopted for ISA23-SSPy. Yield: 3.18 g (79.5 %). Molecular weight values: $\overline{M}_n$=1800, $\overline{M}_w$=3000, PD=1.93. ^{13}C NMR (D_2O): δ= 171.3 (NH-***C***O); 156.6 (N-***C***-S pyridine); 149.8 (N-***C***H pyridine); 139.4 (CH-***C***H=CH- pyridine); 122.8 (CH-CH=***C***H- pyridine); 122.1 (***C***H-CH=CH- pyridine); 56.5-41.5 (-***C***H_2N polymer backbone); 29.9-28.3 (-NCH_2***C***H_2- polymer backbone); 14.2 (***C***H_3- piperazine). ^{1}H NMR (D_2O): δ= 8.40 (m, 1H, N=C***H***-C-pyridine); 7.90-7,84 (m, 2H, =C***H***-C***H***= pyridine); 7.40 (m, 1H, C=C***H***-C pyridine); 3.65-2.88 (br, 2H, NHCOC***H$_2$*** polymer backbone); 2.79-2.70 (br, 2H, $NHCOCH_2C$***H$_2$*** polymer backbone); 1.38 (br, 3H, -C***H$_3$*** piperazine). Loading of –SSPy by ^{1}H NMR: 8.7%.

Preparation of the gelonin template. Gelonin template was incubated over-night at 37 °C under stirring in 10 mL of 2xYT(amp) medium. After this time, the colloidal suspension was centrifuged at 4,000xg for 5 minutes. The supernatant was eliminated and the plasmid purified with Qiagen Miniprep Kit.

Cloning of 6H-V5 Gelonin and Gelonin HA-Cys-V5. Polymerase chain reaction (PCR) was used to engineer the gelonin template with the required functions. 1 µL of template was mixed in a 100 µL Eppendorf tube with 0.5 µL of Taq polymerase, 5 µL of deoxynucleotide triphosphate (dNTPs), 1.25 µL of oligomers 5' and 3', 10 µL of 10x buffer and 81 µL of DNase-free water. The set-up parameters and oligomers used for 6H-V5 Gelonin and Gelonin HA-Cys-6H are reported in Table 3.2.

Table 3.2. Set up parameters used in the PCR experiments.

	Gelonin HA-Cys-6H	6H-V5 Gelonin
		
Taq polymerase	Accuzyme	Accuzyme
Oligos 5’	87 CACCATGAAAGGTAATATGAAAGTG	90 caccTAAAGGAGGaaaggatccATG AAAGGTAATATGAAAGTG
Oligos 3’	89 TTAATCGAAGCCAACCAGGGA	86 TTAatgatgatgatgatgatgTGCGCATCTtg cgtaatctggtacgtcgtaaggataATCGAAG CCAACCAGGGATTC
Program	1 kb	1 kb
Annealing T	55 °C	55 °C

Electrophoresis. Gel electrophoresis assay was used to evaluate the formation of PCR products and plasmid. The samples were subjected to electrophoresis on agarose gel (0.7 % w/v) with ethidium bromide (0.25 µg/mL) for 45 minutes at 70 Volt. The banding pattern was obtained using a UV transilluminator and photographed with a Polaroid camera.

Bacteria transformation. TOPO-cloning has been used to directly insert Taq polymerase-amplified PCR products into a plasmidic vector. 2 µL of a DNA:water solution (1:10 for Gelonin HA-Cys-6H and 1:100 for 6H-V5 Gelonin) were mixed with 1 µL of salt solution, 2.5 µL of water and 0.5 µL of pET151/D-TOPO vector and allowed to equilibrate at room temperature for 20 minutes. The mixture was incubated on ice for 5 minutes, then 10 µL of One Shot® TOP10 Chemically Competent E.coli were added. Heat shock at 42 °C for 30 seconds was performed using a thermocycler. The Eppendorf tube was immediately put on ice and 100 µL of SOC medium added.

100 µL of this resulting solution were spread on an agarose plate and incubate at 37 °C and 5% v/v CO_2. The plasmid of each colony was amplified by PCR using 12.5 µL Green Dream Taq, 11.9 µL of DNase-free water and 0.3 µL of the primers (1 kb program, 55 °C and 60 °C annealing temperature) and evaluated by electrophoresis on agarose gel. The plasmid of the colonies expressing the right molecular weight DNA vector was isolated and purified with Qiagen Miniprep Kit.

Protein expression (Mini-induction). 50 ng of plasmid were mixed with 5 µL of DNase-free water and 10 µL of BL21(DE3) Competent E.coli and incubated on ice for 30 minutes. The solution was heat shocked at 42°C for 30 seconds and immediately put on ice for 2 minutes. Then, 100 µL of SOC medium was added and incubated for 1 hour at 37 °C. After this time the mixture was transferred in 10 mL of 2xYT(amp) medium and incubated at 37 °C under stirring.

Protein purification (Large scale preparation). 5 mL of the Mini-induction solution were mixed with 1 liter of 2xYT(amp) and incubated for 3 hours at 37°C. After this time, 250 µL of 1M IPTG (Isopropil β-D-1-tiogalattopiranoside) were added and the solution incubated again at 37 °C for other 3 hours. The colloidal suspension were put in 500 mL tube and centrifuged at 6000 rcf(g) and 4 °C for 20 minutes. The supernatant was eliminated and the pellet re-suspended in 5 mL of PBS. 100 µL of protein inhibitor and 50 mL of 0,2 % sodium azide were added before cell lysis by French Press. The extract was centrifuged at 22,000 rcf(g) and 4 °C for 20 minutes, the pellets removed and the supernatant centrifuged again at 22,000 rcf(g) and 4 °C for 10 minutes. The resulting clear solution was eluted through a TALON® immobilized metal affinity chromatography resin charged with cobalt. Eight fractions were collected eluting with 500 µL of a 100 mM solution of imidazole in PBS. Bradford test was used to calculate the concentration of the fractions eluted. High concentrated samples were mixed together, dialyzed against 4 liters of PBS for 2 times and filter sterilized.

SDS-Page. Sodium dodecyl sulfate polyacrylamide gel electrophoresis was used to characterize the cloned proteins according to their electrophoretic mobility which is a function of the protein's molecular weight. 10% resolving gel was prepared using 3.3 mL of 30% w/v acrylamide, 2.5 mL of 1.5 M Tris buffer pH: 8.8, 0.1 mL of 10% v/v sodium dodecyl sulfate (SDS), 4 mL of water, 50 µL of 10% w/v ammonium persulfate (APS) and 5 µL of N,N,N',N'-tetramethylethylenediamine (TEMED). Stacking buffer was prepared mixing 5.1 mL of water with 0.66 mL of 30% w/v acrylamide, 0.83 mL of 1 M Tris buffer pH: 6.8, 50 µL of APS, 50 µL of SDS and 10 µL of TEMED. Running time used was 45 minutes at 200 Volt in SDS buffer. Following electrophoresis, the gel was stained with Coomassie Brilliant Blue or processed further (Western blot). Samples were prepared mixing 20 µL of protein in 8 µL of Laemmli buffer and 2 µL of β-mercaptoethanol.

Western immunoblotting. Proteins resolved by SDS-PAGE were transferred to PVDF membrane using Towbin buffer, at 400 Ampere for 60 minutes. After blocking with 1% w/v not fat dryed milk in PBS Tween20 (0,01% v/v), membranes were incubated with 3 µL 6xHis monoclonal primary antibody for 1 hour at 37 °C and then washed 3 times with PBS Tween. 6 µL of Anti-mouse Ig, horseradish whole secondary antibody were incubated over-night at 4 °C. After washing again with PBS-Tween, immunoreactive proteins were visualized using 1 mL of Amersham ECL western blotting detection reagent. Exposure time used were 5 and 10 minutes.

In vitro biological evaluation

Polymer cytotoxiciy. Sterile, flat-bottomed 96-well plates were seeded with B16F10 and Vero cells to a density of $1x10^4$ cells/well and incubated at 37 °C in an atmosphere of 5% v/v CO_2 for 24 hours. Polymers dissolved in RPMI 1640 medium glutaMAX-I (B16F10) or DMEM (Vero) supplemented with foetal bovine serum and PSG (penicillin-streptomicin-glutamine) were filter sterilized and then added to cells to give a final concentration range of 0-5 mg/mL.

After incubation for 69 hours, cell viability was assessed using the MTT assay (3-[4,5-dimethylthiazol-2-yl]-2,5-diphenyltetrazolium bromide). MTT solution (20 µL; 5 mg/mL) was added and the plates were incubated for a further 3 hours (total incubation 72 hours), during which time the yellow tetrazolium dye was converted into an insoluble blue formazan salt by viable cells. Finally, the cell culture medium was removed and the formazan salt crystals formed were dissolved in optical grade DMSO (100 µL). Plates were read spectrophotometrically using a plate-reader set at 550 nm. Viability of cells exposed to test compound was expressed as a percentage of the viability seen in the control untreated cells. Dextran and poly(ethyleneimine) (PEI) were used as negative and positive controls, respectively.

Toxin cytotoxicity. In order to establish a concentration of gelonin that would be non-toxic to B16F10 cells, toxin-dose response assay was first carried out. B16F10 cells were exposed to either 6H-V5 Gelonin and Gelonin HA-Cys-6H (0-200 µg/mL) for 72 hours and viability assessed using the MTT assay as described above. 6H-V5 Gelonin at a concentration of 1.4 µg/mL and Gelonin HA-Cys-6H at a concentration of 1.4 µg/mL and 14 µg/mL caused no decrease in cell viability and, thus, were selected for use in subsequent toxin and polymer cytotoxicity assays.

Evaluation of cytotoxicity of polymer-toxin conjugates. 6H-V5 Gelonin at a concentration of 1.4 µg/mL and Gelonin HA-Cys-6H at a concentration of 1.4 µg/mL and 14 µg/mL were dissolved in RPMI 1640 medium. The polymers used were then dissolved in this medium to give polymer concentration in the range 0-2 g/mL and allow to react for 24 hours at 37 °C. B16F10 cells were exposed to polymer-toxin conjugates for 72 hours and cell viability was measured by the MTT assay as described above. Dextran-toxin and PEI-toxin were used as negative and positive controls respectively.

3.3 RESULTS AND DISCUSSION

The rationale of this work was to obtain a family of smart soluble PAAs-gelonin conjugates sensitive to reductive cleavage via exchange reaction between PAAs bearing pendant 2-ethenyldithiopyridine (PAA-SSPy) moieties and a thiol-containing gelonin. The linkage between protein and PAA chain is a redox sensitive disulfide bond. After internalization, these PAA-gelonin conjugates are expected to be rapidly dissolved, releasing a drug payload, if present.

PAA-SSPy polymers were prepared using two families of PAA with different ionic behavior and widely studied in the past as endosomolitic polymers[18,38,39]: a purely polycationic ISA1-like polymer and an amphoteric ISA23-like polymer.

The strategy adopted consists of a two step synthesis[22,23]. Briefly, a PAA-cystamine networks were first prepared (HG-ISA23 and HG-ISA1) and then converted into linear soluble polymers bearing activated disulfide pendants by exchange reaction with 2,2'-dithiodipyridine (ISA1-SSPy and ISA23-SSPy).

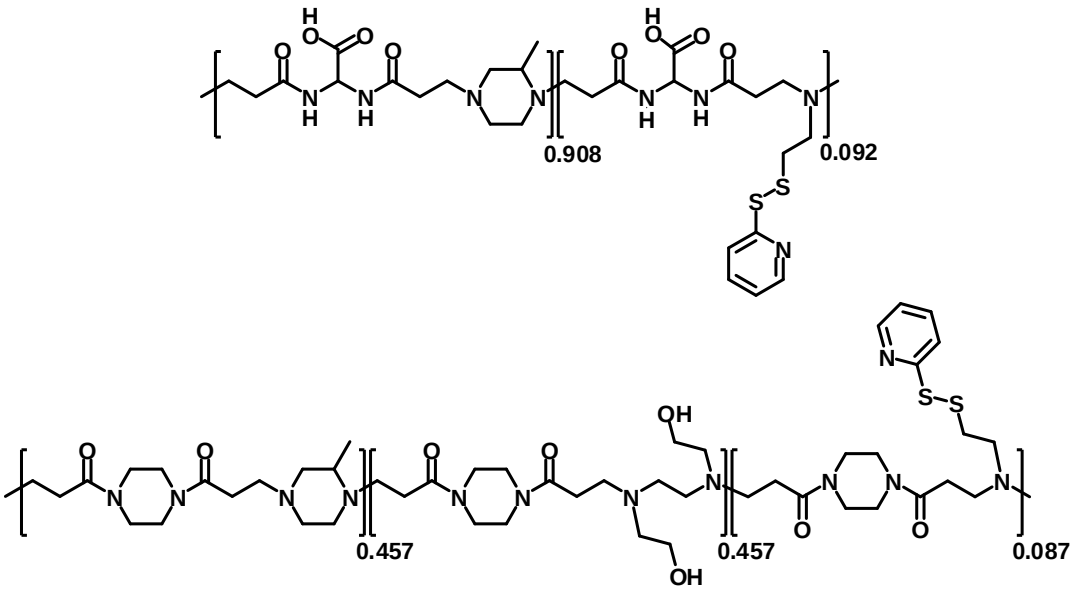

Figure 3.1. Structures of ISA23-SSPy (up) and ISA1-SSPy (bottom).

2-Ethenyldithiopyridine is in fact extremely reactive in thio/disulphide exchange reactions, the driving force being the production of 2-mercaptopyridine that, mostly turning into the tautomeric thiopyrid-2-one form, is an excellent leaving group[39].

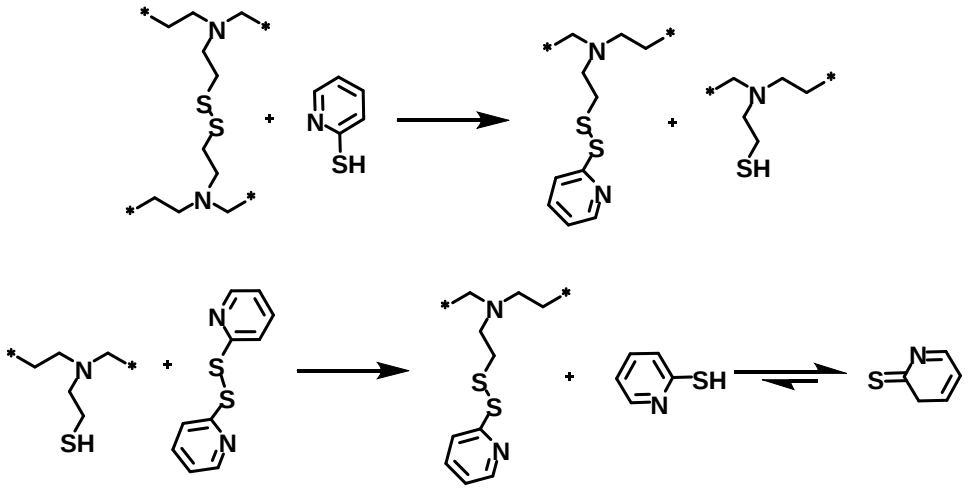

Scheme 3.2. Mechanism of the thiol-disulfide exchange reaction between PAA hydrogels and 2,2'-dithiodipyridine.

In the first synthetic step, HG-ISA23 and HG-ISA1 were prepared using 15% of cystamine over the total number of amine hydrogens.

In the second step, the exchange reactions leading to PAA-SSPy polymers were performed on finely ground PAA networks swollen in ethanol (HG-ISA1) or in 2:1 v/v water/ethanol mixture (HG-ISA23) under slightly alkaline conditions (pH 8.5-9 after dilution with water) and in the presence of a catalytic amount of 2-mercaptopyridine. A 2:1 excess 2,2'-dipirydyldisulfide with respect to cystamine moieties was employed in all cases. The loading of 2-ethenyldithiopyridine was 9.2 % and 8.7 % on a molar basis in ISA23-SSPy and ISA1-SSPy, respectively. The number of pyridyl groups found in these polymers was always somewhat lower than the expected one. However, it is unlikely that the exchange reaction was really incomplete, since the starting hydrogels were in all cases completely solubilized long before the reaction was stopped.

This result can be ascribed to the possible elimination of some highly functionalized low molecular weight fractions during ultrafiltration.

The ribosome-inactivating protein gelonin was used to investigate the ability of ISA1-SSPy and ISA23-SSPy to mediate its intracellular delivery. Gelonin in fact, is a type I RIPs and does not contain the cell-binding subunit that promotes its internalization by endocytosis.

In a previous work, linear and non-functionalised ISA23 and ISA1-like polymers proved able to effectively delivery commercial available ricin A-chain and gelonin on B16F10 cells lines. Ricin and RTA displayed IC_{50} values of 0.3 and 1.4 μg/ml, respectively, and gelonin was non-toxic over the range studied. In all further experiments, non-toxic concentrations of RTA (250 ng/ml) and gelonin (1.4 μg/ml) were used. When B16F10 cells were incubated with a combination of RTA-PAA conjugates (250 ng/ml), the observed IC_{50} fell to 0.65±0.05 mg/ml. Similar results were obtained with gelonin. Moreover, it has been found that the decrease of the IC_{50} was related to the concentration of the PAA used: as the PAA concentration increased, less RTA was required to achieve the IC_{50} level.

In this work, PAA-SSPy polymers were used to prepare PAA-gelonin complexes in which the polymeric chain was linked to the bioactive moieties by a disulfide bridge. Compared to the complexes preaviously obtained using non-functionalized PAA, these new complexes are stable in blood stream and stimuli-responsive to intracellular environment. They can be considered as novel injectable therapeutics.

To achieve this aim, two types of gelonin were synthesized on purpose: a C-terminal Gelonin HA-Cys-V5 containing a cystine residue suitable of exchange reaction with ethenyl-dithiopyridine bearing PAAs and an N-terminal 6H-V5 Gelonin used as reference of proteins that does not contain reactive thiol-groups.

Plasmids expressing both proteins were made by sub-cloning an open reading frame coding for gelonin into a commercially available bacterial expression cassette (pET151/D Topo).

Sub-cloning was performed using the following oligonucleotide PCR primers:

Primer 89: (5') CACCATGAAAGGTAATATGAAAGTG

Primer 89: (3') TTAATCGAAGCCAACCAGGGA

Primer 90: (5') caccTAAAGGAGGaaaggatccATGAAAGGTAATATGAAAGTG

Primer 86: (3') TTAatgatgatgatgatgatgTGCGCATCTtgcgtaatctggtacgtcgtaaggataATCGAAGCCA ACCAGGGATTC

The oligonucleotide primers were used to encorporate the required motif into the gelonin open reading frame. V5 and HA tags were inserted for antibody recognition whereas 6xHIS tag for the final purification of the proteins using a metal affinity resin.

PCR were performed using 1Kb program and 55 °C as annealing temperature. The final Taq polymerase-amplified PCR products were evaluated by gel electrophoresis on agarose gel as reported in Figure 3.2.

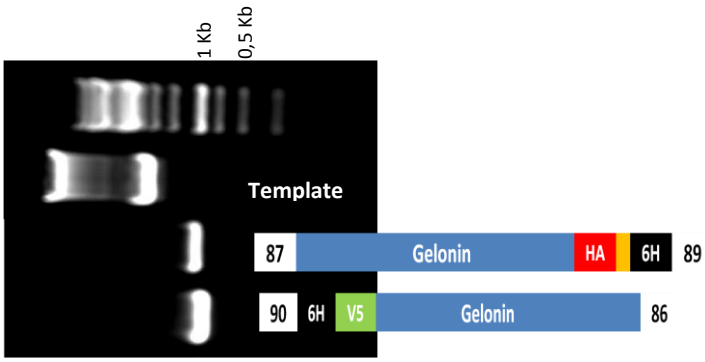

Figure 3.2. Electrophoresis gel of the PCR products.

Having successfully amplified the desired region of the gelonin ORF, the PCR products were purified and inserted into the expression cassette via TOPO-reaction. The technique utilizes the inherent biological activity of DNA topoisomerase I. The biological role of topoisomerase is to cleave and rejoin supercoiled DNA ends to facilitate replication. Vaccinia virus topoisomerase I specifically recognises DNA sequence 5´-(C/T)CCTT-3'.

During replication, the enzyme digests DNA specifically at this sequence, unwinds the DNA and re-ligates it again at the 3' phosphate group of the thymidine base.

The results of these experiments were then transformed into chemically competent E.coli Top10 also following the manufactures recommendations. The resulting colonies were grown over night on selective medium (2xYT agar plates containing a selective marker (Amp)) and individual colonies picked and screened for the presence of the PCR product and its orientation again by PCR (data not reported).

Having ascertained that the PCR product was contained within a specific colony, and that the PCR product was inserted into the vector in the correct orientation, the plasmid was isolated and subject to sequencing. The results of the sequencing efforts were assembled as a contiguous sequence using the LaserGene applications available commercially from DNAStar (Madison WI, USA).

Following the generation of a plasmid map using the above software the ORF was interrogated to ensure there were not deletions that could result in a frame-shift giving rise to an aberrant protein.

Gelonin-HA-Cys-6H

MKGNMKVYWIKIAVATWFCCTTIVLGSTARIFSLPTNDEEETSK
TLGLDTVSFSTKGATYITYVNFLNELRVKLKPEGNSHGIPLLRKKC
DDPGKCFVLVALSNDNGQLAEIAIDVTSVYVVGYQVRNRSYFFK
DAPDAAYEGLFKNTIKTRLHFGGSYPSLEGEKAYRETTDLGIEPRI
GIKKLDENAIDNYKPTEIASSLLVVIQMVSEAARFTFIENQIRNNF
QQRIRPANNTISLENKWGKLSFQIRTSGANGMFSEAVELERAN
GKKYYVTAVDQVKPKIALLKFVDKDPKTSLAAELIIQNYESLVGF
DESLVGFDYPYDVPDYARCAHHHHHH.

6H-V5-Gelonin

MHHHHHHGKPIPNPLLGLDSTENLYFQGIDPFTMKGNMKVY
WIKIAVATWFCCTTIVLGSTARIFSLPTNDEEETSKTLGLDTVSFS
TKGATYITYVNFLNELRVKLKPEGNSHGIPLLRKKCDDPGKCFVL
VALSNDNGQLAEIAIDVTSVYVVGYQVRNRSYFFKDAPDAAYE
GLFKNTIKTRLHFGGSYPSLEGEKAYRETTDLGIEPLRIGIKKLDE
NAIDNYKPTEIASSLLVVIQMVSEAARFTFIENQIRNNFQQRIRP
ANNTISLENKWGKLSFQIRTSGANGMFSEAVELERANGKKYYV
TAVDQVKPKIALLKFVDKDPKTSLAAELIIQNYESLVGFD

Figure 3.3. Sequencing results of 6H-V5 Gelonin and Gelonin HA-Cys-V5.

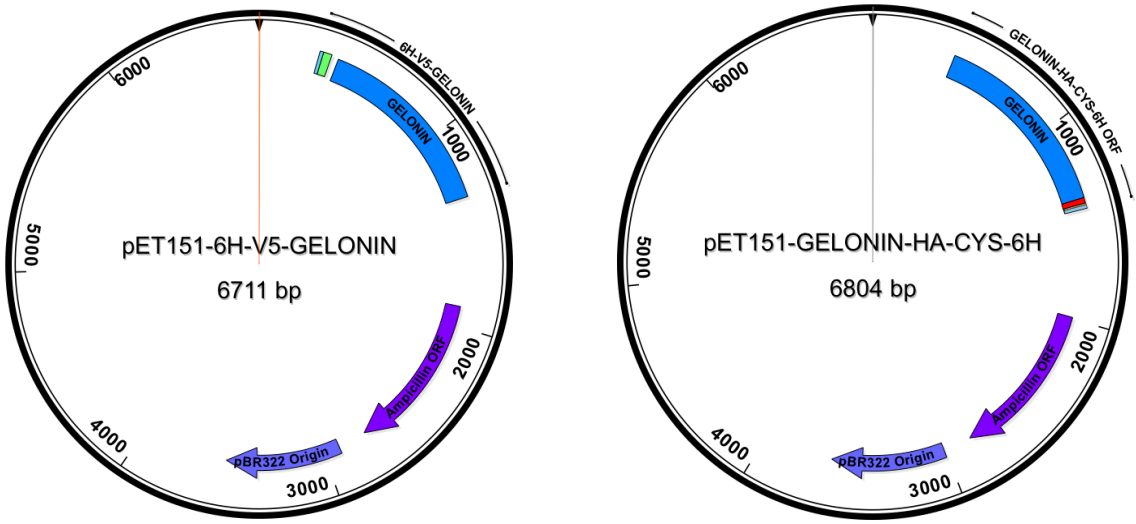

Figure 3.4: Plasmid map of the two type of gelonin cloned.

The purified plasmid was transformed into chemically competent E.coli BL21(DE3) bacteria and mini-induction experiments (as described in the materials and methods section) were performed to ascertain that it was possible to produce protein of approximately the correct molecular weight by both SDS-PAGE followed by Coomassie brilliant blue staining or western immunoblotting using antibodies specific for 6xHis tag.

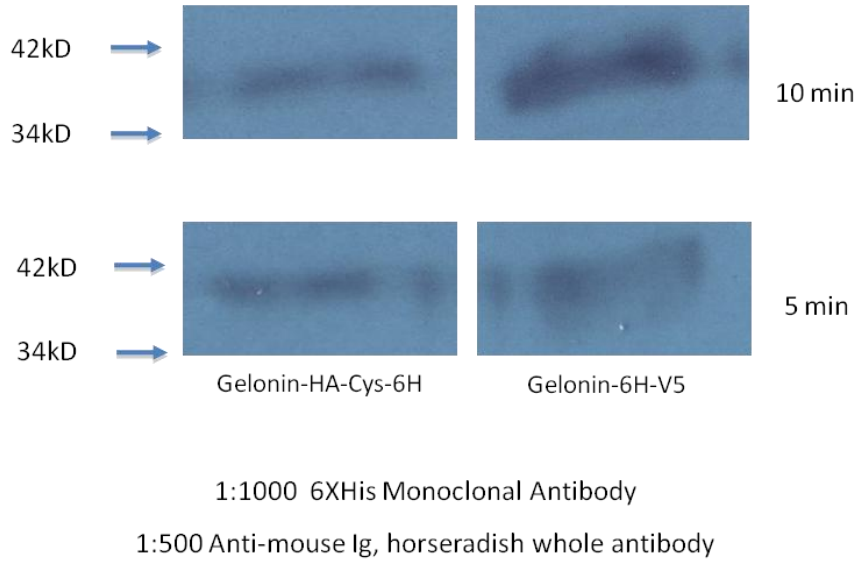

Figure 3.5. Western-immunoblotting of 6H-V5 Gelonin and Gelonin HA-Cys-V5.

Western-immunoblotting confirmed the predicted molecular weight of both the two protein synthesized (40 kDa for 6H-V5 Gelonin and 39 kDa for Gelonin HA-Cys-6H).

For large scale protein production, BL21(DE3) Competent E. coli bacteria were incubated in 2 litres of 2xYT(amp) medium and induced adding 1.5 M IPTG, which is used as a molecular mimic of allolactose, a lactose metabolite that triggers transcription of the *lac* operon[40,41].
Protein purification after cell lysis was achieved using a metal affinity resin complexed with cobalt ions that make it highly selective for polyhistidine-tagged proteins.

In vitro biological evaluation. It was first important to determine whether synthesis of 2-ethenyldithiopyridine bearing copolymers would increase PAA general cytotoxicity, thus making them unsuitable for their potential in vivo applications. Following incubation of the ISA1-SSPy and ISA23-SSPy polymers with B16F10 and Vero cells for 72 hours, all were found being as toxic as the parents ISA 1 and ISA23 homopolymers. The IC_{50} values observed for ISA1-SSPy were 1.5 mg/mL for Vero cells and 2.5 mg/mL for B16F10 cells, whereas for ISA23-SSPy were 5 mg/mL and >5 mg/mL for Vero and B16F10 cells, respectively (Figure 3.6). Dextran and PEI were used as non-toxic and toxic references (Figure 3.7).

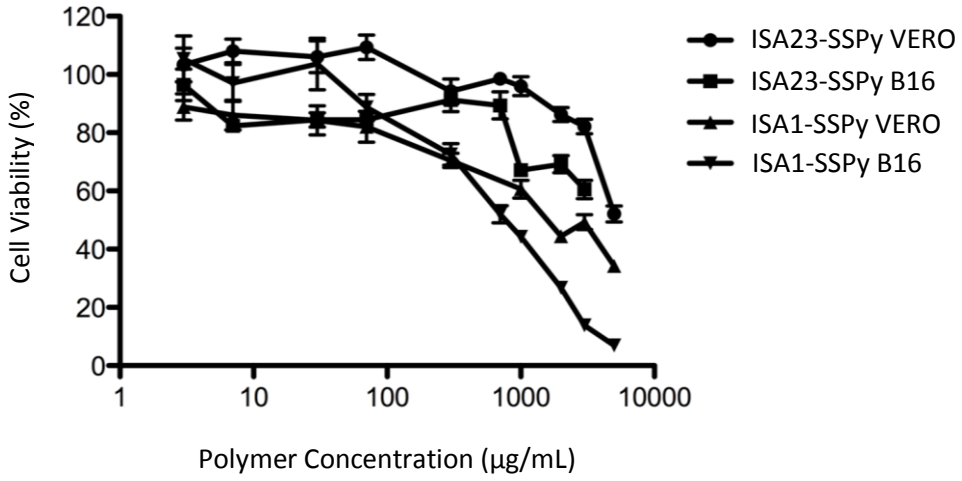

Figure 3.6. Cell viability of ISA1-SSPy and ISA23-SSPy on B16F10 and Vero cells.

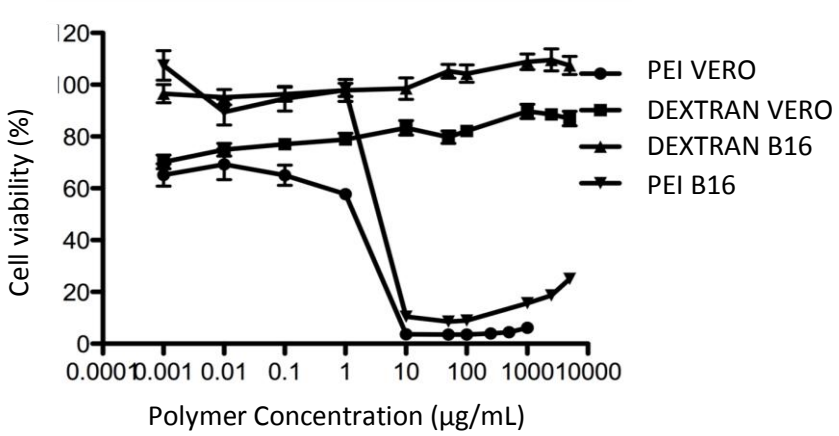

Figure 3.7. Cell viability of dextran and PEI on B16F10 and Vero cells.

To evaluate the ability of PAA-SSPy to mediate the intracellular delivery of Gelonin HA-Cys-6H and 6H-V5 Gelonin, toxin dose-response assay were carried out in order to establish a concentration of both proteins that would be completely non-toxic to B16F10 cells.

6H-V5 Gelonin displayed an IC_{50} value of 15 µg/mL, whereas for Gelonin HA-Cys-6H was 100 µg/mL as reported in Figure 3.8. These values are not unaxpected since gelonin lacks the cell binding domain promoting its internalization into cells and so it is not toxic It's noteworthy that the IC_{50} of Gelonin HA-Cys-6H was 10 times higher than that of 6H-V5 Gelonin. So far, we don't know how to explain this result.

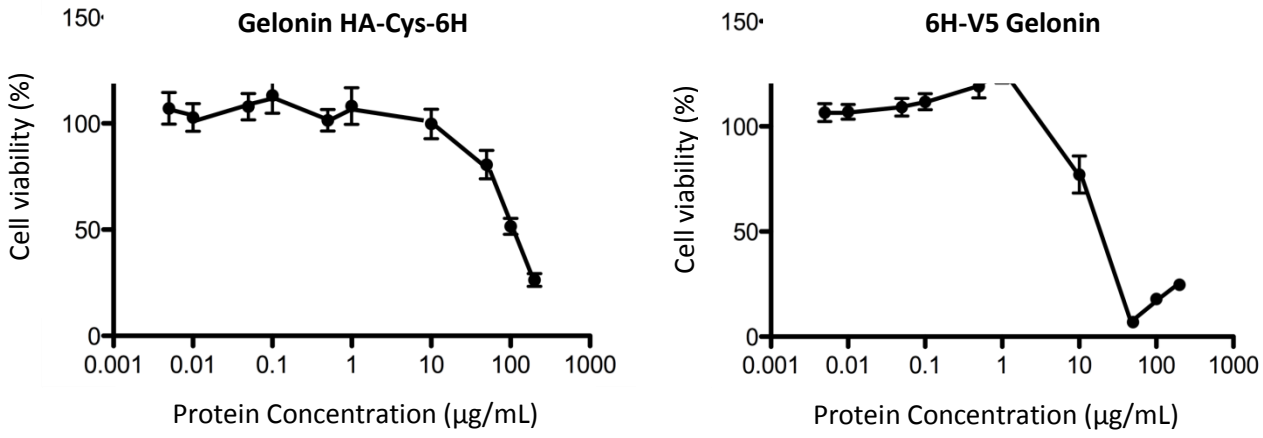

Figure 3.8. Cytotoxicity of toxins against B16F10 cells.

In all further experiments, non toxic concentrations of 6H-V5 Gelonin (1.4 μg/mL) and Gelonin HA-Cys-6H (1.4 μg/mL and 14 μg/mL) were used.

The conjugation of Gelonin HA-Cys-6H to ISA1-SSPy and ISA23-SSPy polymers via thiol-disulfide exchange reaction was performed directly in sterile culture medium for 24 hours. All samples were not ultrafiltred in order to elimite toxic reaction by-products (thiopyridine). The quantity of these products didn't cause any effective toxicity to cells due to their low amount.

Cytotoxicity experiments were performed using fixed concentration of protein and polymer up to 2 mg/mL. The same procedure was also used for dextran and PEI polymers. When incubated with B16F10 cells, the IC_{50} of ISA1-SSPy-6H-V5 Gelonin and ISA1-SSPy-Gelonin HA-Cys-V5 conjugates fell to 100 μg/mL. At increased concentration of Gelonin HA-Cys-6H (14 μg/mL) the IC_{50} observed was 10 μg/mL (Figure 3.9).

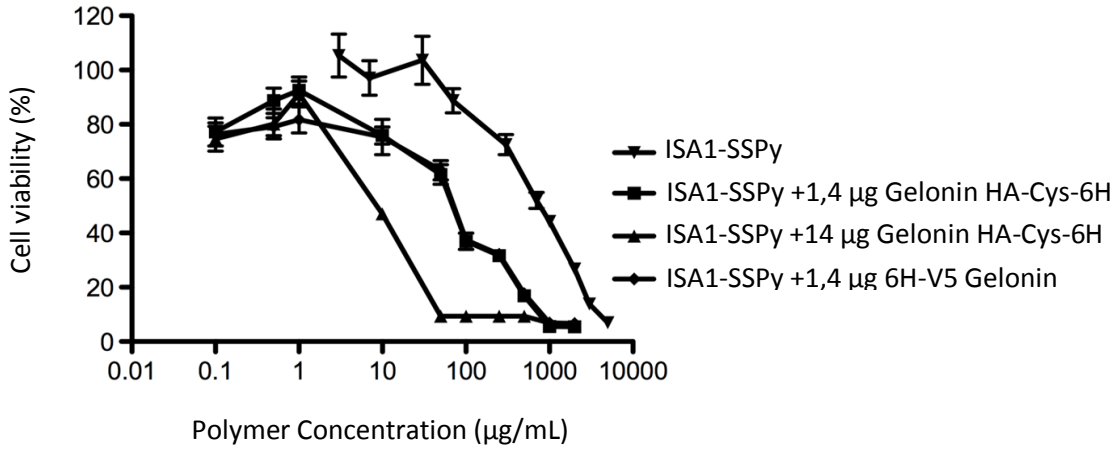

Figure 3.9. Cytotoxicity of ISA1-SSPy-Gelonin conjugates against B16F10 cells.

Like dextran, ISA23-SSPy was unable to mediate toxin delivery in the B16F10 cell line (Figure 3.10 and 3.11).

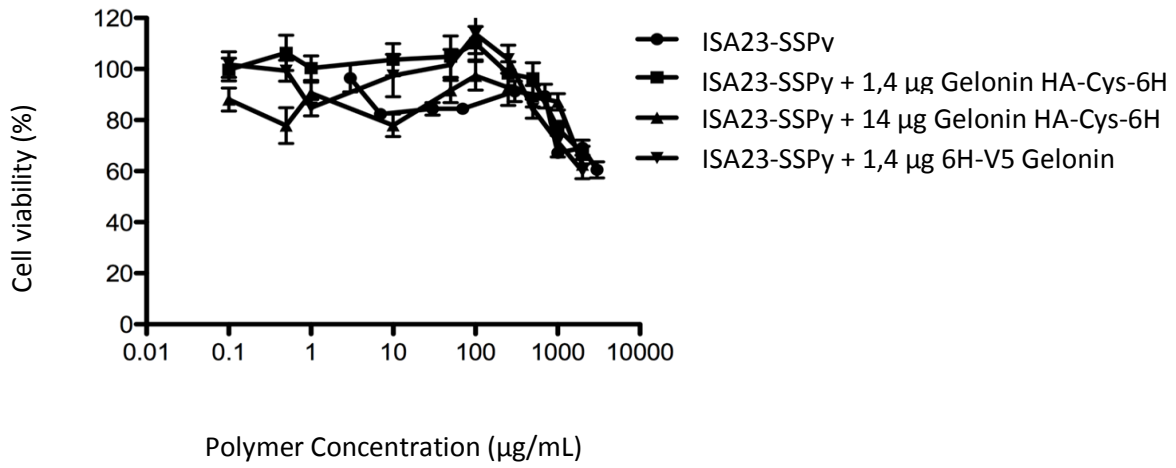

Figure 3.10. Cytotoxicity of ISA23-SSPy-Gelonin conjugates against B16F10 cells.

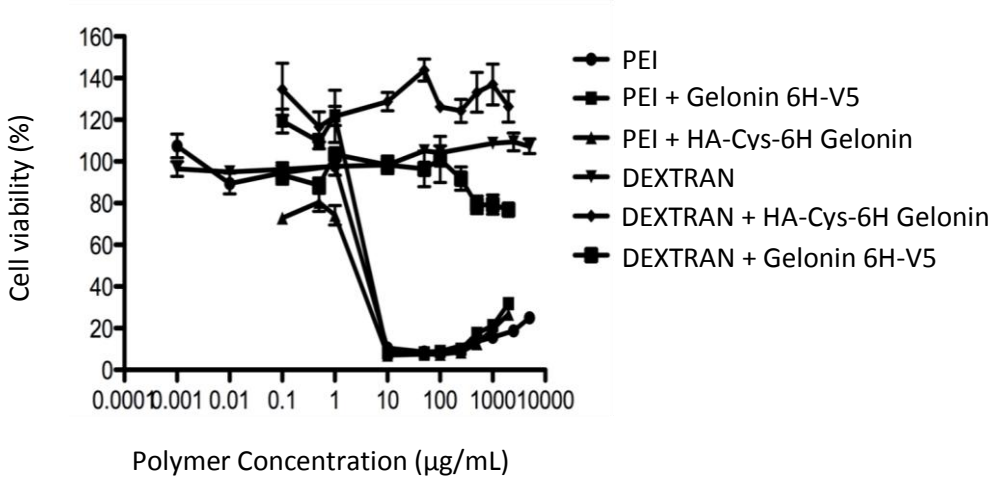

Figure 3.11. Cytotoxicity of Dextran and PEI with Gelonin toxins against B16F10 cells.

ISA1-SSPy promotes the intracytoplasmic delivery of gelonin more efficiently than the parent ISA1 with IC_{50} values 5-times higher for both types of toxins used. The results obtained for ISA1-SSPy-HA-Cys-6H, designed to have a covalent bond between the polymeric vector and the toxin, and ISA1-SSPy-6H-V5 Gelonin were the same, suggesting a non specific conjugation to the thiol groups in the Gelonin HA-Cys-6H.

These findings could be attributed both to the ability of ISA1-SSPy to react with protein's disulfide groups and to the interactions between the ethenyl-dithiopyridine pendants and the hydrophobic domains of the protein, giving stable complexes. It is important to note that in the previous experiment, ISA1 and gelonin were added to B16F10 cells as a mixture and not as a covalent conjugate.

The different ability of ISA1-SSPy and ISA23-SSPy to promote the delivery of the non permanent toxin gelonin is referred to their different intracellular trafficking pathway. ISA23-SSPy is amphoteric with a predominant anionic charge at physiological pH. Thus, they would be expected to enter cells by fluid-phase endocytosis. In contrast ISA1-SSPy is slightly cationic at physiological pH and, thus, would enter by both non-specific adsorptive and the fluid-phase mechanisms of endocytosis.

3.4 CONCLUSIONS

In this work ISA1 and ISA23 polymers bearing ethenyl-dithiopyridine pendants were investigated as intracytoplasmic vectors for the delivery of immunotoxins. Two different recombinant proteins were specifically synthesized: V5-6H Gelonin an Gelonin HA-Cys-6H. The latter proteins were engineered with a cysteine tag in order to covalently bind the polymeric vector via disulfide bound. ISA1-SSPy was effective for the delivery of both the two non-permanent protein whereas ISA23-SSPy wasn't. No differences in the IC_{50} of the two ISA1-SSPy-gelonin conjugates were observed, suggesting a non specific conjugation to the thiol groups in the Gelonin HA-Cys-6H. It's noteworthy that the linear and non-functionalized ISA1 polymer was less effective than the ISA1-SSPy, with an IC_{50} 5-times lower. This finding could be attributed both to the ability of ISA1-SSPy to react with protein's disulfide groups and to the interactions between the ethenyl-dithiopyridine pendants and the hydrophobic domains of the protein.

Further experiments are warranted to investigate the feasibility of using toxin-PAA-SSPy conjugates as therapeutics agents to target various cell types in vivo.

Further studies are needed to determine their mechanism of interaction and the stability.

References:

1. Herbert, A.R.; Arnold M. Seligman, M.D.; Jacob Fine, M.D. *N. Engl. J. Med.* **1952**, *247*, 921-929.
2. Jatzkewitz, H.; *Z. Naturforsch., B: Chem. Biochem.* **1955**, *10*, 27.
3. Davis, F.F. *Adv. Drug Deliv. Rev.* **2002**, *54*, 457-458.
4. Ringsdorf, H. *J. Polymer Sci. Polymer Symp.* **1975**, *51*, 135.
5. Duncan, R. *Nat. Rev. Drug Discov.* **2003***, 2, 214-221.*
6. Duncan, R. *Nature Review* **2006***, 6,* 688-701.
7. Vicent, M.J.; Duncan, R. *TRENDS in Biotechnology* **2006**, *24* (1), 39-47.
8. Matsumura, Y.; Maeda, H. *Cancer Res.* **1986**, *6*, 6387-63-92.
9. Levy H. *J. Pediatr.* **1988**, *113* (5), 908-912.
10. Graham, M.L. *Adv. Drug. Deliv. Rev.* **2003**, *55*, 1293-1302.
11. Iwai, K.; Maeda, H.; Konno, T. *Cancer Res.* **1984**, *44*, 2114-2121.
12. Molineux, G. *Curr. Pharm. Des.* **2004**, *10*, 1235-1244.
13. Reddy, K.R.; Modi, M.W.; Pedder, S. *Adv. Drug. Del. Rev.* **2002**, *54*, 571-586.
14. Wang, Y.S. *Adv. Drug. Del. Rev.* **2002**, *54*, 547-570.
15. Delman, K.A. *Proc. Am. Soc. Clin. Oncol.* **2002**, *96*, abstract 4139.
16. Unger C. *Proc. Am. Soc. Clin. Oncol.* **2005**, abstract 3130.
17. Fang, H.; Sawa, T.; Akaike, T.; Maeda, H. *Cancer Res.* **2002**, *62*, 3138-3143.
18. Griffiths, P.C.; Paul, A.; Khayat, Z.; Ka-Wai Wan; King, S.M.; Grillo, R.; Schweins, R.; Ferruti, P.; Franchini, J.; Duncan, R. *Biomacromolecules* **2004**, *5*, 1422-1427.
19. Richardson, S.C.W.; Pattrick, N.G.; Stella Man, Y.K.; Ferruti, P.; Duncan, R. *Biomacromolecules* **2001**, *2* (3), 1023-1028.
20. Pattrick, N.G.; Richardson, S.C.W.; Casolaro, M.; Ferruti, P.; Duncan, R. *J. Contr. Rel.* **2001**, *77*, 225.
21. Peumans, W.J.; Hao, Q.; Van Damme, E.J.M. *FASEB J.* **2001**, *15*, 1493-1506.
22. Ranucci, E.; Suardi, M.A.; Annunziata, R.; Ferruti, P.; Chiellini, F.; Bartoli, C. *Biomacromolecules* **2008**, *9*, 2693-2704.
23. Ranucci, E.; Ferruti, P.; Suardi, M.A.; Manfredi, A. *Macromol. Rapid Commun.* **2007**, *28*, 1243-1250.

24. Jordan, P.A.; Gibbins, J.M. *Antioxid Redox Signal* **2006**, *8*, 312-324.

25. Reynolds, A.; Laurie, C.; Mosley, R.L.; Gendelman, H.E. *Int. Rev. Neurobiol.* **2007**, *82 (2)*, 99-109.

26. Huber, W.W.; Parzefall, W. *Curr. Opin. Pharmacol.* **2007**, *7*, 404-409.

27. Wu, G.; Fang, Y.Z.; Yang, S.; Lupton, J.R.; Turner, N.D. *J. Nutr.* **2004**, *134*, 489-492.

28. Miller, P.F.; Vandome, A.F.; McBrewster, J. *Cytosol*, Alphascript Publishing, 2009.

29. Arpicco, S.; Dosio, F.; Brusa, P.; Crosasso, P.; Cattel, L. *Bioconjugate Chem* **1997**, *8*, 327-337.

30. Masuho, Y.; Kishida, K.; Saito, M.; Umemoto, N.; Hara, T. *J. Biochem.* **1982**, *91*, 1583-1591.

31. Miyata, K.; Kakizawa, Y.; Nishiyama, N.; Harada, A.; Yamasaki, Y.; Koyama, H.; Kataoka, K. *J. Am. Chem. Soc.* **2004**, *126*, 2355-2361.

32. Saito, G.; Swanson, J.A.; Lee, K.D. *Adv. Drug. Deliv. Rev.* **2003**, *55*, 199-215.

33. Lin, C.; Zhong, Z.; Lok, M.C.; Jiang, X.; Hennink, W.E.; Feijen, J.; Engbersen ,J.F.J. *J. Contr. Rel.* **2007**, *123*, 67-75.

34. Kwok, K.Y.; Park, Y.; Yang, Y.; McKenzie, D.L.; Liu, Y.; Rice, K.G. *J. Pharm. Sci.* 2003, *92* (6), 1174-1185.

35. Ferruti, P.; Ranucci, E.; Trotta, F.; Gianasi, E.; Evagorou, G.E.; Wasil, M.; Wilson, G.; Duncan, R. *Macromol. Chem. Phys.* **1999**, *200*, 1644-1654.

36. Ferruti, P. *Macromol. Synth.* **1985**, *9*, 25.

37. Lavignac, N.; Lazenby, M.; Foka, P.; Malgesini, B.; Verpilio, I.; Ferruti, P.; Duncan, R. *Macromol. Biosci.* **2004**, *4*, 922-929.

38. Ferruti, P.; Manzoni, S.; Richardson, S.C.W.; Duncan, R.; Pattrick, N.G.; Mendichi, R.; Casolaro, M. *Macromolecules* **2000**, *33*, 7793-7800.

39. Bulmus, V.; Woodward, M.; Lin, L.; Murthy, N.; Stayton, P.; Hoffman, A. *J. Contr. Rel.* **2003**, *93*, 105-120.

40. Singh, M.; Yadav, A.; Ma, X.; Amoah, E. *Int. J. of Biotechnology and Biochemistry.* **2010**, *6* (4), 561-568.

41. Baneyx, F. *Current opinion in Biotechnology.* **1999**, *10*, 40-46.

CHAPTER 4

TRICARBONYL-RHENIUM COMPLEXES OF A THIOL-FUNCTIONALIZED POLY(AMIDOAMINE) [1,17,29,31,32]

4.1 INTRODUCTION

Radiopharmaceuticals are molecules containing a radionuclide, and are used routinely in nuclear medicine for the diagnosis or therapy of various diseases (most often tumors)[1-5]. Depending on their medical applications, radiopharmaceuticals can be divided into two primary classes: diagnostics and therapeutics. Diagnostic radiopharmaceuticals are molecules labeled with γ-emitting isotopes for single photon emission computed tomography (SPECT) or positron-emitting isotopes for positron emission tomography (PET). In general, diagnostic radiopharmaceuticals are used at very low concentrations, in the range of 10^{-6} to 10^{-8} M, and are not intended to have any pharmacological effect. Diagnostic radiopharmaceuticals are predominantly metal complexes with an organic bifunctional chelator such as EDTA (ethylenediaminetetraacetic acid), DOTA (1,4,7,10-cyclododecyltetraacetic acid) and DTPA (diethylenetriaminepentaacetic acid) for metal-essential agents or a chelator-biomolecule conjugate for target-specific radiopharmaceuticals. They only provide a method of assessing the disease or disease states and monitoring effect of treatment[6-9]. Therapeutic radiopharmaceuticals are molecules designed to deliver therapeutic doses of ionizing radiation to specific disease site. Generally are α-, β- or Auger-electron emission radionuclide and their applications depend on the size of the tumor, intratumor distribution, pharmacokinetics of the tracer, etc[10,11].

Table 4.1. Selected β-particle emitting radionuclides with therapeutics potential.

Radionuclide	^{32}P	^{47}Sc	^{64}Cu	^{67}Cu	^{89}Sr	^{90}Y	^{105}Rh	^{111}Ag
$t_{1/2}$ (days)	14,3	3,4	0,5	2,6	50,5	2,7	1,5	7,5
max E_β (MeV)	1,71	0,6	0,57	0,57	1,46	2,27	0,57	1,05
γ-ray energy (MeV)		0,159 (68%)	0,511 (38%)	0,184 (38%)			0,319 (19%)	0,342 (6%)
				0,092 (23%)			0,306 (5%)	

Radionuclide	^{117m}Sn	^{131}I	^{149}Pm	^{153}Sm	^{166}Ho	^{177}Lu	^{186}Re	^{188}Re
$t_{1/2}$ (days)	13,6	8	2,2	1,9	1,1	6,7	3,8	0,7
max E_β (MeV)	0,13	0,81	1,07	0,8	1,6	0,5	1,07	2,11
γ-ray energy (MeV)	0,158 (87%)	0,364 (81%)	0,286 (3%)	0,103 (29%)	0,81 (6,33%)	0,113 (6,4%)	0,137 (9%)	0,155 (15%)
						0,208 (11%)		

Because of the constraints due to particle-emission properties such as half-life, specific activity, cost, and availability, only a limited number of radionuclides has been used to design radiopharmaceuticals for application in diagnosis and therapy. ^{131}I-sodium iodide for treatment of thyroid disorders, ^{32}P-phosphate for blood disorders, ^{32}P-sodium phosphate, ^{89}Sr-chloride, and ^{153}Sm-EDTA for pain control in metastatic bone disease, ^{131}I-mIBG for neuroendocrine tumors, and ^{90}Y- or ^{32}P-colloids or -microspheres for intracavitary and intraarterial delivery to tumors are some of the therapeutic radiopharmaceuticals that received FDA approval for routine use in humans and are available on a commercial basis[12-15]. ^{99m}Tc is commonly used for diagnosis procedures, due to its ideal physical properties and easy production from $Na_2{}^{99}MoO_4$ column generators[16].

Critical to the success of using radioactive agents for therapy and diagnosis is the development of compounds labeled with particle-emitting radionuclides that posses the following attributes, either alone or in combination[17]:

- demonstrated ability to in vivo target cancer cells selectively relative to normal cells;

- capability to achieve sufficiently high radioactivity concentration and distributions in the cellular matrixes of tumors to irradiate all cells;
- ability to achieve long-term residualization in the tumor for delivery of cytotoxic radiation doses to the tumor;
- capability to clear the radiolabeled drug or its radioactive metabolites efficiently from non-target tissues in order to minimize radiation-induced side effects.

Different approaches have been studied in order to satisfy these criteria. For the last decade, the direction of research in this area has been shifted towards developing site-directed therapeutic agents based on receptor binding of a radiolabeled receptor ligand in the diseased tissue. The high specificity of receptor binding results in selective uptake and distribution of the radiolabeled receptor ligand[18-23]. Many biomolecules, including monoclonal antibodies, antibody fragments and small peptides have been studied as carriers for radionuclide. While considerable efforts have been devoted to the development of this new class of radiopharmaceuticals, only a few have received approval by the FDA for routine use[24].

Recently, a combination of polymer chemistry and imaging science approaches has led to the generation of polymer-based constructs for the diagnosis and treatment of several diseases using fluorescent agents, quantum dots, paramagnetic contrast agent (usually Gd^{3+} and Mn^{2+}) and radionuclides. These new macromolecular entities take advantages of polymer therapeutics, which have unique pharmacokinetics properties, prolonged plasma half-lives, enhanced stability and targeting, reduced toxicity and preferential accumulation in lesion with blood vessels hypermeability, because of their large sizes (the so called “EPR effect”)[25,26]. An increasing number of biocompatible and water-soluble polymers, including dendrimers, branched, graft and block polymers of PEG and PLL is currently under development and some have already entered the clinical trials for application in MRI and nuclear medicine[27,28].

Based on this premise, we decided to investigate the possibility to design new polymeric radiopharmaceuticals using poly(amidoamine)s polymers (PAA)s and $[Re(CO)_3(H_2O)_3]^+$.

Rhenium has two radioisotopes of interest for nuclear medicine, and both have potential for cancer therapy and diagnosis: ^{186}Re (t½ = 3.7 d, γ = 137 keV, β^- = 1.07 MeV) and ^{188}Re (t½ = 16.94 h, γ = 155 keV, β^- = 2.12 MeV).

At variance with technetium, however, naturally occurring rhenium is in the form of two stable isotopes (^{185}Re and ^{187}Re), so that the preparation and the properties of candidate rhenium radiopharmaceuticals can be preliminarily investigated in cold laboratories. Moreover, due to the similar chemistry of Tc and Re, the non radioactive Re complexes can be used as models of Tc derivatives in preliminary studies aimed at developing novel imaging agents. Among the different species that have been tested for bioconjugation, the $[Re(CO)_3(H_2O)_3]^+$ complex has attracted significant attention, due to its fast preparation and versatile chemistry, arising from the presence of three labile water molecules bound to a stable *fac*-$Re(CO)_3^+$ core. Particularly attractive as polymeric ligand was the ISA23 polymer, which posseses stealth-like properties, prolonged permanence in the blood circle and has been demonstrated able to bind heavy metal ion such as Co, Ni and Cu and[29,30]. In particular we used a thiol-functionalized ISA23 polymer ($ISA23SH_{10\%}$), containing a 9:1 mixture of 2-methylpiperazine and cysteamine-deriving units, which appeared particularly suitable to coordinate *fac*-$Re(CO)_3^+$ fragments, due to the presence of chelating 2-aminoethanethiol loops, which are known to act as good ligands of rhenium or technetium complexes[31,32]. Many articles in literature report the direct labeling of $^{186/188}$Re to thiol-containing proteins and peptides[33].

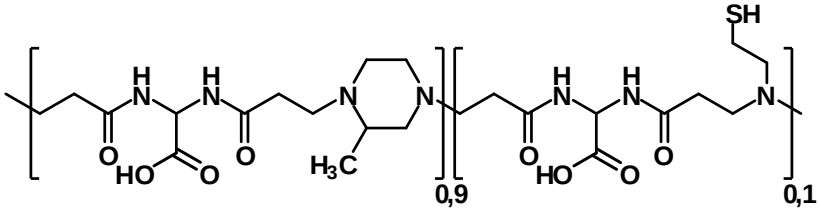

Figure 4.1: Structure of the thiol-functionalized amphoteric ISA23

Two different PAA-Rhenium complexes, complex 1 containing 0.5 equivalent of Re and complex 2 containing 0.8 equivalent, have been obtained and fully characterized by analytical and spectroscopic techniques. Preliminary in vitro and in vivo studies are also reported.

4.2 EXPERIMENTAL PART

Instruments

NMR experiments were performed on a DRX400 Bruker spectrometer (operating at 400.13, 100.62 and 40.55 MHz for ^{1}H, ^{13}C and ^{15}N, respectively), equipped with a Bruker 5-mm BBI Z-gradient probe-head, capable of producing gradients with a strength of 53.5 G/cm. ^{15}N spectra were referred to external CH_3NO_2. All spectra were acquired at room temperature using standard 1D and 2D NMR experiments, on samples typically containing 15-30 mg of lyophilized samples dissolved in 500 μl of D_2O (or of a D_2O/H_2O 1/9 mixture, to identify the NH protons). The π/2 pulse lengths were 6.9 μs (^{1}H), 9.25 μs (^{13}C) and 31.0 μs (^{15}N).

2D ^{1}H-^{13}C and ^{1}H-^{15}N HMBC (Heteronuclear Multiple Bond Correlation) and HSQC (Heteronuclear Single Quantum Coherence) NMR experiments were typically recorded with 2048 data points in ^{1}H dimension, 128-512 increments in the heteronuclei dimension and 32-512 transients per increment; $^{1}J_{HC}$ = 145, $^{n}J_{HC}$ = 10, $^{1}J_{HN}$ = 88 and $^{n}J_{HN}$ = 8 Hz were used.

IR spectra were acquired on a Bruker Vector 22 FT instrument, using 0.1 mm CaF_2 cells.

Microwave assisted reactions were performed using a Milestone MicroSYNTH instrument.

Ultracentrifugations were performed on a Beckman J2-21centrifuge, equipped with a JA-20 35° fixed angle rotor, using Amicon® Ultra-4 or Centricon® centrifugal filter devices (Millipore) with 3000 Nominal Molecular Weight Limit membranes. The solutions were diluted up to 1:10 and centrifugation processes were repeated until the IR spectrum of the filtrate did not show any absorption attributable to $Re(CO)_3$ fragments. Due to its high dilution, the filtrate was normally evaporated in vacuum and dissolved in a very small volume of water (100 μl), to better detect the possible presence of carbonyl IR bands.

In larger preparations, it has been shown that the centrifugation process can be substituted by ultrafiltration using an Amicon® apparatus through a membrane with a 3000 nominal cut off.

The rhenium content in complexes 1 and 2 was determined directly on aqueous solutions of the complexes (5 mg in 10 mL of water), with an IRIS Intrepid TJA Inductively Coupled Plasma spectrophotometer, with TEVA software, using the Re atomic emission lines at 221.4, 227.5 and 346.0 nm, and standard solution at 1000 ppm from Fluka.

The complex morphology was determined by Transmission Electron Microscopy (TEM). TEM analysis was carried out using a Philips CM10 instrument. The rhenium complexes 1 and 2 in aqueous solution were spread onto a Formwar-coated copper grid and air-dried before observation.

Dynamic light scattering measurements were recorded using a 90 Plus instrument (Brookhaven, NY) at a fixed angle of 90° and a temperature of 25 °C. Samples were prepared by dispersing the freeze-dried complexes in filtered water (1 mg/mL) and diluting before analysis.

Size exclusion chromatography (SEC) traces were obtained with Toso-Haas TSK-gel G4000 PW and TSK-gel G3000 PW columns connected in series, using a Waters model 515 HPLC pump equipped with a Knauer Autosampler 3800, a Light Scattering Viscotek 270 Dual Detector, UV detector Waters model 486, operating at 230 nm, and a refractive index detector Waters model 2410. The mobile phase was a 0.1 M Tris buffer pH 8.00 ± 0.05 with 0.2 M sodium chloride. The flow rate was 1 mL/min and sample concentration 1% w/w solutions.

Materials and methods

Analytical grade HPLC solvents were purchased from Fluka and used as received for the synthesis of the polymers. The organic solvents used in the syntheses of the organometallic complexes were purified by standard methods. Ultrapure water (Milli-Q, Millipore, resistivity 18 $M\Omega cm^{-2}$) was used for the preparation of the aqueous solutions. D_2O (99.9%) was purchased from Aldrich and used as received. Triethylamine, purchased from Fluka, was distilled over calcium hydride.

Potassium phosphate monobasic was purchased from Carlo Erba and used as received.

2-Methylpiperazine was purchased from Fluka and used after sublimation. Its final purity (98%) was determined with acidimetric titration. Thin layer chromatography (TLC) was performed using Macherey-Nagel Alugram SIL G/UV254.

2,2-Bis(acrylamido)acetic acid (BAC) was prepared as reported in literature[34] and purity (98%) determined by NMR spectroscopy and titration. $Re_2(CO)_{10}$ was purchased by Sigma-Aldrich and used as received. $Re(CO)_5Br$,[35] $Re(CO)_5(CF_3SO_3)$,[36] and $[Re_4(CO)_{12}(\mu_3\text{-}OH)_4]$[37,38] were synthesized according to literature procedures. For the synthesis of $[Re(CO)_3(H_2O)_3](CF_3SO_3)$ a literature method[39] was used, slightly modified by addition of a small amount of CF_3SO_3H.

N-tert-Butyloxycarbonyl Cystamine Hydrochloride (Cyst-mBoc·HCl).[40] Triethylamine (2.696 g; 26.65 mmol) was added to a dry methanol solution (100 mL) of cystamine bis-hydrochloride (2.00 g; 8.88 mmol), and the solution stirred for 15 minutes at room temperature. Di-tert-butyldicarbonate (1.941 g; 8.88 mmol) was added and the stirring maintained for an additional 2.5 hours, monitoring the reaction progress by TLC (SiO_2, eluent: chloroform/isopropyl alcohol 1:1, Rf product=0.25). The solvent was then evaporated, and a 1 M KH_2PO_4 aqueous solution (60 mL, pH 4.2) was added. The aqueous phase was extracted with diethyl ether (50 mL) to remove di-N,N'-tert-butyloxycarbonyl cystamine, then brought to pH 9 with 1 M NaOH, and extracted with ethyl acetate (6x15 mL). The combined organic phases were dried (Na_2SO_4) and evaporated to dryness. The residue was dissolved in water at pH≥4 (HCl). The clear solution obtained was freeze-dried and N-tert-butyloxycarbonyl-cystamine isolated as hydrochloride. Yield: 1.03 g (40%). ^{1}H NMR (D_2O): δ= 3.31–3.21 (m, 4H, NH_3^+-C***H₂*** and CONH-C***H₂***), 2.83 (t, $^3J_{3,2}$=6.40 Hz, 2H, C***H₂***-S), 2.72 (t, $^3J_{2,3}$= 6.40 Hz, 2H, C***H₂***-S), 1.30 (s, 9H, Boc C***H₃***). ESI-MS: *m/z*=253 (M+1), as free base.

Synthesis of the copolymer ISA23-Cyst-mBoc[41]. BAC (2.076 g; 0.010 mol) and potassium carbonate (1.402 g; 0.010 mol) were dissolved in water (3.4 mL).

Nitrogen was flushed through the reaction mixture for 10 minutes to eliminate all CO_2 produced. When the reaction mixture became clear, Cyst-mBoc·HCl (0.295 g; 0.001 mol) and potassium carbonate (0.150 g; 0.001 mmol) were added. The reaction mixture was then continuously stirred for 24 hours and afterward 2-methylpiperazine (0.931g; 0.009 mol) was added. The solution was maintained for 24 hours at 20 °C under nitrogen atmosphere and with occasional stirring. After this period, the crude reaction mixture was diluted to 300 mL with distilled water, acidified to pH 2.5 with 37% hydrochloric acid and purified by ultrafiltration through a membrane with a nominal cut-off of 5000. The portion retained was recovered by lyophilization. Yield: 1.72 g (45.6%). ^{1}H NMR (D_2O): δ= 5.45 (m, 1H, C***H***-COOH); 3.46-3.21 (b, 2H, C***H₂***-N polymer backbone and piperazine ring); 3.00 (b, 2H, C***H₂*** piperazine ring); 2.79 (b, 2H, CO-C***H₂***); 2.77 (b, 2H, S-C***H₂***); 1.34 (s, 9H, Boc C***H₃***); 1.25 (s, 3H, C***H₃*** piperazine). Molecular weight values: $\overline{M}_n$ =19000, $\overline{M}_w$ =34000, PD=1.8. Content of the disulphide-containing units: 9.85% on a molar basis, determined by NMR.

Synthesis of the co-polymer ISA23SH$_{10\%}$[41]. ISA23-Cyst-mBoc (1.0 g; 0.31 mmol disulfide groups from ^{1}H NMR data) was dissolved in degassed water (30 mL) at pH 8, adjusted by adding a few microliters of NaOH (1.00 N Sigma Aldrich, volumetric standard). 1,4-dithio-D,L-threitol (0.481 g; 3.09 mmol) was then added. The reaction mixture was stirred for 15 hours at room temperature, then diluted with water and ultrafiltered through a membrane with molecular weight cut-off 3000 and eventually freeze-dried. Yield: 0.795 g (79.5%). The NMR spectrum turned to be superimposable to that of ISA23-Cyst-mBoc, apart from the absence of the tert-boc protecting group. Therefore, the content of the sulphidryl-containing units was assumed equal to that of the disulphide units present in the parent polymer. Molecular weight values: $\overline{M}_n$ =10100, $\overline{M}_w$ =17100, PD=1.7. Elemental analysis: Found= C, 46.87; H, 8.05; N, 16.80; S, 0.87% (calculated for $(C_{13}H_{22}N_4O_4)_{0.9015}(C_{10}H_{17}N_3O_4S)_{0.0985}\cdot 1.5H_2O$ = C, 47.23; H, 7.65; N, 16.91; S, 0.98); Found = N/C, 0.358; S/C, 0.019 (calculated = N/C, 0.358; S/C, 0.021).

Reaction between ISA23SH$_{10\%}$ and [Re(CO)$_3$(H$_2$O)$_3$](CF$_3$SO$_3$). A sample (17.7 mg) of the co-polymer ISA23SH$_{10\%}$ (effective cysteamine unit = 9.85%) was dissolved in 1.2 mL of water and treated with 30 μL of a 0.1 M solution of $[Re(CO)_3(H_2O)_3]^+$, leading to a 2.5 mM rhenium concentration. The pH was adjusted to 5.5 by NaOH addition and the solution was heated at 80°C for 15 minutes. The IR spectrum showed that the ν_{CO} bands of the starting material (2037s, 1916vs cm^{-1}) were replaced by new ν_{CO} bands (2011sh, 2004s, 1909vs cm^{-1}), attributable to complex 1. After centrifugation (3000 cut-off filter, 7000 rpm, 25°C for 20 minutes) the IR spectrum of the retained fraction showed the ν_{CO} bands of 1, while no CO bands were present in the IR spectrum of the filtrate. The retained fraction was lyophilized, affording a very fine white powder, used for NMR and ICP analyses. Elemental analysis: Found = C, 42.56; H, 7.95; N, 15.17; S, 0.79; Re, 2.8% (calculated for $(C_{13}H_{22}N_4O_4)_{0.9015}(C_{10}H_{15}N_3O_4S)_{0.0985}(C_3O_3Re)_{0.04925}\cdot 3H_2O$ = C, 42.50; H, 7.58; N, 15.04; S, 0.87); Found = N/C, 0.356; S/C, 0.019 (calculated = N/C, 0.354; S/C, 0.020).

An analogous procedure was used for the reaction with 1 equivalent of $[Re(CO)_3(H_2O)_3]^+$, that afforded complex 2 in 30 minutes at 80°C. Longer reaction times did not cause any spectral changes of the reaction mixture. Elemental analysis indicated the presence of 0.85 equivalent of rhenium per thiol group: Found = C, 41.08; H, 7.31; N, 14.44; S, 0.74; Re, 4.2% (calcolated for $(C_{13}H_{22}N_4O_4)_{0.9015}(C_{10}H_{15}N_3O_4S)_{0.0985}(C_3O_3Re)_{0.0837}\cdot 3H_2O$ = C, 41.77; H, 7.39; N, 14.67; S, 0.85); Found = N/C, 0.352; S/C, 0.018 (calculated = N/C, 0.351; S/C, 0.020).

Microwave synthesis of complex 1. A sample of ISA23SH$_{10\%}$ (30.1 mg) dissolved in 2 mL of water was treated with 50 μL of a 0.1 M solution of $[Re(CO)_3(H_2O)_3](CF_3SO_3)$, leading to a 2.5 mM rhenium concentration, in an open glass vessel, under N_2 atmosphere. After adjusting the pH value to 5.2, the mixture was exposed to microwave radiation, at 500 W for 20 seconds to reach 80°C, then at 100 W for 2 minutes, while the temperature was maintained constant at 80°C. The IR spectrum showed the replacement of ν_{CO} bands of the starting material with those of complex 1.

Centrifugation, as above described, and IR spectra of retained fraction and filtrate confirmed the occurrence of the interaction. The reaction was repeated at a lower concentration, using 10.5 mg of $ISA23SH_{10\%}$, dissolved in 70 mL of water, and 17.5 μL of a 0.1 M solution of $[Re(CO)_3(H_2O)_3](CF_3SO_3)$, leading to a $2.5x10^{-5}$ M rhenium concentration. The pH of the solution was 5.5. The mixture was exposed to microwave radiation, at 500 W for 1 minute to reach 80°C, then at 100 W for 30 minutes, while the temperature was maintained constant at 80°C. The solution was centrifuged, as above, and IR spectra of both the retained fraction and the filtrate were recorded, showing the formation of complex 1.

Stability of complexes 1 and 2 in physiological conditions. A sample of complex 1 (10.0 mg) was dissolved in 10 mL of a 0.9% w/v NaCl solution, at pH 7.4, affording a 0.15 mM solution (referred to the rhenium concentration). The solution was maintained at 25°C for 36 hours, and then centrifuged. No ν_{CO} bands were observed in the IR spectrum of the filtrate, while the retained fraction showed the bands of the starting complex, confirming that rhenium coordination to the polymer had been maintained. The experiment was repeated in the same conditions with complex 2, obtaining the same results. Moreover, stability of complex 1 was ascertained in much more diluted conditions ($4x10^{-5}$ M) at 37 °C, for 30 hours.

Stability of complexes 1 and 2 in the presence of cysteine. A sample of complex 1 (15.0 mg) was dissolved in 0.75 mL of water (affording a 3 mM solution, referred to the rhenium concentration) and treated with 0.73 mL of a 6.6 mM solution of cysteine (0.0048 mmol). The pH was adjusted to 7.4 and the solution was maintained at room temperature for 24 hours, and then centrifuged. No ν_{CO} bands were observed in the IR spectrum of the filtrate, while the retained fraction showed the bands of the starting complex. The experiment was repeated in the same conditions with complex 2, obtaining the same results.

In vitro biological evaluation

Hemolytic activity. The hemolytic activity of the rhenium complexes 1 and 2 was evaluated on human blood. Different quantities of the two complexes were added to a suspension of erythrocytes (30% v/v) in phosphate buffer pH 7.4 to give the following final concentrations: 1.2, 2.0, 3.0, 4.5 and 5.5 mg/mL. A suspension (30% v/v) of erythrocytes in phosphate buffer pH 7.4 was used as blank. Another erythrocyte suspension added with an excess of ammonium chloride was used to obtain complete hemolysis of erythrocytes as 100% hemolytic control. After 90 minutes of incubation at 37 °C all the samples were centrifuged at 2000 rpm for 10 minutes and the supernatants were analyzed using a Lambda 2 Perkin-Elmer spectrophotometer at a wavelength of 543 nm. The percentage of hemolysis was calculated versus the 100% hemolysis control.

Cytotoxicity and biocompatibility determination. The in vitro cytotoxicity of the rhenium complexes was evaluated on Hela cells using the MTT test. To test the effect of complexes on cell viability, Hela cells were seeded at a density of $5x10^2$ in 96-well plates in RPMI-1640 supplemented with 10% of serum (200 μL). The cells were allowed to attach for 72 hours, and seeding medium was removed and replaced by experimental medium supplemented with two different rhenium concentrations (50 ng/mL and 100 ng/mL). $ISA23SH_{10\%}$ and the parent tricarbonyl rhenium complex $[Re(CO)_3(H_2O)_3](CF_3SO_3)$ were used as negative controls at the same concentrations. After 48 hours cell viability was determined by Microplate Reader model 450 at 560 nm. The effect on cell viability of each complex at different concentrations was expressed as a percentage, by comparing treated cells with cells incubated with culture medium alone (untreated cells). For the assay, the experiments were performed in triplicate.

In vivo biological evaluation

Acute toxicity was determined in mice according to standard protocols by INTOX company (India). Preliminary in vivo experiments were performed on 6-10 weeks old mice (CD1, Charles River) to evaluate the biocompatibility of the two complexes. Volumes (100 or 200 μL) of 2 mg/mL aqueous solution of each rhenium complex were administered intravenously in three mice. The animals were daily controlled for 15 days to observe possible signs of toxicity.

The animal experiments complied with the rules set forth in the NIH Guide for the Care and Use of Laboratory Animals.

4.3 RESULTS AND DISCUSSIONS

In this work, $[Re(CO)_3(H_2O)_3]^+$ complex was chosen as starting reagent for obtaining the PAA-rhenium complexes, due to its versatility and ease of the preparation methods[34,42,43], some of which suitable for preparing radioactive derivatives containing the $^{186,188}Re$ isotopes[44,45]. A literature method which involves refluxing for 1 hour $[Re(CO)_5OTf]$ (OTf = CF_3SO_3) in water was attempted[39]. However, in our experiments this procedure always afforded $[Re(CO)_3(H_2O)_3]OTf$ contaminated by the "cubane-like" tetranuclear complex $[Re_4(CO)_{12}(\mu_3\text{-}OH)_4]$[37,38] (ca. 20% from the IR data). A slight modification, which consisted in adding to the starting solution a few microliters of CF_3SO_3H (up to pH 2), to depress the formation of neutral "$Re(CO)_3(OH)$" fragments, gave $[Re(CO)_3(H_2O)_3]^+$ in substantially quantitative yields.

As polymeric ligand we used a thiol-functionalized amphoteric ISA23 co-polymer, constituted by a piperazine majority part, with a minority component bearing cysteamine-deriving fragment, suited to chelate metal centers such as the $Re(CO_3)^+$. The strategy adopted consist of a two step synthesis: first a ISA23-Cyst-mBoc was synthesized using 10% on a molar basis of N-tert-butyloxycarbonyl-cystamine as co-monomer.

In fact, cystamine having two primary amine groups, reacted in polyaddition reaction as tetra-functional monomer, thus generating a hydrophilic insoluble tri-dimensional network. In the second step the disulphide bond was reduced using DTT giving the finally thiol-containing ISA23 co-polymers as reported in scheme 4.1.

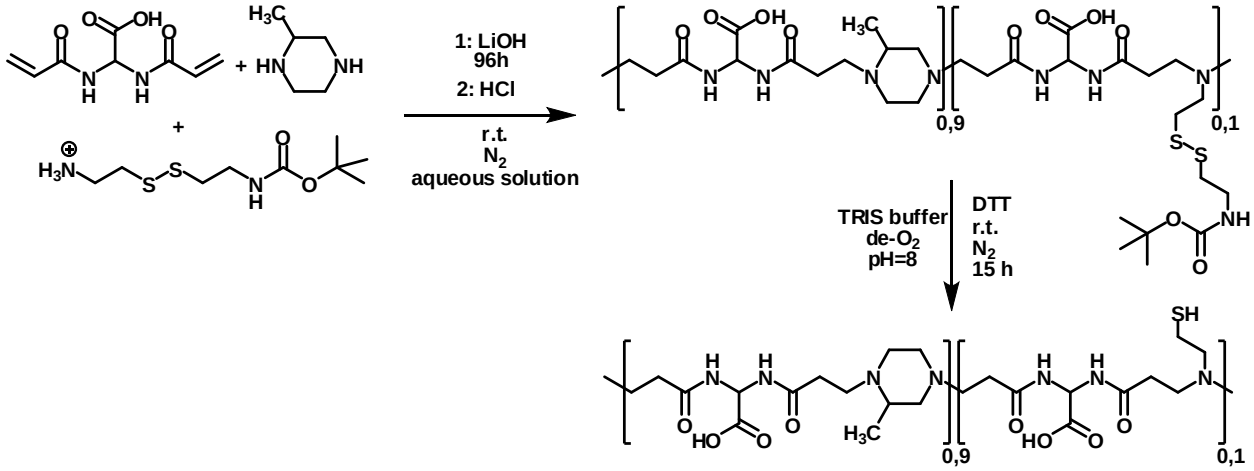

Scheme 4.1. Synthetic pathway leading to ISA23$_{10\%}$.

The reactions between ISA23SH$_{10\%}$ and $[Re(CO)_3(H_2O)_3]^+$ were monitored by IR spectroscopy. Indeed, the CO stretching absorptions (ν_{CO}) are strong and sensitive to the coordination environment.

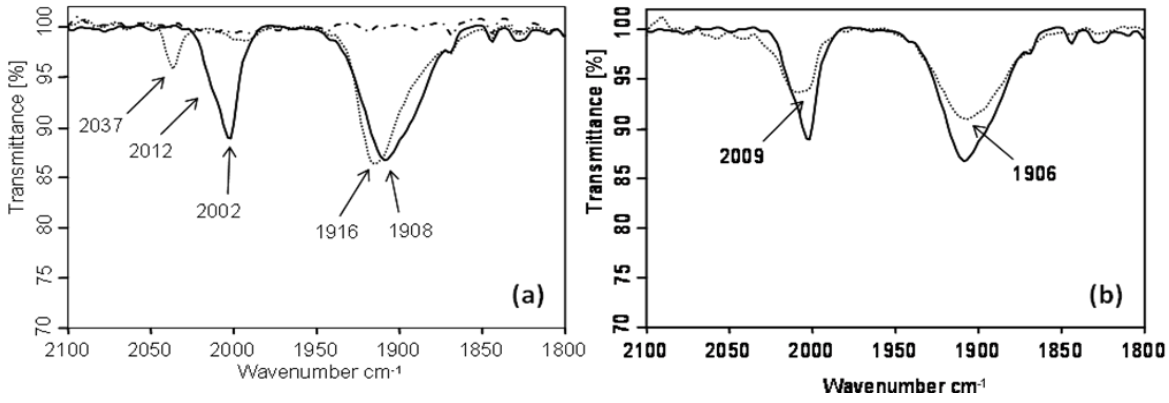

Figure 4.2. FTIR spectra in the ν_{CO} region in H_2O solution of (a) complex 1 (—), the starting material $[Re(CO)_3(H_2O)_3]^+$ (····), and the filtrate after ultracentrifugation (·-·-) and (b) complex 1 (—) and complex 2 (····).

The IR spectrum of a 5 mM water solution of $ISA23SH_{10\%}$ treated with 0.5 equiv of $[Re(CO)_3(H_2O)_3]^+$ (pH 5.5, 80 °C) showed the appearance of two new broad ν_{CO} bands peaking at 2002 and 1908 cm^{-1} with a shoulder at 2012 cm^{-1}, shifted to lower frequencies with respect to those of the starting tris-aquo complex (2037 and 1916 cm^{-1}) as reported in figure 4.2. The reaction was complete in 15 minutes, as ascertained by the IR data and by the lack of ν_{CO} bands in the filtrate, obtained by ultracentrifugation with a 3000 cutoff filter, to eliminate all rhenium complexes not bound to the polymer. The portion retained from the centrifugation was then freeze-dried, affording a white powder (complex 1) containing 2.8% w/w of Re, as shown by ICP analysis. The reaction time was further reduced to 2 minutes by using microwave heating, which is in agreement with a recent report on the microwave syntheses of $[Re(CO)_3(H_2O)_3]^+$ and its bioconjugates[46]. The reaction with 0.5 equivalent of rhenium per thiol was found to be effective even down to $2.5x10^{-5}$ M rhenium concentration. In this case, the reaction time at 80 °C was 3 hours, reduced to 30 minutes by microwave heating. A complex 2 with a higher rhenium content (4.2% w/w) was obtained by an analogous procedure on treating the copolymer $ISA23SH_{10\%}$ with 1 equivalent of $[Re(CO)_3(H_2O)_3]^+$ per thiol (pH 5.5, 30 minutes at 80 °C, ν_{CO} at 2009 and 1906 cm^{-1}, Figure 4.2(b)). Both complexes were completely stable after 36 hours of incubation (a time fully consistent with the half life of the ^{99m}Tc and ^{188}Re radioisotopes) under physiological conditions (pH 7.4 and 0.9% w/v NaCl) at a 10^{-4} M concentration. The IR spectrum of the filtrate did not show any metal-carbonyl stretching bands, whereas the IR spectrum of the retained portion was identical to that of the complexes before the incubation. The same complexes were also stable for 18 hours in the presence of cysteine, a potential in vivo ubiquitous competitor for the metal coordination.

Nuclear magnetic resonance characterization. A detailed multinuclear (^1H, ^{13}C, and ^{15}N) NMR characterization of the copolymer $ISA23SH_{10\%}$ and of its complex with 0.5 equivalent of rhenium per thiol (complex 1) was undertaken in collaboration with Prof. D'Alfonso and co-workers.

This study was performed with the aim of obtaining information on which of the potential binding sites present in the polymer (SH, COOH, and amines) was actually involved in rhenium coordination. The rhenium content of complex 1 is already adequate for biological applications, and subsequent work was mainly focused on it.

Typical ^{1}H and $\{^{1}H\}^{13}C$ NMR spectra at pH 3.5 are reported in Figures 4.3 and 4.4, respectively, whereas the attributions are referred to the labels in Table 4.2.

Table 4.2. ^{1}H, ^{13}C and ^{15}N chemical shift (ppm) of the free polymer ISA23SH$_{10\%}$ at pH 3,5.

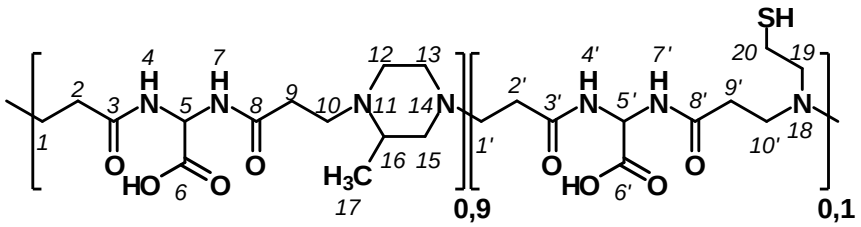

δ	1(1')	2(2')	3(3')	4(4')	5(5')	6(6')	7(7')	8(8')	9(9')	10(10')
^{1}H	3,50	2,65		8,69	5,48		8,76		2,61	3,1
	3,13	(2,80)							(2,80)	(2,60)
	(3,46)									
^{13}C	48,19	29,90	171,88		58,26	173,05		172,4	30,65	52,36
	(28,72)	(48,89)	(171,29)						(28,72)	
^{15}N				-249,8			-248,9			

δ	11	12	13	14	15	16	17	18	19	20
^{1}H		3,47	3,31		3,29	3,31	1,28		3,36	2,9
		3,08	2,88			2,71				2,82
^{13}C		48,81	49,58		56,17	55,43	14,00		56,07	18,50
^{15}N	-333,7			-324,7				-328,5		

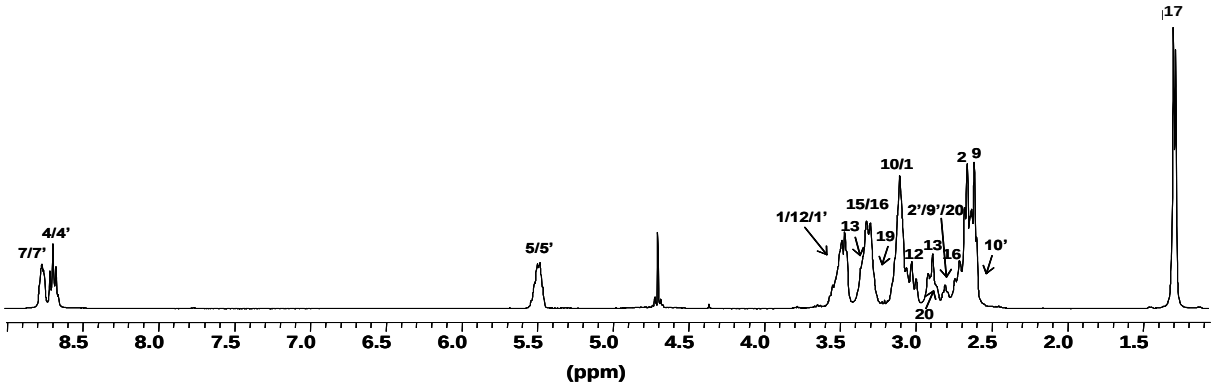

Figure 4.3. ^{1}H NMR spectrum of the free polymer ISA23SH$_{10\%}$.

The resonances of the thiol-bearing units were hardly detectable in the spectra, being weak and largely overlapped with those of the major constituents. However, the proton spectra in Figure 4.3 showed, in the narrow gap between the multiplets of methylenes 13 and 16, a group of signals that by heterocorrelation experiments were assigned to the protons in the sites 2′, 9′, and 20. The corresponding carbon resonances were also detectable in the ^{13}C spectra, together with those of carbons 1′ and 3′ (Figure 4.4).

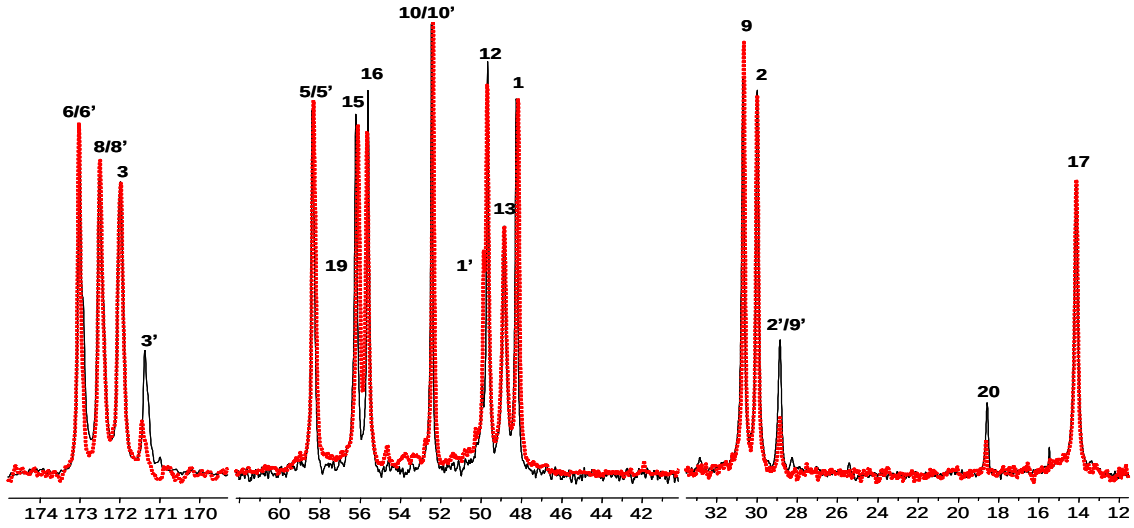

Figure 4.4. ^{13}C NMR spectra of ISASH23$_{10\%}$ (red dotted line) and ISA23$_{20\%}$ (black line).

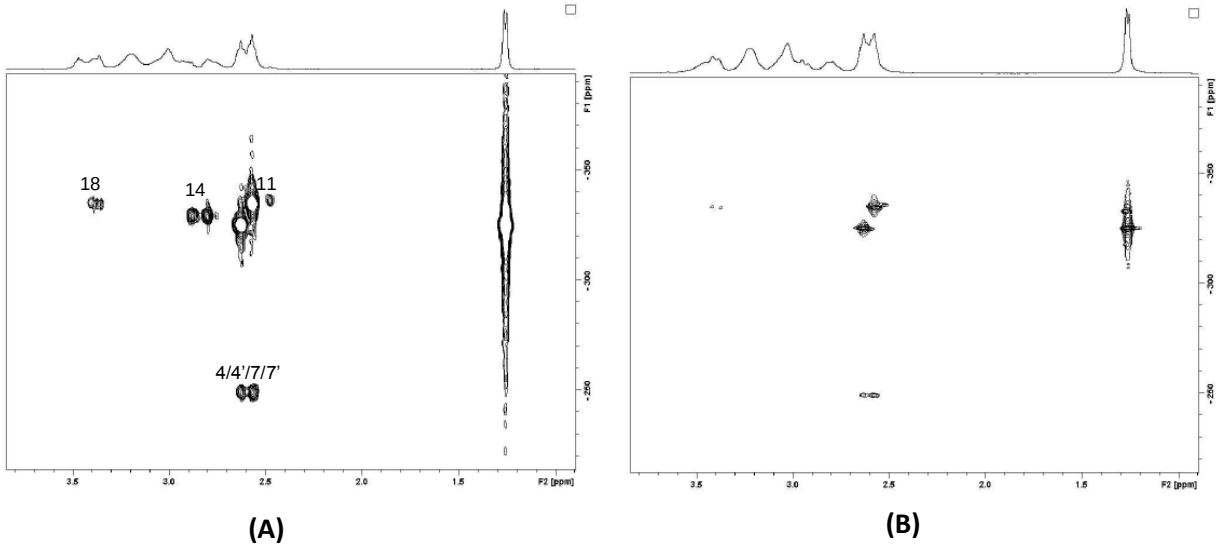

Figure 4.5. ^{1}H-^{15}N HMBC of ISA23SH10% (A) and complex 1(B).

The attribution of these signals to the thiol-bearing portion is well supported by the comparison with the spectra of the analogous copolymer with a double percentage of SH ($ISA23SH_{20\%}$). The ^{15}N signals of the amide groups N4′ and N7′ were also overlapped with the corresponding signals N4 and N7 of the majority part, whereas the signal of the cysteamine N18 was detected at -328.5 ppm as shown in Figure 4.5-A. The ^{1}H and $\{^{1}H\}^{13}C$ spectra of the complex 1 showed only minimal variations with respect to those of the parent polymer. However, these variations had a diagnostic value because they specifically involved the resolved signals of the thiol-bearing units, as apparent in the ^{13}C spectrum reported in Figure 4.6. The most significant change, besides the broadening of the ^{13}C signals 2′, 3′, and 9′, was the disappearance of the signal at 18.5 ppm due to carbon atom α to SH group (C20).

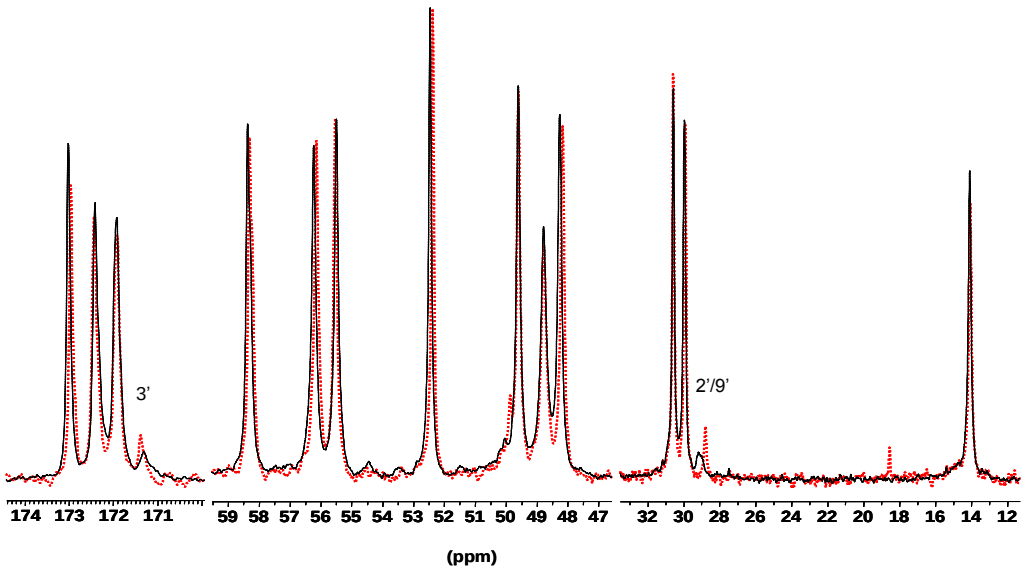

Figure 4.6. ^{13}C NMR spectra of $ISA23SH_{10\%}$ (red dotted line) and complex 1 (black trace).

As to the sixth coordination position around the rhenium atom, it might be occupied either by an amide nitrogen atom or a water molecule, possibly stabilized by a hydrogen-bond interaction with the carboxylate anion (scheme a or b, respectively, in Figure 4.7).

However, the complete disappearance of the CH_2SH resonance at 18.5 ppm upon the addition of only 0.5 equivalent of rhenium strongly suggests that in complex 1 this coordination site is occupied by another thiolate group belonging to a cysteamine moiety of the same or of a different polymer coil (c in Figure 4.7). The contribution of form c explains the impossibility of binding to the polymer an amount of rhenium exactly corresponding to the amount of thiol groups.

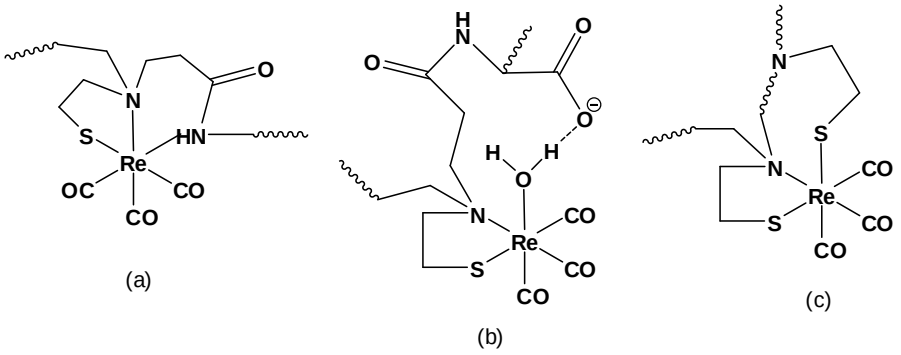

Figure 4.7. Possible coordination environments of Rhenium in complexes 1 and 2.

Further support for the involvement of the cysteamine-deriving moiety in the binding of rhenium was provided by the ^{15}N NMR data. A ^{1}H-^{15}N HMBC experiment on complex 1 showed that the signal of N18 of cysteamine was no more detectable (Figure 4.5-B), whereas the signals of the piperazine nitrogen atoms (N11 and N14) were observed at the same positions of the free polymer.

Moreover, $ISA23SH_{10\%}$ completely inhibits the condensation of the $Re(CO)_3$ units to the "cubane-like" derivative $[Re_4(CO)_{12}(\mu_3\text{-}OH)_4]$, which occurs upon heating solutions of $[Re(CO)_3(H_2O)_3]^+$ at pH 5.5. The same inhibitory effect does not occur with ISA23, indicating that the coordination sites of rhenium ions are the cysteamine moieties, as confirmed by the NMR data.

Morphological evaluation. The morphology of complexes 1 and 2 was evaluated by TEM analysis in collaboration with Prof. Cavalli and co-workers.

Both complexes formed nanoparticles with a quite spherical morphology, average diameter <25 nm, and a narrow size distribution, as shown in Figure 4.8. In particular, the size of complex 1 ranged from about 5 to 15 nm, whereas the size of complex 2 ranged from about 7 to 20 nm. The DLS determinations showed a mean diameter of ∼15 nm for complex 1 and of ∼22 nm for complex 2, with polydispersity indices of 0.1.

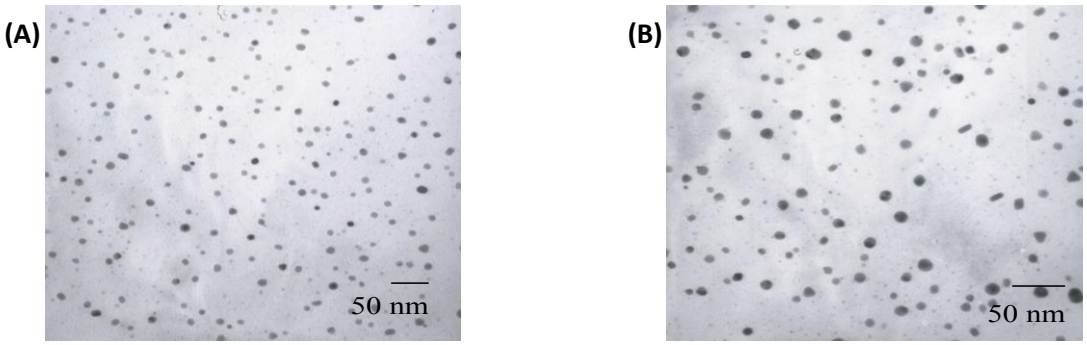

Figure 4.8. TEM photomicrographt of PAA-rhenium complexes: (a) complex 1 (magnification 105 000x) and (b) complex 2 (magnification 145 000x).

Preliminary biological evaluation. Preliminary biological evaluation were performed by Prof. Cavalli and co-workers. No hemolytic activity was observed for $ISA23SH_{10\%}$ and the two rhenium complexes up to a concentration of 5.5 mg/mL. No significant toxic effects were observed for the two rhenium complexes on Hela cells up to 100 ng/mL after 48 hours of exposure as reported in Figure 4.9. This observation time was considered to be amply sufficient for the envisaged medical application, which requires storage time and in vivo stability consistent with the stability of the radiopharmaceutical involved. The parent polymer $ISA23SH_{10\%}$ and the free tricarbonyl rhenium complex did not show any cytotoxic effect at the tested concentrations. Acute toxicity experiments carried out according to standard protocols gave a maximum tolerated dose (MTD) value of 500 mg/kg for $ISA23SH_{10\%}$.

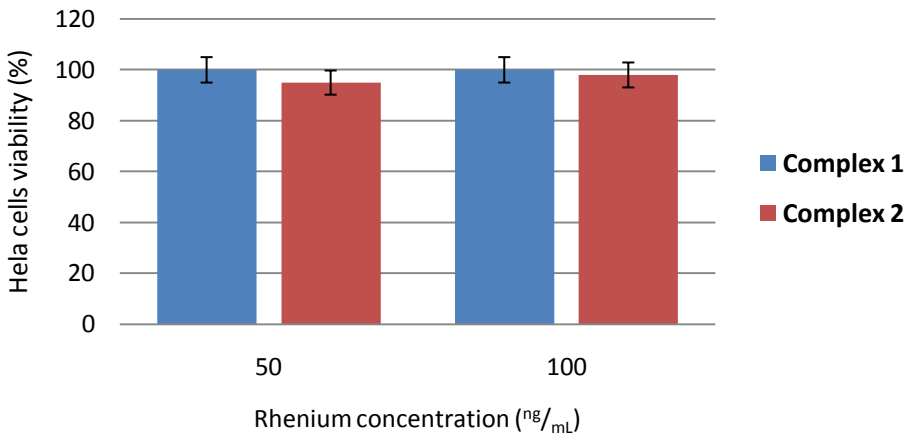

Figure 4.9. Viability of Hela cells after 48h incubation with the complex 1 and 2 with respect to untreated cells as positve control (100%).

Preliminary in vivo studies were performed on the two rhenium complexes, which were intravenously injected in mice in doses up to 20 mg/kg, corresponding to rhenium doses up to about 1 mg/kg. All mice survived, and no toxic signs were observed.

4.4 CONCLUSIONS

In this study an ISA23 polymer containing cysteamine-deriving moieties has been prepared and used to tightly bind $Re(CO)_3^+$ fragments, up to a 0.85:1 Re/SH molar ratio. Nanosized complexes have been easily obtained upon thermal or microwave activation of the reagents. Rhenium chelation occurred through the S and N atoms of the cysteamine moiety, as demonstrated by ^{1}H, ^{13}C, and ^{15}N NMR spectroscopy. The ISA23-Re complexes formed spherical nanoparticles stable under physiological conditions and non toxic, as evidenced by preliminary in vitro and in vivo studies. Owing to these favorable properties, coupled to the intrinsic tumor targeting capability of the amphoteric ISA23, these rhenium-complexing polymers warrant a significant diagnostic and therapeutic potential for preparing radiopharmaceutical formulations of rhenium and technetium.

References:

1. Spencer, R.P.; Suvers, R.H.; Friedman, A.M. *Radionuclides in Therapy*, CRC Press, Boca Raton, Florida, 1987.
2. Winston, M.A. *Semin. Nucl. Med.* **1979**, *2*, 114-120.
3. Hoefnagel, C.A. *Anti-Cancer Drugs* **1991**, *2* (2), 107-132.
4. Kaplan, E. *Therapy in Nuclear Medicine*, Spencer R. Ed., Grune & Stratton, 1978.
5. Britton, K.E. *Nucl. Med. Commun.*, **1997**, *18*, 823-826.
6. Volkert, W.A.; Goeckeler, W.F.; Ehrhardt, G.J.; Ketring, A.R. *J. Nucl. Med.* **1991**, *32* (1), 174-185.
7. Ehrhardt, G.J.; Ketring, A.R.; Ayers, L.M. *Appl. Radiat. Isot.* **1998**, *49*, 295-297.
8. Troutner, D.E. *Int. J. Radiat. Appl. Inst.* **1987**, *14*, 233.
9. Attard, A.R.; Chappell M.J., Bradwell A.R.; Br. J. Radiol., vol. 68; 1995.
10. Howel, R.W.; Rao, D.V.; Sastry, K.S. *Med. Phys.* **1989**, *16*, 66-74.
11. Kassis, A.I.; Wen, P.Y.; Van den Abbeele, A.D.; Baranowska-Kortylewicz, J.; Makrigiorgos, G.M.; Metz, K.R.; Matalka, K.Z.; Cook ,C.U.; Sahu, S.K.; Black, P.McL.; Adelstein, S.J. *J. Nucl. Med.* **1998**, *39*, 11-48-1154.
12. Illdge, T.M.; Brock, S. *Curr. Phar. Des.* **2000**, *9*, 1399-1418.
13. Potamianos, B.; Varvarigou, A.D.; Archimandritis, S.C. *Anticancer Res.* **2000**, *20*, 925-948.
14. Vriesendorp, H.M.; Quadri, S.M.; Borchardt, P.E. *BioDrugs* **1998**, *10* (4), 275-293.
15. Wun, T.; Kwon, D.S.; Tuscano, J.M. *Biodrugs* **2001**, *15* (3), 151-162.
16. Dilworth, J.R.; Parrott ,S.J.; *Chemical Society Review* **1998**, *27*, 43-55.
17. Volkert, W.A.; Hoffman, T. *Chem. Rev.* **1999**, *99*, 2269-2292.
18. Sgouros, G.J *J. Nucl. Med.* **1995**, *36*, 1885-1894.
19. Fritzber, A.R.; Gustavson, L.M.; Hylarides, M.D.; Reno, J.M. *Chemical and Structural Approaches to Rational Drug Design*, Weiner D.B, Williams M.V. Eds., CRC Press, Boca Raton, Florida, 1995.
20. Schubiger, P.A.; Alberto R.; Smith, A. *Bioconjugate Chem.* **1996**, *7* (2), 165-179.
21. Otte, A.; Mueller-Brand, J.; Dellas, S.; Nitzsche, E.U.; Herrmann, R.; Maecke, H.R. *Lancet.* **1998**, *351*, 417-418.
22. Zhu, H.; Jain, R.K.; Baxter, L.T. *J. Nucl. Med.* **1998**, *39*, 65-76.

23. Wilbur, D.S.; Hamlin, D.K.; Buhler, K.R.; Pathare, P.M.; Vessella, R.L.; Stayton, P.S.; To, R. *Bioconjugate Chem.* **1998**, *9* (3), 322-330.
24. Shuang, L. *Chem. Soc. Rev.* **2004**, *33*, 401-461.
25. Duncan, R. *Nat. Rev. Drug Discov.* **2003**, *2*, 214-221.
26. Maeda, H.; Matsumura, Y. *Crit. Rev. Ther. Drug Carrier.* **1989**, *6* (3), 193-210.
27. Kim, J.H.; Park, K.; Nam, H.Y.; Lee, S.; Kim, K.; Kwon, I.C. *Prog. Polym. Sci.* **2007**, *32*, 1031-1053.
28. Lu, Z.R.; Ye, F.; Vaidya, A. *J. Contr. Rel.* **2007**, *122* (3), 269-277.
29. Ferruti, P.; Ranucci, E.; Bianchi, S.; Falciola, L.; Mussini, P.R.; Rossi, M. *Journal of Polymer Science: Part A: Polymer Chemistry.* **2006**, *44* (7), 2316-2327.
30. Richardson, S.C.W.; Ferruti, P.; Duncan, R. *J. Drug Targeting.* **1999**, *6*, 391-404.
31. Lipowska, M.; Hansen, L.; Xu, X.; Marzilli, P.A.; Taylor, A.; Marzilli, L.G. *Inorg. Chem.* **2002**, *41*, 6417-6425.
32. Lazarova, N.; Babich, J.; Valliant, J.; Schaffer, P.; James, S.; Zubieta, J. *J. Inorg. Chem.* **2005**, *44*, 6763-6770.
33. Griffiths G.L. CRC Press, Inc.: Boca Ranton, Chapter 7, 1995.
34. Ferruti, P.; Ranucci, E.; Trotta, F.; Gianasi, E.; Evagorou, G.E.; Wasil, M.; Wilson, G.; Duncan, R. *Macromol. Chem. Phys.* **1999**, *200*, 1644-1654.
35. Schmidt, S.; Trogler, W.; Basolo, F. *Inorg. Synth.* **1985**, *23*, 41-46.
36. Schmidt, S.; Nitschke, J.; Trogler, W. *Inorg. Synth.* 1989, *26*, 113-117.
37. Herberhold, M.; Suess, G. *Angew. Chem. Int. Ed. Engl.* **1975**, *14*, 700.
38. Herberhold, M.; Suess, G.; Ellerman, J.; Gaebelein, H. *Chem. Ber.* **1978**, *111*, 2931-2941.
39. He, H.; Lipowska, M.; Xu, X.; Taylor, A.T.; Carlone, M.; Marzilli, L. *Inorg. Chem.* **2005**, *44*, 5437-5446.
40. Jacobson, K.A.; Fischer, B.; Ji, X. *Bioconjugate Chem.* **1995**, *6*, 255-263.
41. Garnett, M.; Ferruti, P.; Ranucci, E. Univeristy of Nottingham, Univeristà degli Studi di Milano, Patent WO/2008/038038; 2008.
42. Alberto, R.; Egli, A.; Abram, U.; Hegetschweiler, K.; Gramlich, V.; Schubiger, A. *J. Chem. Soc. Dalton Trans.* **1994**, 2815-2820.
43. Lazarova, N.; James, S.; Babich, J.; Zubieta, J. *J. Inorg. Chem. Commun.* **2004**, *7*, 1023-1026.

44. Schibli, R.; Schwarzbach, R.; Alberto, R.; Otner, K.; Schmalle, H.; Dumas, C.; Egli, A.; Schubiger, A. *Bioconjugate Chem.* 2002, *13*, 750-756.
45. Alberto, R.; Schilibi, R.; Egli, A. Mallinckrodt Medical Int., Patent WO/1998/048848; 1998.
46. Causey, P.W.; Besanger, T.R.; Schaffer, P.; Valliant, J.F. *Inorg. Chem.* **2008**, *47*, 8213-8221.

CHAPTER 5

NOVEL POLY(AMIDOAMINE)-BASED HYDROGELS AS SCAFFOLD FOR TISSUE ENGINEERING APPLICATIONS

3,8,20,23,37,55,56

5.1 INTRODUCTION

Tissue lost or end-stage organ failure caused by injury or other types of damage is one of the most devastating and costly problems in human health care. Surgical strategies that have been developed to deal with these problems include organ transplantation from one individual to another, tissue transfer from a healthy site to the diseased site in the same individual and replacement by using mechanical devices such as joint prosthesis or dialysis machine. Moreover, medical treatment encompassed supplementation of metabolic products of the non-functional tissue. Though significant advances have been achieved in terms of health care by these therapeutic options, many limitations and unsolved issues remain[1]. The number of organs available for transplantation is far exceeded by the number of patients needing such procedures. In the Italy in 2010 alone, approximately 9,300 people were on the waiting list for an organ transplant due to end-stage organ-failure, but only 3,100 transplants were performed[2]. Tissue transfer cannot replace all the functions of the original tissue and bears the risk of donor-site complications.

Tissue engineering "is an interdisciplinary field that applies the principles of engineering and of life science towards the development of biological substitutes that restore, maintain or improve tissue or organ function." This definition was based on several articles, by Langer and Vacanti, that were published in the 90s[3-6]. In those articles tissue engineering was proposed as an alternative to organ transplantation when all the other treatments failed using three main strategies. First, the utilization of isolated cells, which has the great advantage to replace just the cells that are really needed and to eventually genetically manipulate them before infusion. This strategy allows for minimal invasive surgery, but there is always the possibility of immunological rejection or failure in maintaining new functions. The second approach is that of using tissue-inducing substances like, for instance, growth factors, or cytokines. However, drawbacks of this solution are purification and large-scale production issues, and it will always be necessary to have a system to deliver the bioactive molecule to its target.

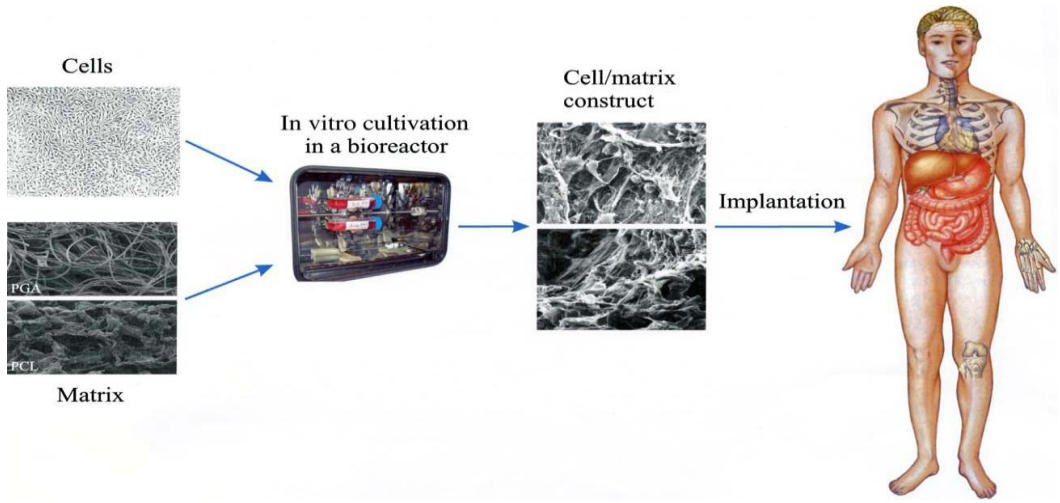

Figure 5.1. Tissue engineering process (Image from reference 1).

Finally, the third strategy utilizes cells that are placed on a scaffold that serves as a synthetic extracellular matrix to organize cells into a three-dimensional architecture and to present stimuli which direct the growth and formation of a desired tissue[7]. This strategy is currently used in tissue engineering.

Scaffolds can be produced from natural materials or synthetic polymers. In general, the ideal scaffold should be three-dimensional, highly porous with an interconnected pore network, and biocompatible with a controlled degradation rate, should have an appropriate surface for cell adhesion, proliferation, and differentiation and should maintain proper mechanical properties. Among all the synthetic polymeric materials that have been found to be suitable for tissue engineering applications, special attention has been given recently to biodegradable polymers and hydrogels. Several reviews in literature describe the use of natural[8-15] and synthetic[16-20] biodegradable polymers as well as some non-biodegradable[21,22] polymers, which are currently used for cartilage, nerve repair, bone, cardiac, vascular graft and many other tissue engineering applications. Among synthetic materials, increasing attention has been paid on hydrogels due to their tissue-like properties for interaction with living cells, such as similar water content and permeability to oxygen and metabolites[23]. Synthetic hydrogels, as opposed to naturally derived materials are more advantageous, giving the possibility of a complete control over hydrogel composition, surface properties and other key parameters such as water absorption and (bio)degradation time. Moreover, hydrogel structures could be used to encapsulate cells, proteins and signaling factors, as well as bioactive moieties to be slowly released during cell growth.

Peripheral nerve injuries present a significant clinical challenge across the world[24]. Injuries to the peripheral nervous system are common and are a major source of disability, impairing the ability to move muscles and/or feel normal sensations, or resulting in painful neuropathies. Due to the difficulties in treating such injuries, many patients are left without any benefit of medical intervention. Even among the patients who receive treatment for traumatic peripheral nerve injuries, more than 50% show no measurable signs of recovery, or else suffer from drastically reduced muscle strength[25].

After nerve trauma, the standard clinical operating procedure is to oppose the two nerve ends and suture them together without generating tension where possible.

If the gap is large a nerve autograft – typically the patient's own sural nerve – is used as a bridge. While autografts are the best clinical bridges available today because they are biocompatible, non toxic and provide a support structure to promote axonal adhesion, there are many drawbacks to this procedure. These include the need for a secondary surgery, loss of donor site function, limited availability, modality mismatch (arising from a sensory nerve being used to repair a motor or mixed nerve), and neuroma formation at the donor or graft site.

Various tissue engineering strategies have been used to influence different aspects of the regenerative process with hope for functional recovery using natural and synthetic tubular scaffolds. The design criteria for fabrication of scaffolds should address various factors including composition[26] and dimensions of the tubular scaffold[27], the addition of exogenous factors such as fibrin precursors[28] and growth factors, the incorporation of glial cells, most often Schwann cells and fibroblasts[29,30], the elastic modulus, permeability, topography, swelling ratio, degradation rate, size and clearance of the degradation products[31]. In particular the elastic modulus of the scaffold should be at least 1,200 kPa in order to resist compressive and tensile forces that are generated both during the surgery as well as from surrounding tissue post-implantation[32].

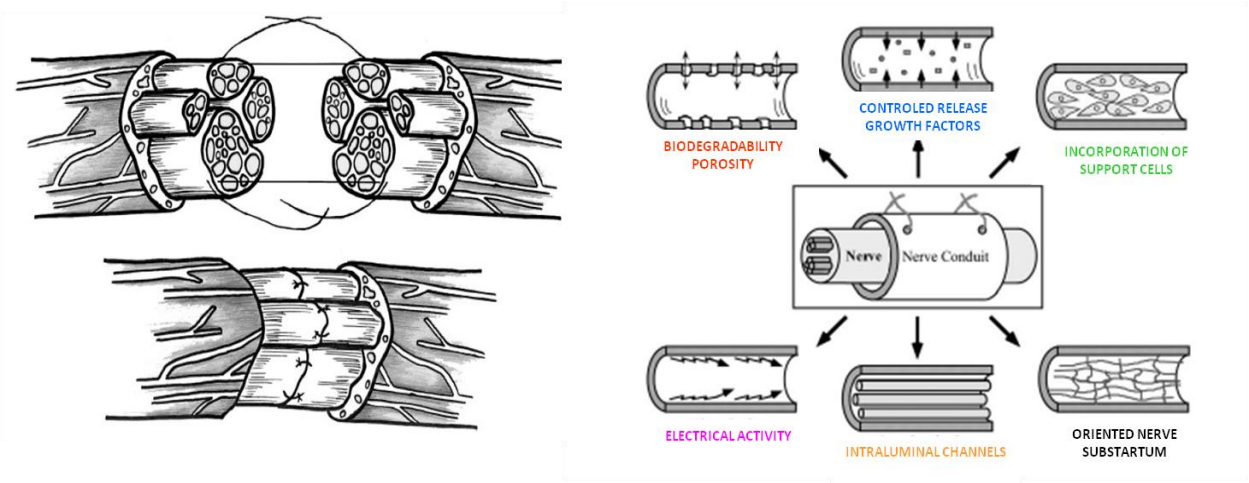

Figure 5.2. Surgical (right) and tissue engineering (left) strategies designed to facilitate the regeneration of peripheral nerves.

Different natural and synthetic materials have been used to facilitate nerve regeneration. Among natural tubular scaffolds, autogenous venous and arterial nerve grafts have been the most successful in achieving functional recovery across 10-mm nerve gaps[33-35]. Venous grafts remain intact throughout the process of nerve regeneration and are easier to extract compared to arterial grafts[33]. While natural materials have good biocompatibility, they often collapse when used in longer nerve gaps. Additionally, issues related to the limited availability of these explants as well as autograft-triggered immune response are a few among many reasons that prompted exploration of alternative materials to direct nerve growth[36]. Synthetic tubular scaffolds have similar advantages to natural scaffolds but additionally provide mechanical and structural control[37]. In the recent past, several guidance techniques using artificial nerve conduits have been developed to guide nerve regeneration towards the distal stump[38]. The isolated environment provided by guidance channels helps confine and concentrate neurotrophic factors that are released by supporting cells while protecting the axons against collapse and invasion from immune cells[33]. The use of guidance channels eliminates functional loss at the donor site, a condition that is commonly associated with the use of autografts. Initial studies employing the use of short impermeable silicone tubes showed promising nerve regeneration across 3mm gaps[39], although significant fibrosis and nerve compression was subsequently associated with the use of these tubes[40–42]. Biodegradable polymers such as poly(L-lactic acid), polyglycolic acid and poly(lactic-co-glycolic) acid were originally the materials of choice for synthesizing conduits, due to their relative abundance and applicability[43-45]. In addition to poly(esters), biodegradable poly(urethane)[46], poly(organo-phosphazene)[47] and poly(3-hydroxybutyrate)[48] have shown a capacity for guiding regeneration. Nevertheless, these materials don't fulfill all the requirements that a scaffold for in vivo application should have. For instance, a common inconvenience of biodegradable polyesters is to cause inflammation in the surrounding tissues giving rise to a local concentration of acids upon degradation.

In recent years, special attention has been given to hydrogels. Hydrogels are insoluble and swellable materials that are widely used in the biomaterial field due to their biocompatibility, which derives from their high water absorption and surface properties. Hydrogels exhibit overall properties similar to those of soft tissues, having tunable elasticity, nutrient permeability, biocompatibility and low interfacial tension.

Among natural hydrogels, gelatin-based tubular scaffolds[49], alginate-based capillary hydrogels[50] and multichannel collagen nerve conduits[51] were used to guide axonal growth in animal experiments. Synthetic hydrogels include poly(ethyleneglycol)[52] and poly(2-hydroxyethyl methacrylate-co-methyl methacrylate)[53].

Although these materials showed promising results in terms of nerve regeneration, their properties, such as permeability, degradability and mechanical strength are not yet satisfactory[54].

Biocompatible and biodegradable PAA-based hydrogels have also been studied as scaffold for tissue engineering. Paricularly promising was the amphoteric but prevealing cationic Agma1 hydrogel, obtained using 4-aminobutyl guanidine (Agmatine) as amine monomer and ethylenediamine (EDA) as cross-linking agent. This material showed excellent adhesion and proliferation properties towards different cell lines: Mouse Embryo Fibroblast (3T3/BalbC Clone A3); Madin-Darby Canine Kidney Epithelial Cells (MDCK Line); Phaeochromocytoma of rat adrenal medulla (PC12 cell)[55-57]. The cell adhesion on the Agma1 substrates was comparable to that on tissue culture plastic substrates and significantly enhanced with respect to the non functionalized controls. We argued that this interesting property was related to the presence of side-guanidine groups, which, together with the carboxyl and the amide groups gave rise to a repeating unit bearing a close resemblance to the Arg-Gly-Asp (RGD) peptide sequence, well known for its ability to interact with integrins[58,59].

Recently, an ISA23-based hydrogel has been used for the synthesis of patterned substrate using a scanning electron microscope[60]. These experiments showed that proteins, growth factors and the PC12 cell lines were selectively attached along the pattern.

Using this technique a neural network of differentiated PC12 cells has been prepared in which all the single cells were connected each other by neuritis extended along the patterned surface.

All the above considerations point to the general conclusion that amphoteric PAA hydrogels have a definite potential as biomimetic materials and deserve to be further considered for different biotechnological applications such as substrates for cell culture. Unfortunately, their mechanical properties were not satisfactory in view of a use as scaffolds for tissue engineering, in that their strength is still very low and they are very soft and breakable on handling.

To overcome this problem, in this work a new synthetic method has been developed leading to hydrogels with similar composition and exhibiting the same biological properties but with improved mechanical strength. In particular a different two-step pathway has been followed as reported in scheme 5.1. In the first step an acryloyl end-capped linear PAA oligomer was synthesised using a controlled excess of the bisacrylamide; in the second step the oligomer was photopolymerized by UV irradiation producing hydrogels with the required mechanical characteristics.

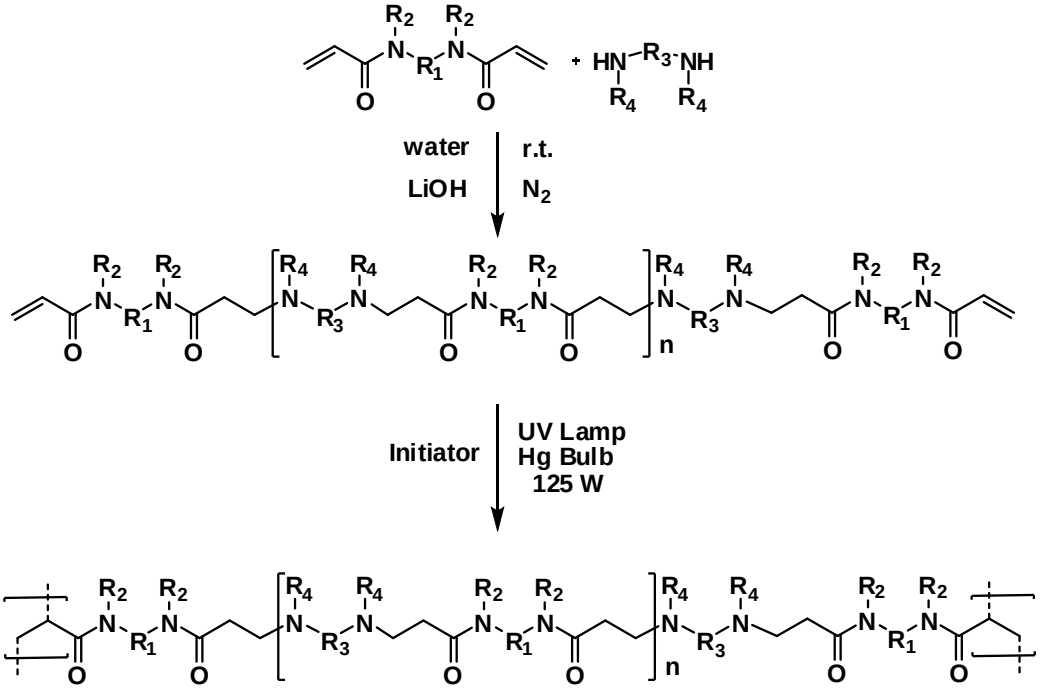

Scheme 5.1. Synthetic pathway leading to UV-made PAA hydrogels.

Using these new hydrogels large sheets and tubular scaffold of various sizes have been prepared. Adhesion and proliferation test results were similar to PAA-based hydrogels with ethylenediamine as cross-linker. Preliminary in vivo tests were performed on living rat in order to demonstrate the potential application of these kinds of PAA hydrogels in tissue engineering and in particular in neural tissue repair.

5.2 EXPERIMENTAL PART

Instruments

NMR experiments were run on a Brüker Advance 400 spectrometer operating at 400.132 (^{1}H) and 100.623 (^{13}C) MHz. All spectra were acquired at room temperature, on samples typically containing 15-30 mg of lyophilized samples dissolved in 500 μl of D_2O.

Size exclusion chromatography (SEC) traces were obtained with Toso-Haas TSK-gel G4000 PW and TSK-gel G3000 PW columns connected in series, using a Waters model 515 HPLC pump equipped with a Knauer Autosampler 3800, a Light Scattering Viscotek 270 Dual Detector, UV detector Waters model 486, operating at 230 nm, and a refractive index detector Waters model 2410. The mobile phase was a 0.1 M Tris buffer pH 8.00 ± 0.05 with 0.2 M sodium chloride. The flow rate was 1 mL/min and sample concentration 1% w/w solutions.

Materials and methods

The solvents and reagents, unless otherwise indicated, were analytical-grade commercial products and were used as received. 2,2-Bis(acrylamido)acetic acid (BAC) was prepared as reported in literature and purity (99,7%) determined by NMR and titration[61]. Phosphate buffer solution (PBS) 10 mM was prepared using Sigma Aldrich tablets according to manufacturer's instructions. D_2O (99.9%) was purchased from Aldrich and used as received. Photopolymerization reactions were performed using a 125 W Hg bulb UV lamp.

Synthesis of Agma1 acryloyl end-capped oligomer. In a 10 mL round bottomed flask BAC (2 g; 10.06 mmol) was added under nitrogen atmosphere and stirring to an aqueous lithium hydroxide solution (LiOH monohydrate, 426.58 mg; 10.06 mmol in 3.4 mL). When the solution was clear, Agmatine (2.13 g; 9.06 mmol) and LiOH (383.93 mg; 9.06 mmol) were added and dissolved. The mixture was allowed to react at room temperature, in inert atmosphere and in the dark for 72 hours. After this time it was diluted to 200 mL with water and brought to pH 4.0 with 37% hydrochloric acid. The product was finally recovered by lyophylisation. Yield: 2.7 g (95.95%). ^{13}C NMR (D_2O): δ= 173.5 (CH-***C***OOH); 171.3 (NH-***C***O); 155.1 (NH_2***C***NN guanidine group); 129.6 (***C***H_2CH acryloyl residue); 128.6 (CH_2***C***H acryloyl residue); 56.0 (COOH-***C***H); 52.5 (NH***C***H_2 agmatine monomer); 49.1 (NHCO***C***H_2 polymer backbone); 40.4 (CH_2N***C***H_2 agmatine monomer); 28.9 (NHCOCH_2***C***H_2 polymer backbone); 25.0 (NHCH_2***C***H_2 agmatine monomer); 22.3 (NHCH_2CH_2***C***H_2 agmatine monomer). ^{1}H NMR (D_2O): δ= 6.75 (m, 2H, C***H*****$_2$**CH acryloyl residue); 5.74 (m, 1H, CH_2C***H*** acryloyl residue); 5.55 (s, 1H, COOH-C***H***); 3.44 (br, 2H, NHCOC***H*****$_2$** polymer backbone); 3.19 (m, 4H, NHC***H*****$_2$** and NC***H*****$_2$** agmatine monomer); 2.79 (br, 2H, NHCOCH_2C***H*****$_2$** polymer backbone); 1.76 (br, 2H, NHCH_2C***H*****$_2$** agmatine monomer); 1.61 (br, 2H, NHCH_2C***H*****$_2$** polymer backbone). Molecular weight values: $\overline{M}_n$ =10100, $\overline{M}_w$ =17100, PD=1.7.

Synthesis of Agma1 hydrogel tubes by photopolymerization. In a 10 mL round bottomed flask Agma1 oligomer (1 g; 0.31 mmol of acryloyl functions) was dissolved under nitrogen atmosphere in 1.5 mL of bidistilled water and 0.5 mL of an aqueous solution of 4,4'-azobis(4-cyanovaleric) acid (250 mg in 5 mL of bidistilled water). The mixture was stirred for 1 minute, retrieved with a syringe, injected in a silanized tubular glass with 0.7 mm inner diameter and exposed for 2 hours to UV irradiation. The PAA hydrogel obtained was washed twice with 200 mL of water and finally with 200 mL of PBS 0.1 mM.

Swelling test. The native hydrogels were cut into 10x10x0.3 mm^3 parallelepiped, freeze-dried to obtain the dry weight (mean weight 212 ± 15 mg) and placed inside a Falcon tube containing 50 mL of the desired solvent at the room temperature until the maximum swelling was reached. The swelling percentage was calculated using the following formula:

$$Swelling\ (\%) = \frac{W_{wet}}{W_{initial\ dry}} \times 100 \qquad \text{(Eq. 5.1)}$$

where W_{wet} is the weight of the swelled hydrogel *and* $W_{initial\ dry}$ is the weight of the initial dry hydrogel.

Degradation test. Samples of dry AGMA1 hydrogels were weighed (average weight 20 ± 5 mg) and placed each in a test tube containing 50 mL phosphate buffered solution 0.1 M at pH 7.4. The samples were closed, placed in an incubator at 37°C and retrieved at different times. The recovered samples were blotted dry and weighed, then they were freeze dried to define the dry weight. The proportional weight rest was calculated as:

$$Weight\ rest\ (\%): = \frac{W_{final\ dry}}{W_{initial\ dry}} \times 100 \qquad \text{(Eq. 5.2)}$$

where $W_{initial\ dry}$ is the weight of the initial dry hydrogel and $W_{final\ dry}$ is the weight of the final dry hydrogel.

Rheometry. Viscoelastic measurements were performed using a strain-controlled rheometer (Rheometric Scientific ARES). Samples were prepared in the form of disks with a 28 mm diameter and 1 mm thickness in the swollen state. Samples were tested using a parallel plate geometry with a 25 mm diameter. The samples were placed between the rheometer plates, and a slight compressive force of about 50 g was applied. The frequency sweep test was conducted with a strain of 0.2% from 0.05 to 10 Hz at 25 °C.

In vitro biological evaluation

Cell viability assay. Cell viability tests were also carried out for MTT assay procedure. $4x10^4$ PC12 cells were seeded on AGMA1 hydrogels and TCPS within a 48-well tissue culture plates for 24 hours. Non-adherent cells were removed by washing at one and three hours from seeding. Then, 500 µl 10% MTT solution (5 mg/mL in PBS) was added to each sample and the plates were incubated for 3 hours at 37°C. The supernatant was discarded and the formazan salt was dissolved in an equal volume of an isopropanol-HCl 0.04 M solution. The absorbance was measured at 570 and 650 nm using a Perkin Elmer Lambda EZ210 spectrophotometer, elaboration program PESSW version 1.2. Images were collected with a Power Shot G6 Canon digital camera mounted on a Zeiss Axiovert 40 CFL inverted optical microscope using 10X objective lens.

In vivo biological evaluation

Animals. Sprague-Dawley adult 3-months old male rats (Charles River, Italy) were anaesthetized with an intraperitoneal injection of pentobarbital (30 mg/kg), then underwent surgical procedures. In all cases, all efforts were made to minimize pain and discomfort. All experiments were performed according to institutional guidelines and in compliance with the policy on the use of animals approved by the European Communities Council Directive (86/609/EEC).

Surgical procedure. Animals were divided in two experimental groups (each consisting of 5-6 animals), sham operated and injured rats that were guide-implanted. The animals were anesthetized and the right sciatic nerve was exposed after the skin incision, and separation of muscles around the nerve tissues. Subsequently, in the injured rats the right sciatic nerve was severed in the middle, giving proximal and distal segments.

The conduits were implanted securing both the proximal and the distal stumps with 9-0 nylon and leaving a 5-mm gap between stumps. The muscle layer was re-approximated with 4-0 nylon sutures, and the skin closed with 4-0 sutures. Each rat received one implant that was removed at different time points (30, 90, 180 days post surgery).

Immunocytochemistry. Sciatic nerves were fixed in 4% paraformaldehyde in phosphate buffered saline. 10 µm thick coronal sections were used for immunohistochemistry with a mouse monoclonal anti-neurofilament of medium/high density antibody (clone RMdO20, diluted 1:500). The slides were incubated overnight at 4 °C in PBS containing 0.25% bovine serum albumin, 0.1% Triton X-100 and the primary antibody. Following washes, the slides were incubated for 2 hours with a secondary antibody goat anti-mouse FITC conjugate (diluted 1:500). Nuclei were stained with Dapi (diluted 1:1000) and the slides were mounted. Controls for antibody specificity included a lack of a primary antibody, or substitution with pre-immune serum.

The image analysis was done using a Zeiss Axioskop200 microscope and Adobe Photoshop 5.0.2.

Light microscopy. For the light microscopy sciatic nerves were fixed with 2% paraformaldehyde - 2% glutaraldehyde in 0.1 M sodium cacodylate. After rinsing in buffer sciatic nerves were postfixed with 1% OsO_4. The specimens were then dehydrated and embedded in Epon-Araldite resin. Semi-thin (0.5 µm) sections, toluidine blue stained were examined by light microscopy (Pro Plus Imaging software) at a final magnification of 1500X.

Gait analysis. Rats with their hind feet stained with black ink were placed on a 100 cm long gangway, which yielded 8-10 footprints per rat. Footprints were analyzed with the Footprint 1.22 program[62].

We evaluated the area touched by a single step, the toe spreads 1-5 and 2-4, the length of the foot step, the stride width and the stride length. Rats did not undergo any training to perform the test.

Thermal sensitivity. Responses to thermal stimuli were performed on both paws of control (sham operated) and hydrogel-implanted rats. Heat hypersensitivity was tested according to the Hargreaves procedure[63] using the Basile Plantar test apparatus. Briefly, rats were placed in a clear Plexiglass cubicles and allowed to familiarize themselves. A constant intensity radiant heat source (beam diameter 0.5 cm and intensity 20 I.R.) was aimed at the midplantar area of the hind paw. The time from the heat source activation until paw withdrawal was recorded (in seconds).

5.3 RESULTS AND DISCUSSIONS

In this work a new Agma1-like hydrogels have been prepared and tested as nerve guidance by an alternative method consisting of the UV triggered radical polymerisation of acrylamide-end capped Agma1 oligomers. This procedure is a general method for preparing UV made cross-linked PAAs. The oligomer was prepared using a 10% stoichiometric excess of 2,2-bis(acrylamido)acetic acid with respect to 4-aminobutylguanidine. The final hydrogel has been obtained by radical photopolimerization of an acqueous solution of the reactive oligomer inside a mold consisting in an external thin-walled glass tube previously treated with trimethylchlorosilane containing an internal non-adhesive rod of the required diameter. 4,4'-Azobis(4-cyanovaleric) acid was used as initiator (Scheme 5.2). The polymerization reaction was complete after 2 hours and purification from unreacted monomers or occasional impurities carried out by extensive extractions with doubly-distilled water.

Hydrogel tubes of different dimensions (length 10-30 mm, 3 mm external diameter and 0.5-1.2 mm internal diameter) were obtained (Figure 5.3); however, the preferred dimensions for rat implantation were 10 mm length and 1 mm inner diameter.

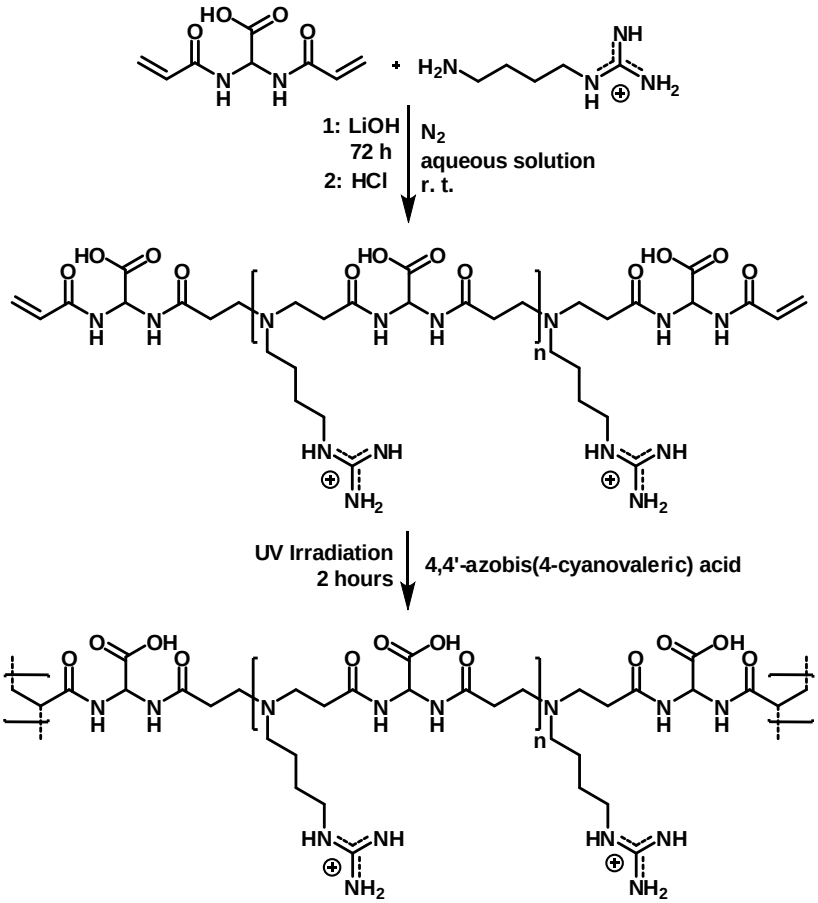

Scheme 5.2. Synthetic pathway leading to Agma1 hydrogels.

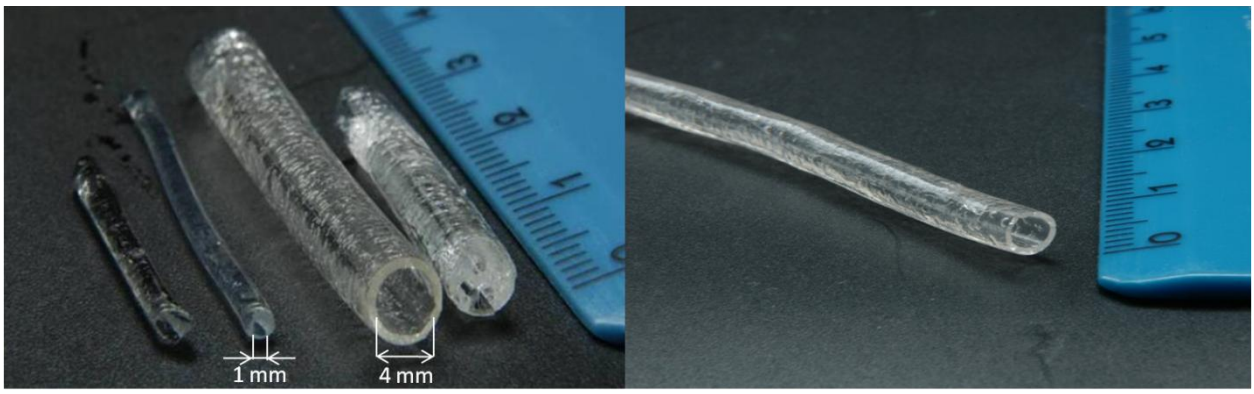

Figure 5.3. Agma1 tubular hydrogels obtained by UV photopolymerization.

The cross-linking degree of the resulting hydrogels depends on the chain length of the starting oligomer which, at the same time, is related to the bis-acrylamide excess in the polymerization recipe. High excess of the bis-acrylamide leads to short chain length and high cross-linking degree. In the case of Agma1, a 10% excess of the 2,2-bis(acrylamido)acetic acid acid (on molar basis) represented the optimum stoichiometric unbalance, yielding hydrogels pliable and transparent when fully swollen in aqueous media. Lower and higher excess of the bis-acrylamide leads to materials unsuitable as scaffold, being in the former case exceedingly soft and in the later case opaque and brittle when fully swollen in water. This new kind of hydrogel contains an hydrophilic PAA segment combined with an hydrophobic polyvinyl chain, whose relative amount depends on the bis-acrylamide excess in the reacting oligomer and influences the swelling degree and the mechanical behavior.

Cross-linked PAAs obtained by ethylenediamine as cross-linking agent were proved to swell in water giving very soft hydrogels[55-57]. Swelling tests carried out on the UV-made Agma1 hydrogels in doubly distilled water and 0.1 M PBS solution pH 7.4 showed a 200% absorption in both cases, 3 times lower than the ethylenediamine-made cross-linked Agma1 as reported in Figure 5.4. Degradation tests were carried out under conditions mimicking the physiological environment, that is, PBS 0.1 M at pH 7.0 and 37 °C. The mechanism of degradation seems to be purely hydrolytic as no acrylic groups have been detected by NMR spectroscopy.

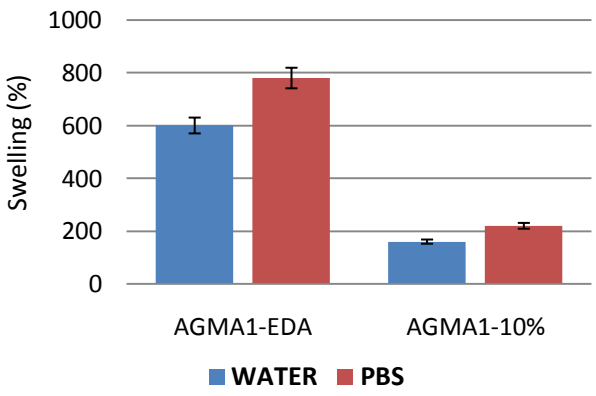

Figure 5.4. Comparison of the swelling percentage in water and PBS 0.1 M between UV-made and ethylenediamine-made Agma1 hydrogels.

Dynamic mechanical characterizations were performed by Prof. Laus on Agma1 hydrogels in the swollen state. A sinusoidal deformation of constant peak amplitude was applied over the range of frequencies from 0.05 to 10 Hz. As reported in Figure 5.5, the storage shear modulus, G', is higher than the loss shear modulus, G'', over the entire frequency region for both hydrogels. This indicates that the elastic response of the material is stronger than the viscous response so Agma1 hydrogels cross-linked by UV irradiation display a predominantly solid-like behavior.

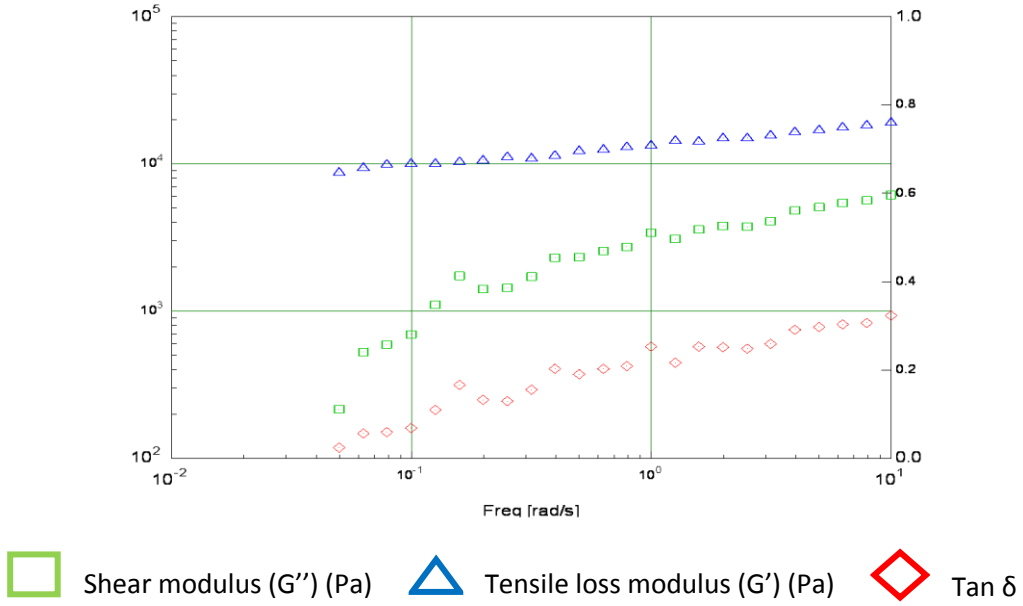

Figure 5.5. Frequency sweep test of an Agma1-UV made hydrogels.

The shear modulus obtained was 15kPa. It's noteworthy that under the same conditions, Agma1 hydrogels obtained using ethylenediamine as cross-linker were not measurable due to their poor mechanical properties.

In vitro biological evaluation. MTT assay was performed for obtaining a quantitative evaluation of cell viability. PC12 cells were seeded at appropriate density and the hydrogels were placed in direct contact with cell monolayer for 24 hours.

Figure 5.6 shows that cells viability on UV-made Agma1 hydrogels is lower but yet satisfactory than that of TCPS and Agma1 hydrogels cross-linked with ethylene diamine. The morphology of cells grown onto the surface of both hydrogels was comparable with that of cells grown on the control.

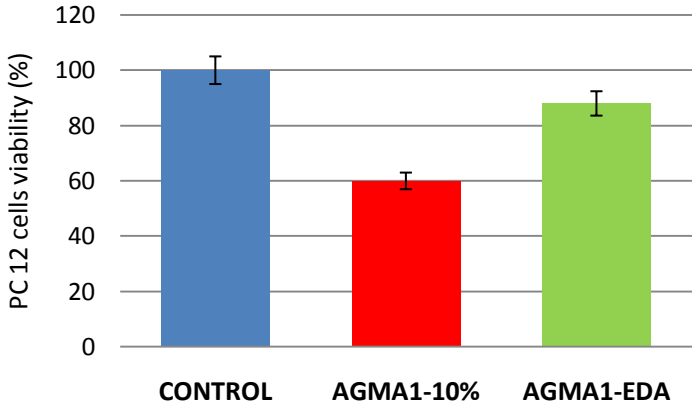

Figure 5.6. MTT assay: PC12 were plated at 4x10^4 cells/well on UV-made Agma1, Agma1-EDA and TCPS.

In vivo biological evaluation. In vivo experiments were performed in collaboration with Dr. Magnaghi (animals) and Dr. Cortese (surgery). The right sciatic nerve of the rats was cut in the middle and an hydrogel conduit having 10 mm legth and 1 mm inner diameters was implanted leaving the nerve gap of 5 mm (Figure 5.7). All rats survived and no complications related to operation occurred, since all wounds healed spontaneously.

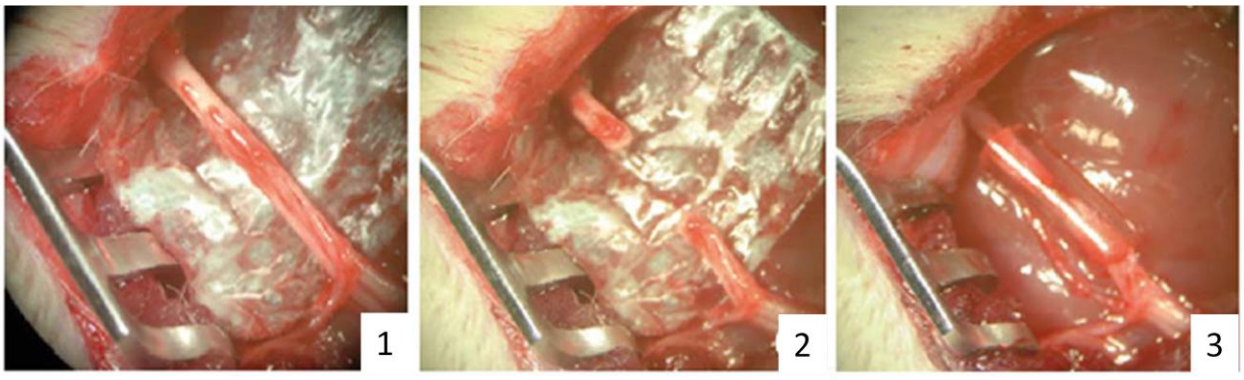

Figure 5.7. Normal intact right sciatic nerve was cut in the middle (1), removing 4-5 mm nervous tissue. Agma1 hydrogel tube has been used to regenerate the gap (3).

The progression of the nerve regeneration was extensively analyzed at different time points, namely 30, 90 and 180 day post surgery. 30 days after implantation the conduit appeared well integrated and no dislocations were observed. The regenerated nerve was resistant to mechanical traction showing no evidence of interruption. No apparent sign of inflammatory reaction or serum infiltrate were found, even if a thin fibrotic sheet surrounding the conduit was observed. Regeneration between the upper and lower nerve stump occurred inside the scaffold guide as demonstrated by the presence of nerve fibers filling the original gap. The conduit was largely degraded but not completely reabsorbed, since two large scaffold fragments (h) were embedded in the epineurium surrounding the nerve (Figure 5.8-A). At 90 days post surgery a complete nerve structure was evident with some detritus still included in the fibrotic tissue around the nerve (Figure 5.8-B), whereas at 180 day the scaffold was grossly reabsorbed, with only a few detritus in the surrounding epineurium (Figure 5.8-C).

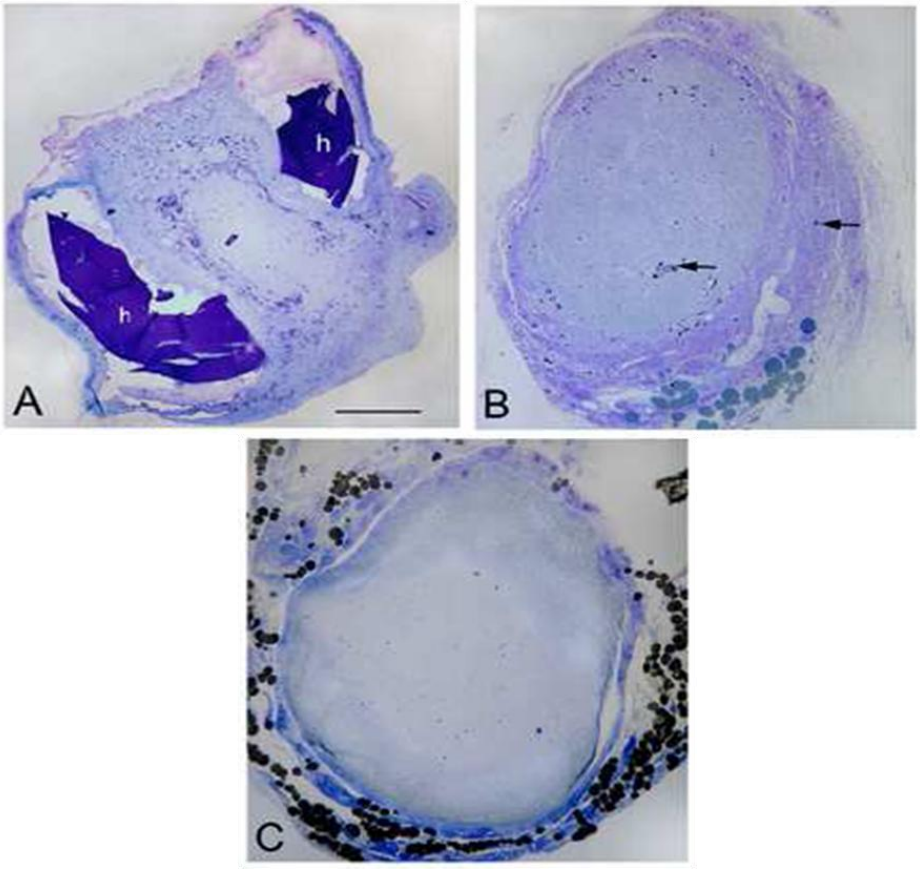

Figure 5.8. Toluidine-blue semi thin transverse section of regenerating nerves in the medial part of the nerve guide at 30 (A), 90 (B) and 180 (C) days post-surgery.

Morphological evaluations have been focused on 30 days after surgery, since the nerve regeneration was apparently satisfactory and not significantly different from that observed at 90 and 180 days post implantation. (Data from Dr. Magnaghi and Dr. Procacci)

The axonal regeneration at 30 days was confirmed by immunofluorescent analysis of longitudinal sections of the sciatic nerve stump through the conduit. Nerve fibers were labeleld in green with anti neurofilament M/H antibody and Schwann cells nuclei were stained in blue with nuclear marker DAPI. Figure 5.9-A shows the continuity of green labeling for the heavy chain of axon neurofilaments. A stronger neurofilament immunopositivity at 90 days post surgery was consistent with a higher, complete axonal regeneration (Figure 5.9-B).

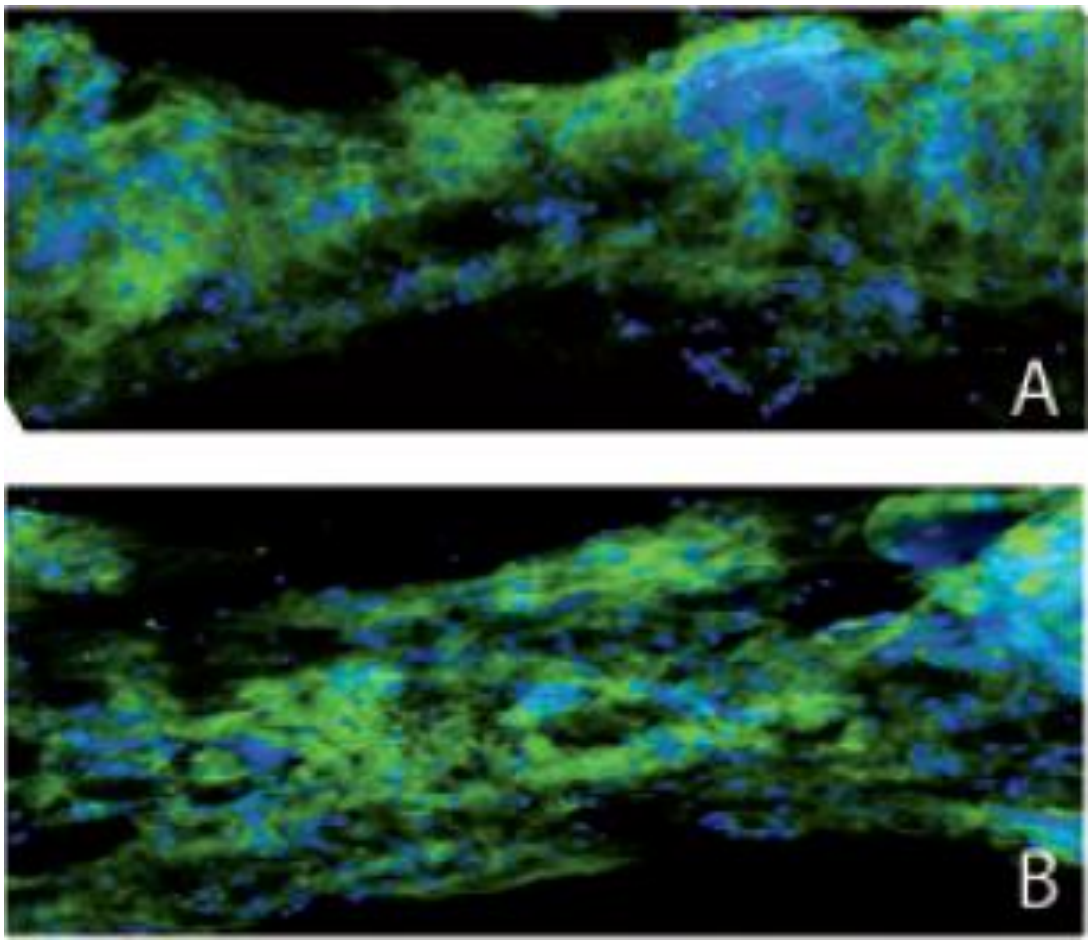

Figure 5.9. Immunofluorescence image of the regenerated nerve inside the hydrogel tube at 30 (A) and 90 (B) days post surgery.

The regenerated nerves showed several interesting signs of morphological improvements. Compared to the sham operated animal used as controls, which presented normal myelinated fiber (Figure 5.10), in the proximal part of the transected sciatic nerve, several thinly myelinated fibers and numerous proliferating Schwann cells were evident at 30 days post surgery, in accordance with an active regenerative process. Fiber compartmentalization was also observed, due to the interposition of connective tissue among nerve fibers. This phenomenon became more evident at 90 and 180 days (Figure 5.10-proximal). In the medial part of the regenerated nerve, covering the gap, some small fibers in active regeneration were present already at 30 days post surgery. At that time the conduit was still partially present (see Figure 5.7-A), and infiltration of macrophages was observed in the re-absorption areas (Figure 5.10-medial). At 90 and 180 days post surgery nerve morphology gradually improved, since the number of thinly myelinated fibers increased, and the myelin thickness resembled that of control animals. The distal stump of the transected sciatic nerve turned to be mostly affected by a fine fibrotic process and a neurodegenerative process called Wallerian degeneration[64,65] at 30 days post surgery. However, an active regenerative process was progressively evident at 90 and 180 days post surgery. In the distal part (Figure 5.10-distal), although this process resulted in only a small number of myelinated axons in comparison with the proximal and medial parts of the regenerated nerve. In the distal part collagen was abundant and organized in mini-compartments, which enveloped small groups of axons jointed in foci of regeneration (Figure 5.10-distal). The number of nerve fibers with normal diameter rose progressively up to 180 days post surgery, when the myelin thickness resembled that of sham operated animals (Figure 5.10).

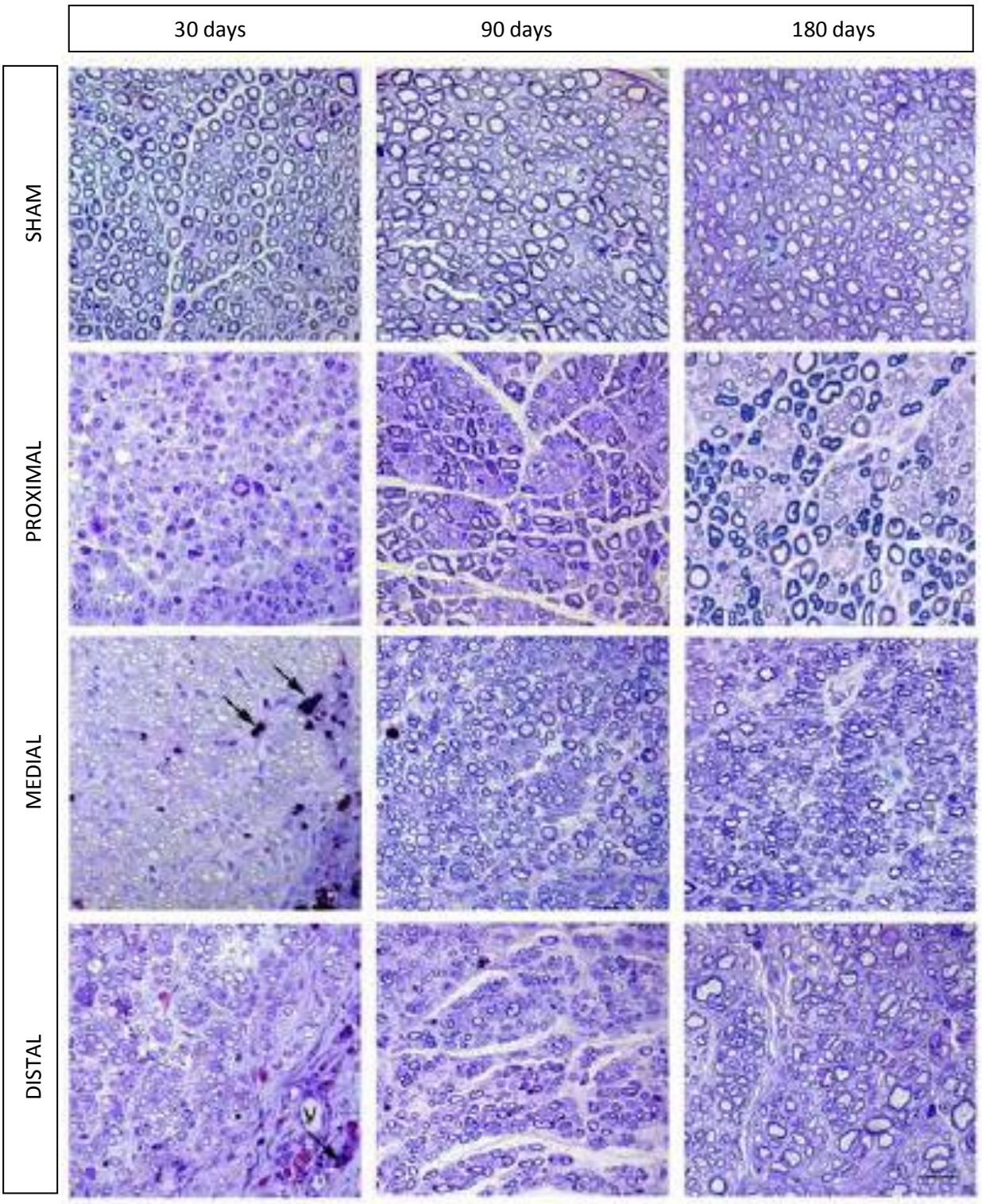

Figure 5.10. Semi thin traverse sections of sham operated nerves compared to the proximal, medial and distal part of the nerve guide of regenerating nerves at 30. 90 and 180 days post surgery.

Gait analysis and thermal sensitivity evaluation. The quality of functional recovery was further assessed performing the gait analysis, which is a standardized method to measure the motor coordination and synchrony. Unfortunately, except for the sham operated, the implanted animals showed a tendency for auto-mutilation of their digits in the operated limb, making this analysis extremely difficult. Consequently, we evaluated only the qualitative appearance of trails. As shown in Figure 5.11, 10 days after surgery sham rats show normal gait trail, while operated rats assumed a limping gait, with right dragging feet. At 1 month after surgery gait in operated resembled that of sham rats, either in term of stride length or stride width.

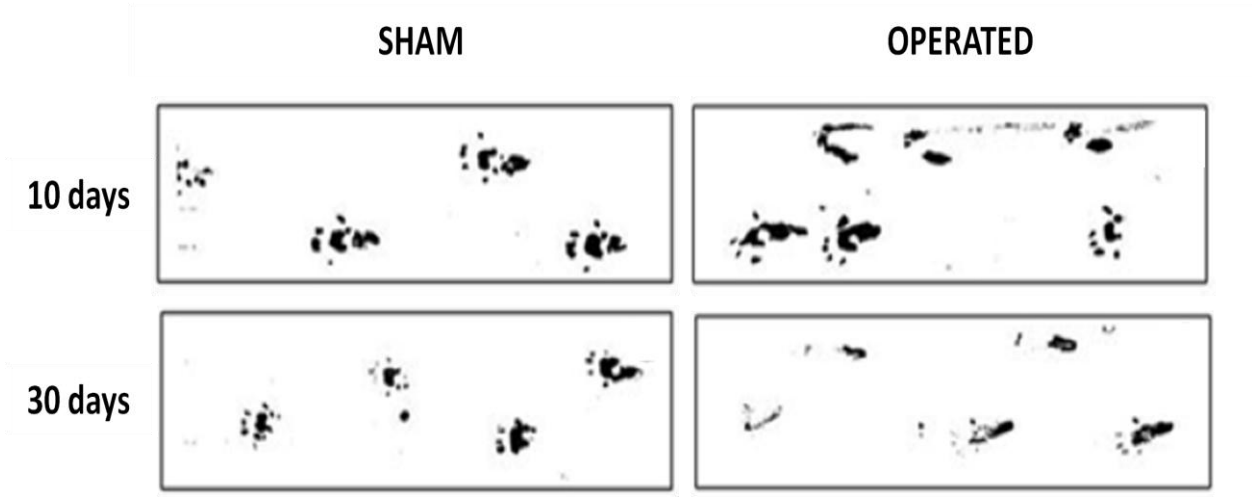

Figure 5.11. Representative footprints analysis performed on sham versus operated rats.

The thermal sensitivity test was used to evaluate the quality of functional recovery after transection, in particular the sensory nerve recovery. Thermal sensitivity was assessed at lower extremities using the plantar test, according to the Hargraves method (Figure 5.12). After a slight increase, sham operated rats showed a paw latencies lasting over times. Operated rats showed a decrease in paw latencies at 30 and 60 days after surgery, indicating an hyperalgesic state, which back to sham operated levels at later time analyzed.

Gait analysis and thermal sensitivity evaluations were performed by Dr. Magnaghi and Dr. Procacci.

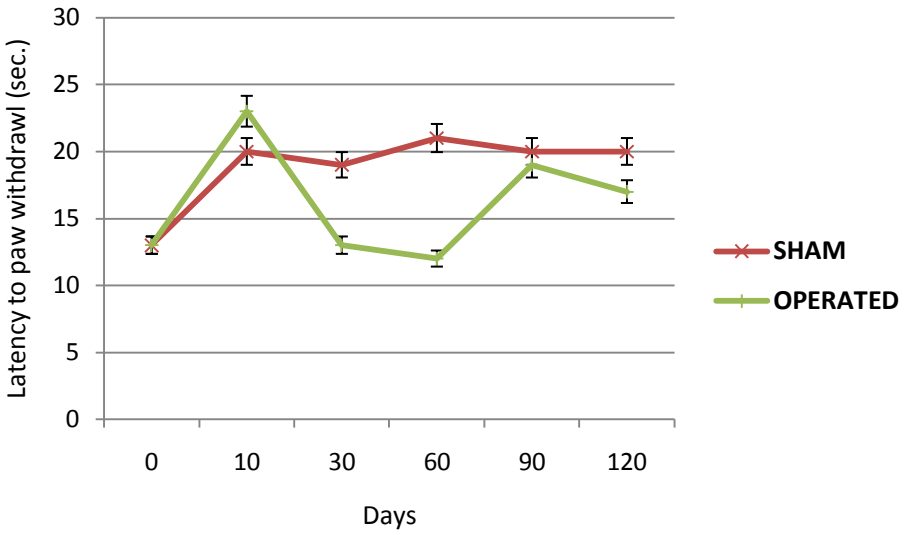

Figure 5.12. Functional evaluation of nerve regeneration by nociceptive analysis in sham versus operated rats.

5.4 CONCLUSIONS

In this work a novel Agma1-like hydrogel has been obtained by an alternative method consisting of the radical polymerisation of acrylamide-end capped Agma1 oligomers inside hollow cylinder molds in less than 2 hours. These hydrogels were remarkably less swollen in water and had improved mechanical strength if compared to the previous ones prepared using ethylenediamine as cross-linking agents. Agma1 tubular scaffolds were implanted in living rat as guide for sciatic nerve regeneration. Good surgical outcomes were achieved with no signs of inflammation or neuroma. Moreover, nerve regeneration was morphologically comparable to that of control animals and the quality of functional recovery satisfactory. Up to now, no PAA hydrogels have been tested as scaffold for in vivo tissue regeneration.

References:

1. Shieh, S.J.; Vacanti, J.P. *Surgery* **2005**, *137*, 1-7.
2. Italian Ministry of Health, National Center for Transplant, 2009-2010.
3. Langer, R.; Vacanti, J.P. *Science* **1993**, *260*, 920-926.
4. Vacanti, J.P.; Langer, R. *Lancet* **1999**, *354*, 32-34.
5. Langer, R.; Vacanti, J.P. *Sci. Am.* **1999**, *280*, 86-89.
6. Langer, R.; Vacanti, J.P. *Sci. Am.* **1995**, *273*, 130-133.
7. Yang, S.; Leong, K.F.; Du, Z.; Chua, C.K. *Tissue Eng.* **2001**, *7* (6), 679-689.
8. Freyman, T.M.; Yannas, I.V.; Yokoo, R.; Gibson, L.J. *Biomaterials* ***2001***, *22*, 1085-1093.
9. Guest, J.D.; Rao, A.; Olson, L.; Bunge, M.B.; Bunge, R.P. *Exp. Neurol.* **1997***, 148*, 502-522.
10. Marijnissen, W.; Osch, G. Van; Aigner, J.; Veen, S.W. van der; Hollander, A.P.; Verwoerd-Verhoef, H.L. *Biomaterials* **2002**, *23* (6), 1511-1517.
11. Pomahac, B.; Svensjo, T.; Yao, F.; Brown, H.; Eriksson, E. *Crit. Rev. Oral Biol. Med.* **1998**, *9*, 333-344.
12. Liu, S.; Peulve, P.; Jin, O.; Boisset, N.; Tiollier, J.; Said, G.; Tadie, M. *J. Neurosci. Res.* **1997**, *49*, 425-432.
13. Xu, X.; Zhang, S.X.; Li, H.; Aebischer, P.; Bunge, M. *Eur. J. Neurosci.* **1999**, *11*, 1723-1740.
14. Sieminski, A.L.; Padera, R.F.; Blunk, T.; Gooch, K.J. *Tissue Eng.* **2002**, *8* (4), 1057-1069.
15. Dar, A.; Shachar, M.; Leor, J.; Cohen, S. *Biotechnol. Bioeng.* **2002**, *80*, 305-312.
16. Nicolini Aldini, N.; Fini, M.; Rocca, G.; Giavaresi, G.; Giardino, R. *Int. Orthop.* **2000**, *24* (3), 121-125.
17. Lee, J.Y.; Lee, J.W.; Schmidt, C.E. *J. R. Soc. Interface* **2008**, 6, 801-810.
18. Dubin, R.A.; Callegari, G.; Kohn, J.; Neimark, A. *IEEE Trans. Nanobiosci.* **2008**, *7* (1), 11-14.
19. Malarkey, E.B.; Parpura, V. *Neurodegener. Dis.* **2007**, *4* (4), 292-299.
20. Cellot, G.; Clia, E.; Cipollone, S.; Rancic, V.; Sucapane, A.; Giordani, S.; Gambazzi, L.; Markram, H.; Grandolfo, M.; Scaini, D.; Gelain, F.; Casalis, L.; Prato, M.; Giugliano, M.; Ballerini, L. *Nat. Nanotechnol.* **2009**, *4*, 126-133.
21. Li, W.J.; Tuan, R.S. *Macromol. Symp.* **2005**, *227*, 65-75.

22. Godbey, W.T. *Aust. J. Chem.* **2005**, *58*, 689-690.
23. Alexander, C.; Shakesheff, K.M. *Adv. Mater.* **2006**, *18*, 3321.
24. Robinson, L.R. *Muscle Nerve* **2000**, *3* (6), 863-873.
25. Lee, S.K.; Wolfe, S.W. *J. Am. Acad. Orthop. Surg.* **2000**, *8* (4), 243-252.
26. Aebischer, P.; Guenard, V.; Winn, S.R.; Valentini, R.F.; Galletti, P.M. *Brain Res.* **1988**, *454*, 179-187.
27. Williams, L.R.; Varon, S. *J. Coump. Neurol.* **1985**, *231*, 209-220.
28. Williams, L.R.; Danielsen, N.; Muller, H.; Varon, S. *J. Coump. Neurol.* **1987**, *264*, 284-290.
29. Ansselin, A.D.; Fink, T.; Davey, D.F. *Neuropathol. Appl. Neurobiol.* **1997**, *23*, 387-398.
30. Koshimune, M.; Takamatsu, K.; Nakatsuka, H.; Inui, K.; Yamano, Y.; Ikada, Y. *Biomed. Mater. Eng.* **2003**, *72*, 223.
31. Atzet, S.; Curtin, S.; Trinh, P.; Bryant, S.: Ratner, B. *Biomacromolecules* **2008**, *9*, 3370-3377.
32. Midha, R.; Munro, C.A.; Dalton, P.D.; Tator, C.H.; Shoichet, M.S. *J. Neurosurg.* **2003**, *99*, 555.
33. Weiss, P. *Science* **1940**, *93*, 67-68.
34. Foidart-Dessalle, A.; Dubuisson, A.; Lejeune, A.; Seveyns, A.; Manassis, Y.; Delree, P.; Crielaard, J.M.; Bassleer, R.; Lejeune, G. *Exp. Neurol.* **1997**, *148* (1), 236-246.
35. Tseng, C.Y.; Hu, G.; Ambron, R.T.; Chiu, D.T. *J. Reconstr. Microsurg.* **2003**, *19*, 113-118.
36. Kim, Y.T.; Haftel, V.K.K.; Bellamkonda, S.R.V. *Biomaterials* **2008**, *29*, 3117.
37. Belkas, J.S.; Munro, C.A.; Shoichet, M.S.; Midha, R.; *Restor. Neurol. Neurosci.* **2005**, *23*, 19-29.
38. Nicoli Aldini, N.; Perego, G.; Cella, G.D.; Maltarello, M.C.; Fini, M.; Rocca, M.; Giardino, R. *Biomaterials* **1996**, *17*, 959-962.
39. Lundborg, G.; Dahlin, L.B.; Danielsen, N. *Scand. J. Plast. Reconstr. Surg. Hand Surg.* **1991**, *25*, 79-82.
40. Merle, M.; Dellon, A.L.; Campbell, J.N.; Chang, P.S. *Microsurgery* **1989**, *10*, 130-133.
41. Lundborg, G.; Rosen, B.; Dahlin, L.; Holmberg, I.; Rosen ,J. *J. Hand Surg.* **2004**, *29* (2), 100-107.
42. Braga-Silva, J. *J. Hand. Surg.* **1999**, *24*, 73-77.
43. Belkas, J.S.; Shoichet, M.S.; Midha, R. *Neurol. Res.* **2004**, *26* (2), 151-160.
44. Hudson, T.W.; Evans, G.R.; Schmidt, C.E. *Clin. Plast. Surg.* **1999**, *26*, 617-628.
45. Doolabh, V.B.; Hertl, M.C.; Mackinnon, S.E. *Rev. Neurosci.* **1996**, *7*, 47-84.

46. Soldani, G.; Varelli, G.; Minnocci, A.; Dario, P. *Biomaterials* **1998**, *19*, 1919-1924.

47. Nicoli Aldini, N.; Fini, M.; Rocca, M.; Giavaresi, G.; Giardino, R. *Int. Orthop.* **2000**, *24*, 121-125.

48. Young, R.C.; Wiberg, M.; Terenghi, G. *Br. J. Plast. Surg.* **2002**, *55*, 235-240.

49. Gamez, E.; Goto, Y.; Nagata, K.; Iwaki, T.; Sasaki T.; Matsuda, T. *Cell Transplantation* **2004**, *13* (5), 549-564.

50. Prang, P.; Muller, R.; Elijaouhari, A.; Heckmann, K.; Kunz, W.; Weber, T.; Faber, C.; Vroemen, M.; Bogdahn, U.; Weidner, N. *Biomaterials* **2006**, *27*, 3560-3569.

51. Yao, L.; de Reiter, G.C.W.; Wang, H.; Knight, A.M.; Spinner, R.J.; Yaszemski, M.J.; Windebank, A.J.; Pandit, A. *Biomaterials* **2010**, *31*, 5789-5797.

52. Runge Brett, M.; Dadsetan, M.; Baltrusaitis, J.; Ruesink, T.; Lu, L.; Windebank, A.J.; Yaszemski, M.J. *Biomacromolecules* **2010**, article ASAP.

53. Belkas, J.S.; Munro, C.A.; Shoichet, M.S.; Johnston, M.; Midha, R. *Biomaterials* **2005**, *26*, 1741-1749.

54. Gunn, J.W.; Turner, S.D.; Mann, B.K. *J Biomed Mater Res A* **2005**, *72* (1), 91-97.

55. Ferruti, P.; Bianchi, S.; Ranucci, E.; Chiellini, F.; Piras, A.M. *Biomacromolecules* **2005**, *6* (4), 2229-2235.

56. Jacchetti, E.; Emilitri, E.; Rodighiero, S.; Indrieri, M.; Gianfelice, A.; Lenardi, C.; Podestà, A.; Ranucci, E.; Ferruti, P.; Milani, P. *Journal of Nanobiotechnology* **2008**, *6,* 14.

57. Emilitri, E.; Guizzardi, F.; Lenardi, C.; Suardi, M.; Ranucci, E.; Ferruti, P. *Macromol. Symp.* **2008**, *266*, 41-47.

58. Ferruti, P.; Franchini, J.; Bencini, M.; Ranucci, E.; Zara, G.P.; Serpe, L. *Biomacromolecules* **2007** , *8* (5), 1498-1504.

59. Franchini, J.; Ranucci, E.; Ferruti, P.; Rossi, M.; Cavalli, R. *Biomacromolecules* **2006**, *7* (4), 1215-1222.

60. Dos Reis, G.; Fenili, F.; Gianfelice, A.; Bongiorno, G.; Marchesi, D.; Scopelliti, P.E.; Borgonovo, A.; Podestà, A.; Indrieri, M.; Ranucci, E.; Ferruti, P.; Lenardi, C.; Milani P. *Macromolecular Bioscience* **2010**, *10*, 842-852.

61. Ferruti, P.; Ranucci, E.; Trotta, F.; Gianasi, E.; Evagorou, G.E.; Wasil, M.; Wilson, G.; Duncan, R. *Macromol. Chem. Phys.* **1999**, *200*, 1644-1654.

62. Klapdor, K.; Dulfer, B.G.; Hammann, A.; Van der Staay, F.J. *J. Neurosci. Methods* **1997**, *75* (1), 49-54.

63. Hargreaves, K.; Dubner, R.; Brown, F.; Flores, C.; Joris, J. *Pain* **1988**, *32* (1), 77-88.

64. Mukhatyar, V.; Karumbaiah, L.; Yeh, J.; Bellamkonda, R. *Advanced Materials* **2009**, *21*, 4670-4679.

65. Stoll, G.; Muller, H.W. *Brain Phatology* **1999**, *9*, 313-325.

CHAPTER 6

NEW CATIONIC POLY(AMIDOAMINE) AS NON-VIRAL VECTORS FOR GENE THERAPY [1,19,29,30,43,44,47]

6.1 INTRODUCTION

Gene therapy can be defined as the treatment of human disease by the transfer of genetic material into specific cells of the patient[1]. Initially, gene therapy was viewed as an approach for treating hereditary diseases, but its potential role in the treatment of genetic diseases such as hemophilia[2], muscular dystrophy[3-5] or cystic fibrosis[6] is now widely recognized. However, the gene therapy approaches are also being developed for treatments of virtually all forms of cardiovascular diseases[7], neurological diseases[8-10], infectious diseases[11], wound healing[12] and cancer[13-15]. In these instances, the delivered genes may be intended to augment naturally occurring proteins (e.g growth factors or cytokines), to alter the expression of existing genes facilitating a desired cellular or tissue response, or to produce cytotoxic proteins or pro-drug-activating enzymes, for example, to kill tumor cells in the cancer treatment.

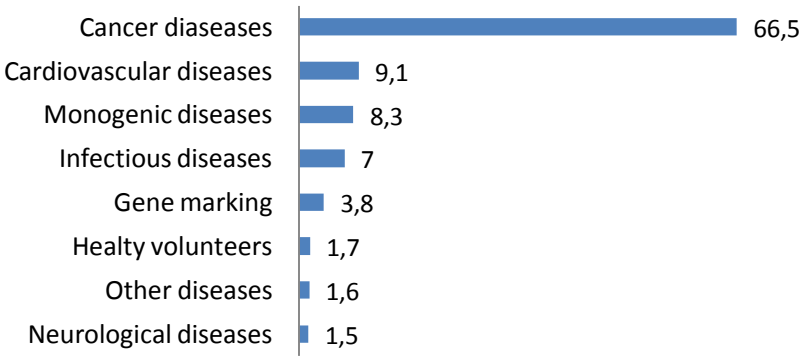

Figure 6.1. Gene therapy clinical trials.

Historically, there have been three different approaches applied to gene delivery. The first approach consists on the use of naked DNA. Direct injection of free DNA to the tumor site has been shown to produce high levels of gene expression and the simplicity of this approach led to its use in a number of experimental protocols[16,17]. This strategy appears to be limited to tissues that are easily accessible by direct injection such as the skin and muscles[18] and is unsuitable for systemic delivery due to the presence of serum nuclease. The second approach involves genetically altered viruses. Viral vectors are biological systems derived from naturally evolved viruses capable of transferring their genetic materials into the host cells. Viruses can be transformed into gene delivery vehicles by removing part of the virus genome and replacing it with a therapeutic gene. If done carefully, the resulting recombinant virus will retain the functions essential for infection of specific target cells, but will be rendered incapable of replication and, hence, will be nonpathogenic. Many viruses including the retrovirus, adenovirus, herpes simplex virus and adeno-associated virus have been modified to eliminate their toxicity and maintain their high capacity for gene transfer[19] hence presenting various advantages[20-22]. Despite the high efficiency of viral vector in vitro, clinical trials are often limited by several concerns such as toxicity, immunogenicity, inflammatory properties, the limited size of the DNA, production and packing problems, and the high cost. In addition, an overwhelming immune reaction against adenovirus occurred in a patient at Pennsylvania University in 1999[23,24] and a leukemia-like disease were reported in a French patient in 2002[25,26]. The third approach for delivery systems concerns non-viral vectors, which are mainly of a cationic nature. Such materials have included cationic peptides, proteins, polymers, and liposomes. Various synthetic vectors, including (diethylamino)ether-dextran[27] and calcium phosphate[28], have been extensively used for in vitro gene transfer studies since 1960s. In general, polymeric vectors are materials that bind electrostatically to DNA or RNA, condensing the genetic material into nanometer-scale polyplexes (a few tens to several hundred nanometers in diameter) that protect the genes and allow them to enter cells.

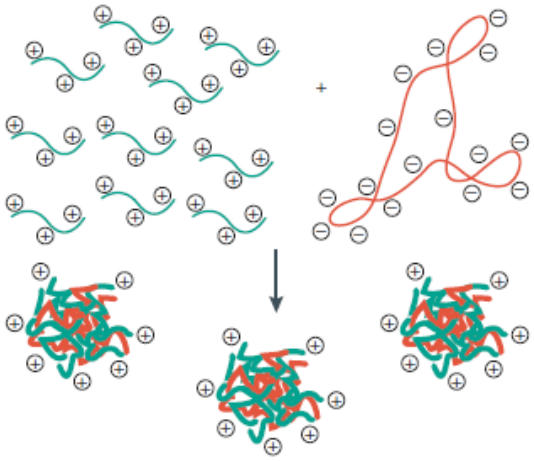

Figure 6.2. Example of poliplex formation.

For effective polyplex-mediated gene delivery, the cationic polymer carrier has to fulfill a series of drug delivery functions in the extracellular and intracellular transport of the DNA vector. When polyplexes encounter the cells, they may interact with the negatively-charged cellular membrane and are taken up into the cells via endocytosis. In the intracellular environment, the polyplexes are normally located in endosomes that become acidified and finally fuse with lysosomes.

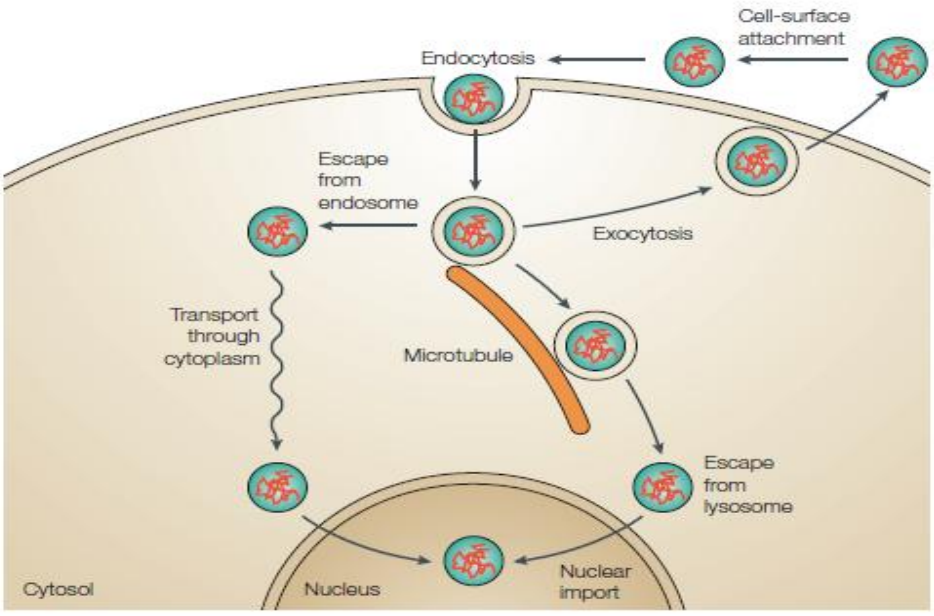

Figure 6.3. Schematic illustration of cationic polymer-mediated gene delivery (Image from Reference 47).

In this case, DNA is prone to degradation by lysosomal enzymes. In order to transfer their DNA cargo successfully to the nucleus, polyplexes must escape from the endosome by some transmembrane mechanism or endosomolytic process such as the "proton sponge effect"[29]. After endosomal escape, polyplexes are located in the cytoplasm where, at present, their fate is not fully understood. However, it is clear that the polyplexes have to unpack DNA to deliver it to a suitable site near the nucleus or in the nucleus. In addition, the polymer should be nontoxic, non-immunogenic and biodegradable.

Although cationic polymers are regarded as promising vectors for non-viral gene delivery for many years, their clinical application is limited by the relatively low transfection efficacy. Different from viral vectors, simple cationic polyplexes do not possess all the mechanisms to efficiently overcome the extra- and intracellular barriers encountered in the temporal-spatial pathway to gene transfection. To overcome this problem many types of polymers have been specifically designed for use as gene delivery vectors. In many cases, the polymers were designed to address one of the perceived gene delivery barriers described above.

Polylysine (PLL) was one of the first cationic polymers to be used in the modern era of gene delivery research[30]. Polyplexes of DNA and polylysine itself are poor gene-delivery vectors and require the addition of exogenous endosomolytic agent for even moderate transfection activity. Early studies on polylysine were promising, but it now seems unlikely that polylysine-based polyplexes will find clinical applications because of their relatively low efficiency. This is generally accepted to be the result of poor escape from the endocytic pathway. In recent years, polylysine has been relegated to a role in mechanistic studies or as a point of comparison to more promising polymers.

Poly(ethylenimine) (PEI), one of the most effective gene-delivery polymers studied to date, has been used as a gene-delivery vector since 1995[29]. Importantly, PEI mediates gene delivery efficiently in the absence of any exogenous endosomolytic agent.

The relatively high gene-transfer activity of PEI is believed to be due in large part to efficient escape from the endocytic pathway through the proton-sponge mechanism[29,31]. However, the high amount of positive charges and their non-biodegradability resulted in a fairly high toxicity of PEI polymers in vivo[32].

Dendrimers are spherical, highly branched polymers. The most currently used dendrimers are polyamines, polyamides or polyesters, but the most commonly encountered are polyamidoamine (PAMAM) dendrimers because of their high transfection efficiency. Dendrimers bear primary amine groups on their surface and tertiary amine groups inside. The primary amines participate in DNA binding, compact it into nanoscale particles and promote its cellular uptake, while tertiary amine groups act as a proto-sponge in endosome and enhance the release of DNA into the cytoplasm. Due to their relatively high gene-delivery efficiency and good biocompatibility compared to PEI, PAMAM dendrimers have recently been used in several in vivo gene-delivery studies[33,34].

Many others synthetic polymers, such as poly(2-(dimethylamino)ethyl methacrylate), PEG and poly(β-aminoester) are now under investigation as transfection promoters.

Different PAA polymers have been tested in the past as gene delivery systems. The ability of linear PAAs to promote the transfection in vitro of HEPG2 cells by pSV-β galactosidase was first demonstrated for ISA1 and ISA23-like polymers[35]. Interestingly, ISA 23 was equi-effective when compared with PEI and LipofectIN and more effective than Lipofect-ACE. When protonated at pH 6.5, PAAs inherently destabilize endosomal membranes and this is consistent with the mechanisms of polycation-mediated bilayer destabilization seen using polymers such as PLL. Moreover, in contrast to PLL and PEI, PAAs showed pH-dependent hemolysis. In particular, they caused more hemolysis at pH 5.5 (the lysosomal pH) than at pH 7.4. The given explanation, was that lowering the pH led to protonation of the polymer backbone, increasing its capacity to interact with the anionic red blood cell membrane and, consequently, to cause concentration dependent membrane perturbation.

For this reason, it was supposed that the same PAAs could make the intracellular trafficking of DNA and proteins easier by promoting their escape from endosomes into the cytosol. Subsequently, other PAAs have been considered as transfection promoters[36-39].

Several PAAs with pendant primary amines were synthesized by Michael polyaddition of different diamine to N,N-methylenebisacrylamide and proved able to condense plasmid DNA in nanosized polyplexes by electrostatic interactions. The trasnfection efficiency of some of these polymers was comparable to that of commercial branched PEI 25000[40].

Disulfide-containing cystaminebisacrylamide was employed as a co-monomer yielding PAAs with variable amounts of bioreducible disulfide linkages in the main chain. Transfection experiments with COS-7 cells showed that polyplexes from PAAs with disulfide linkages gave significant higher transfection than those from PAAs lacking the disulfide linkage. Variation of the disulfide content revealed that polyplexes of PAA copolymers with appropriate disulfide content have largely improved biophysical properties, yielding enhanced levels of gene expression along with low toxicity[41].

Pendant thiol moieties have been incorporated into PAA homopolymer and a PEG-PAA-PEG copolymer as a self-assembling system. When mixed with DNA, small monodisperse sterically stabilized particles were formed in quantity yields. This cross-linked formulation has been successfully tested in both freshwater and estuarine field trials as a water tracer[42].

Although these polymers showed promising results in terms of transfection efficacy, their cytotoxicity is still not acceptable for in vivo applications.

Recently, a new linear and amphoteric but prevailing cationic PAA, nicknamed Agma1 has been successfully tested as trasfection promoters in vitro on Hela cells[43-44]. This polymer is completely non-toxic, with an IC_{50}> 5 g/mL on HT29 cells despite its polycationic behavior and is not appreciably hemolytic both at pH 7.4 and at pH 4.0. These peculiar properties are probably due to the structural similarities of Agma1 with the tripeptide arginine-glycine-aspartic (RGD sequence).

The aim of this work is to evaluate the effect of the molecular weight of three Agma1 samples, named Agma5, Agma10 and Agma20 with lower (Agma5) and higher (Agma10 and Agma20) molecular weight as transfection promoters.

Finally, the most effective sample has been tested in vivo. Up to now, however, no PAAs have been reported as in vivo DNA carriers.

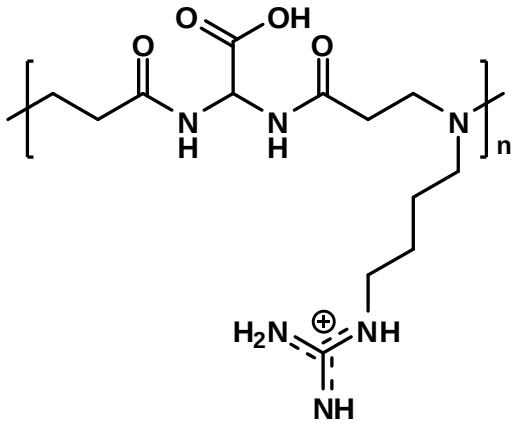

Figure 6.4. Structure of Agma1-like polymer.

6.2 EXPERIMENTAL PART

Instruments

^{1}H and ^{13}C NMR spectra were run on a Brüker Advance 400 spectrometer operating at 400.132 (^{1}H) and 100.623 (^{13}C) MHz. Size exclusion chromatography traces were obtained with a Knauer Pump 1000 equipped with a Knauer Autosampler 3800, TSKgel G4000 PW and G3000 PW TosoHaas columns connected in series, Light Scattering Viscotek 270 Dual Detector and a refractive index detector Waters model 2410. The mobile phase was a 0.1 M Tris buffer pH 8.00 ±0.05 with 0.2 M sodium chloride. The flow rate was 1 mL/min and sample concentration 1% w/w. Fluorimetric measurements were performed with an RF 551 Shimadzu fluorimeter.

Materials and methods

Ultra-pure water was obtained using a 1-800 Milli-Q (Millipore) system. Fluorescein 5-isothiocyanate (FITC), ethidium bromide and Etoposide were purchased from Fluka. DNase I was supplied by Sigma. Plasmidic DNA was purified with Qiagen Midiprep Kit. Agarose was purchased from BIO-RAD Laboratories S.r.l and JetPEI from Polyplus-Transfection. All other reagents (ACS grade) were from Sigma-Aldrich and were used as received. High-performance liquid chromatography solvents were from Carlo Erba. 2,2-Bis(acrylamido)acetic acid (BAC) was synthesized as described in literature and its purity (99,7%) determined titrimetrically[45].

Synthesis of Agma5, Agma10 and Agma20 [43]. Agmatine sulfate (2.000 g; 8.5 mmol) and lithium hydroxide monohydrate (0.360; 8.5 mmol) were added to a solution of BAC (1.689 g; 8.5 mmol) and lithium hydroxide monohydrate (0.360 g; 8.5 mmol) in distilled water (2.8 mL). This mixture was maintained under nitrogen atmosphere and occasionally stirred for 48 (AGMA5), 78 (AGMA10), or 240 (AGMA20) hours. After this time, it was diluted with water (2.8 mL), acidified with hydrochloric acid to pH 4-4.5, and then ultrafiltered through membranes with nominal cut-off 3000 (AGMA5), 5000 (AGMA10) and 10000 (AGMA20), respectively. The fractions retained in each case were freeze-dried and the product obtained as a white powder. Yields: 2.1 g, 1.9 g and 1.75 g. ^{13}C NMR (D_2O): δ= 173.5 (CH-***C***OOH); 171.3 (NH-***C***O); 155.1 (NH_2***C***NN guanidine group); 56.0 (COOH-***C***H); 52.5 (NH***C***H_2 agmatine monomer); 49.1 (NHCO***C***H_2 polymer backbone); 40.4 (CH_2N***C***H_2 agmatine monomer); 28.9 (NHCOCH_2***C***H_2 polymer backbone); 25.0 (NHCH_2***C***H_2 agmatine monomer); 22.3 (NHCH_2CH_2***C***H_2 agmatine monomer). ^{1}H NMR (D_2O): δ= 5.55 (s, 1H, COOH-C***H***); 3.44 (br, 2H, NHCOC***H_2*** polymer backbone); 3.19 (m, 4H, NHC***H_2*** and NC***H_2*** agmatine monomer); 2.79 (br, 2H, NHCOCH_2C***H_2*** polymer backbone); 1.76 (br, 2H, NHCH_2C***H_2*** agmatine monomer); 1.61 (br, 2H, NHCH_2C***H_2*** polymer backbone). Molecular weight values: Agma5: $\overline{M}_n$ =3300, $\overline{M}_w$ =4500, PD=1.38; Agma10: $\overline{M}_n$ =7800, $\overline{M}_w$ =10100, PD=1.29; Agma20: $\overline{M}_n$ =16400, $\overline{M}_w$ =20500, PD=1.25.

Synthesis of fluorescent Agma10 (FITC-Agma10)[44]. Labeled AGMA10 (FITC-AGMA10) was prepared by treating with a FITC solution in methanol (0.2 mg/mL) a 10 mg/mL solution in buffer pH 7.4 of an AGMA10 sample (AGMA10-NH_2) carrying amine groups as side substituents. In turn, AGMA10-NH_2 was obtained by substituting 7% on a molar basis of mono(*tert*-butoxycarbonyl)ethylenediamine for agmatine. The mixture was stirred overnight at room temperature and then centrifuged to eliminate insoluble impurities. The resultant clear solution was then dialyzed and the fluorescein-labeled polymer isolated by freeze-drying the retained portion. The recovery was practically quantitative. The conjugation of AGMA10-NH_2 with FITC was confirmed by NMR and fluorescence microscopy and the efficiency of the labeling procedure was determined by measuring the fluorescence intensity at λ_{ex}=480 nm and λ_{ex}=520 nm of a solution of FITC-AGMA10 of known concentration versus a standard FITC solution.

ζ-potential measurements. The ζ-Potential values of AGMA5, AGMA10 and AGMA20 were determined in aqueous solutions at increasing pH values, ranging from 4.0 to 7.4, to verify the polymer charge distribution as function of the pH. A 90 Plus Brookhaven instrument was used to determine the electrophoretic mobility and the ζ-Potential of the three polymers. For the determinations, the aqueous solutions of the polymers were placed in the electrophoretic cell, where an electric field of about 15 V/cm was applied. Each value reported is the average of ten measurements. The electrophoretic mobility measured was converted into ζ-Potential using the Smoluchowsky equation[46].

Preparation of the DNA complexes. The DNA/AGMA complexes were prepared at different pH values. PAA aqueous solutions (1.6 mg/mL) were added under stirring to plasmidic DNA solutions (30 μg/mL) in 20 mM HEPES buffer pH 7.4 or lower, adjusted by adding diluted hydrochloric acid. Different w/w DNA/polymer ratios, namely, 1:5, 1:10, 1:15, 1:20 and 1:30 were used for AGMA5, AGMA10 and AGMA20. In the case of AGMA5 two further ratios, that is, 1:90 and 1:100, were tested.

In all cases, complexes were incubated for 30 minutes at room temperature before characterization.

Characterization of the DNA complexes. The average diameters and polydispersity indices of the DNA/AGMA complexes were determined by photocorrelation spectroscopy (PCS) using a 90 Plus Brookhaven instrument at a fixed angle of 90° and a temperature of 25 °C. Each reported value is the average of five measurements of three different samples. The electrophoretic mobility and ζ-Potential were determined, as previously described in the case of polymers. The morphology of DNA complexes was determined by Transmission Electron Microscopy (TEM). TEM analyses were carried out using a Philips CM10 instrument. DNA/AGMA complexes in solution were dropped onto a Formwar-coated copper grid and dried before observation.

Gel retardation assay. Gel electrophoresis assay was used to evaluate the formation of DNA/AGMA complexes. The complexes were subjected to electrophoresis on agarose gel (0.7 % w/v) with ethidium bromide (0.25 µg/mL) for 1 hour at 100V to confirm the DNA complexation. The banding pattern was obtained using a UV transilluminator and photographed with a Polaroid camera.

DNase degradation assay. To determine the complex ability to protect DNA from enzymatic degradation, DNA (10 µg/mL) and the DNA complexes (1 mg/mL) were incubated at 37 °C with DNase I (1000 units/mL) in phosphate buffer pH 7.4. At fixed times (up to 1 hour) samples were withdrawn, centrifuged and the supernatants analyzed at 260 nm using a Perkin-Elmer Lambda II UV spectrophotometer. Results were expressed as a percentage of the control degradation (naked DNA).

In vitro biological evaluation

Hemolytic activity. Hemolytic activity of AGMA5, AGMA10 and AGMA20 was studied on human blood. Increasing amounts of the polymers up to 15 mg/mL were added to a suspension of erythrocytes (30% v/v) in phosphate buffer pH 7.4 and then incubated for 90 minutes at 37 °C. A suspension containing only a 30% v/v of erythrocytes in phosphate buffer pH 7.4 was used as blank. Another suspension added with an excess of ammonium chloride was used to obtain complete hemolysis as 100% hemolytic control. After centrifugation at 2000 rpm for 5 minutes the supernatants were analyzed using a Lambda 2 Perkin-Elmer spectrophotometer at a wavelength of 543 nm. The percentage of hemolysis was calculated versus the 100% hemolysis control.

Cytotoxicity of AGMA polymers. The in vitro cytotoxicity of the polymers was evaluated on Hela cell using the MTT test. Appropriate dilution was made in order to obtain a concentration of 2x 10^4 cells/mL in culture medium. The measurement was performed at 24 and 48 hours using different concentrations of polymers. The viability of the treated cells was compared to untreated cells and to cells treated with Etoposide (0.1 µg/µL) as negative compound.

Cytotoxicity of DNA/AGMA complexes. The cytotoxicity of the DNA/polymer complexes was evaluated by MTT assay. Cells were cultured for 24 and 48 hours after transfection then 0.2 mg/mL of MTT in DMEM medium without Phenol Red was added. After 3 hours of incubation with MTT the supernatant was removed and 200 µL of DMSO added to dissolve the formazan crystal. Optical density value of each sample was measured at wavelength of 595 nm. All experiments were performed in triplicate.

In vitro DNA transfection studies. Transfection experiments were performed on Hela cell lines. Hela cells line was grown in DME (Cambrex) supplemented with 10% FCS, 2 mM L-Glutamine (Cambrex) and antibiotics. Cells were transfected in 6-wells plate at $4.5x10^5$ cells per well. The DNA (pEGFP) and the polymers were pre-incubated in a 150 nM NaCl solution pH 5.5 for 30 minutes at room temperature. The DNA quantity used for transfections in 6 and 24-wells plate were 3.5 and 0.7 µg respectively. Before transfection, cells medium was replaced with serum-free medium and the complex of transfection was added the culture medium for 3 hours.

Nuclear localization of DNA/AGMA10 complexes. After transfection, cells were washed, fixed with 4% paraformaldehyde for 10 minutes, stained with DAPI, mounted and analyzed with a confocal laser-scanning microscope (TCS SP2 with DM IRE2; Leica) equipped with 63X/1.40 HCX Plan-Apochromat oil-immersion objective. Confocal images are maximun projections of a z section of ≈3 µm. Nuclear localization was quantified with high resolution confocal images stacks reconstructed by isosurface rendering using Imaris software (version 6.2.0, Bitplane, AG). Isosurface is a computer generated representation of specified range of fluorescence intensities that allows the creation of an artificial solid object of a specific area.

In vivo biological evaluation

In vivo administration of DNA/AGMA10 complexes. Preliminary in vivo experiments were performed on 6-10 weeks old Balb/c mice. To four groups of six mice 10 µg DNA (pEGFP) as 100 µL solution in 5% w/w glucose of 1:30 DNA/AGMA10 polyplex prepared at pH 6.0 was injected in the tail vein. Free DNA and AGMA10 solutions at the same concentrations were used as controls. Three mice of each group were sacrificed at 24 hoursvand three at 48 hours after the intravenous administration, and samples of liver, heart, kidney and lungs collected. All tissues were washed with saline and freezed. Then they were homogenized in PBS solution pH 7.4 using a Politron homogenizer before the evaluation of the in vivo gene expression.

The animal experiments complied with the rules set forth in the NIH Guide for the Care and Use of Laboratory Animals.

Western blot experiments. Total proteins were extracted in Laemmli buffer (62.5 mM Tris-HCl pH 6.8, 2% SDS, 10% glycerol), quantified and equal amounts of each sample were resolved by SDS-PAGE and transferred to PVDF membrane. After blocking with TBS/0.1% Tween 20/5% BSA, membranes were incubated with primary antibody over-night at 4 °C. Primary antibodies were: α-Akt, α-GFP , α-tubulin and α-actin. Immunoreactive proteins were identified with secondary antibody coupled to horseradish peroxidase (HRP) antibody and visualized by ECL.

6.3 RESULTS AND DISCUSSION

In this work, three samples of an amphoteric Agmatine-containing PAA of the same structure, but different molecular weights, named AGMA5, AGMA10 and AGMA20, were tested as nucleic acid carriers. In a previous work, we found that the repeating unit of AGMA polymers contains three ionizable groups, a strong acid (pK_a= 2.3), a medium-strength base (pK_a= 7.4) and a strong base ($pK_a \geq$ 12.1). As a consequence, this polymer is prevailing cationic up to pH 10.5. At pH 7.4 the average positive charge is 0.55 per unit. In spite of that, AGMA polymers proved nontoxic and nonhemolytic in vitro and exhibited a good transfection efficiency, suggesting a significant ability of transporting a DNA payload in the cytoplasm of cells not related to any measurable membranolytic activity[43]. This feature is hardly influenced by the molecular weight of the sample, as it depends primarily from the chemical groups present in the repeating units. To establish the relationship between the molecular weight of the samples and their gene transfer ability, we carried out transfection experiments in vitro on Hela cells using three AGMA samples that were prepared by Michael polyaddition of 4-aminobutylguanidine (Agmatine) to 2,2-bis(acrylamidoacetic) acid in water.

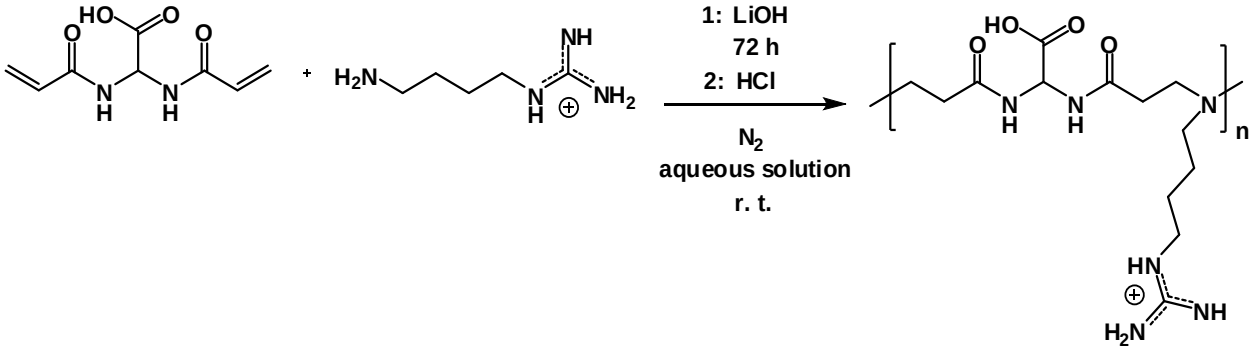

Scheme 6.1. Synthetic pathway leading to AGMA polymers.

The molecular weights of the samples were tuned adopting different reaction times and different cut-off membranes for the final ultrafiltration step during isolation. Table 6.1 reports the SEC results of the three AGMA samples.

Table 6.1. Molecular weight data of AGMA polymers.

Sample	$\overline{M}_n$	$\overline{M}_w$	PD
AGMA5	3700	5100	1.38
AGMA10	7800	10100	1.29
AGMA20	16400	20500	1.29

These values should be compared with those of the previously studied AGMA1 sample: $\overline{M}_n$ = 4800, $\overline{M}_w$ = 7200, PD=1.50. It is noteworthy that the new samples studied in this work had a lower polydispersity (PD) value.

Preparation and characterization of DNA/Agma complexes, as well as, in vivo and in vitro biological evaluation were performed in collaboration with Prof. Cavalli and co-workers.

All samples were positively charged in aqueous solution at pH 7.4 and the positive charge increased by lowering the pH to 4.0. The ζ-Potential values relative to AGMA10, are reported in Table 6.2. The values obtained with AGMA5 and AGMA 20 were similar.

Table 6.2. ζ-Potential values of AGMA10 at different pH values.

ζ-Potential (mV)				
	pH= 4.0	**pH= 5.0**	**pH= 6.0**	**pH= 7.4**
AGMA10	+21.00 ± 1.16	+15.32 ± 0.74	+11.10 ± 0.52	+2.10 ± 0.37

No significant hemolytic activity was observed for all AGMA samples after 90 minutes incubation in blood at pH 7.4 up to a concentration of 15 mg/mL. Moreover, the three polymers showed no cytotoxic effects on Hela cells after 48 hours incubation up to a concentration of 7 mg/mL.

All the samples were able to complex DNA at different weight ratios and pH values forming nanoparticles with spherical shape.

The lower molecular weight sample, AGMA5, under the conditions adopted formed larger polyplex nanoparticles than AGMA10 and AGMA20, suggesting a weaker or incomplete binding ability. In particular, AGMA10 and AGMA20 polyplexes had sizes lower than 100 nm, which varied according to the DNA/polymer ratio, but did not increase over time, nor after freezing and did not change morphology. This size is considered suitable for cell internalization both in vitro and in vivo.

A moderate excess of AGMA (5:1) shifts the negative ζ-Potential of DNA to positive values already at pH 7.4.

The results of the ζ-Potential and the avarege diameters and polydispersity index of the AGMA/DNA complexes are reported in Table 6.3.

Table 6.2. ζ-Potential values and Average diameters and polydispersity index of AGMA/DNA complexes at different pH values and different weight/weight ratio.

Sample	DNA/AGMA Ratio ($^{w}/_{w}$)	ζ-Potential (mV)			Average diameters and PD index (nm)			
		pH= 4.0	pH= 6.0	pH= 7.4	pH= 5.0		pH= 7.4	
					Avarage Diameter	PD Index	Avarage Diameter	PD Index
DNA/AGMA 5	1:5	+12.3±0.77	+8.55±0.65	+3.23±1.0	108.2±3.2	0.26	450±10.0	0.23±0.02
	1:15	+18.23±0.81	+17.29±0.60	+5.23±0.70	189.3±4.7	0.30	310±5.0	0.22±0.01
	1:30	+23.81±1.25	+20.16±0.77	+13.29±0.88	197.5±4.3	0.30	333±21.3	0.15
DNA/AGMA 10	1:5	+17.62±0.63	+11.44±0.77	+5.23±0.70	85.2±5.6	0.10	161±15.4	0.20
	1:15	+19.53±0.81	+17.95±0.60	+6.11±0.46	78.9±1.2	0.12	158±9.4	0.18
	1:30	+27.61±1.25	+18.70±1.5	+13.29±0.46	72±2.3	0.10	148±0.52	0.21
DNA/AGMA 20	1:5	+24.20±1.25	+10.5±1.91	+5.62±0.86	107.3v5.9	0.33	271.9±20.8	0.25
	1:15	+29.31±0.92	+18.71±0.41	+9.34±0.54	95±3.4	0.18	115±10.8	0.16
	1:30	+31.61±1.07	+21.04±1.74	+13.54±0.74	89.5±7.9	0.18	94.6±22.3	0.21

Direct observation by TEM revealed that the DNA/AGMA polyplexes were obtained in the form of discrete nanospheres (Figure 6.5), whose average size and polydispersity depended on the DNA/AGMA ratio, the molecular weight of the AGMA polymer and also the pH of the medium.

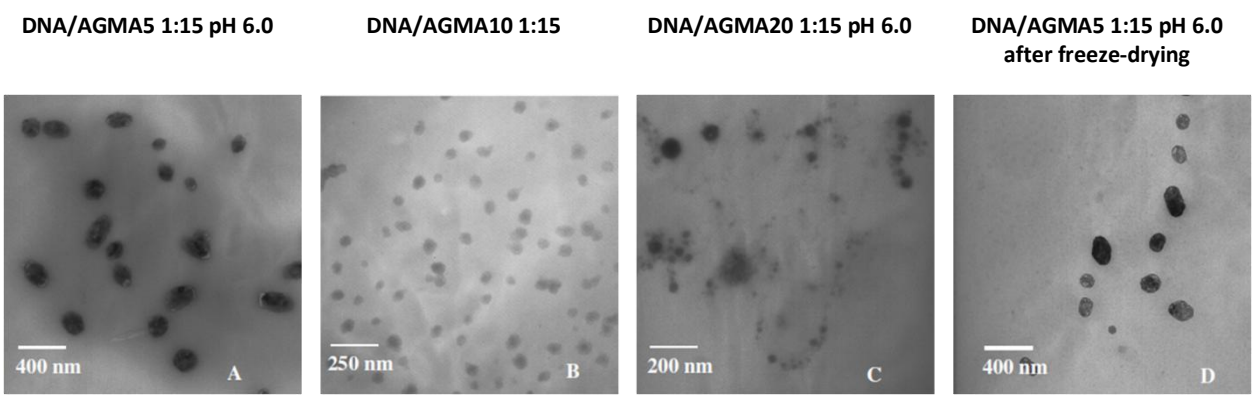

Figure 6.5. TEM microphotograph of DNA/AGMA complexes at different w/w ratio.

The ability to complex DNA was also confirmed by the strong electrophoretic retardation (Figure 6.6), showing the disappearance of the free DNA band for AGMA10 and AGMA20 and a strong reduction but not complete disappearance for AGMA5.

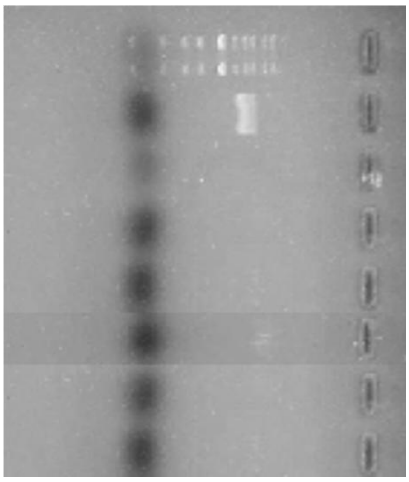

Figure 6.6. Electropheresis assay of DNA/AGMA complexes at different w/w ratio.

AGMA5, AGMA10 and AGMA20 significantly protected DNA from degradation by DNAse I. For instance, the protection afforded by 1:20 DNA/AGMA polyplexes is shown in Figure 6.7. It may be noticed that after 1 hour less than 10% of the DNA in the DNA/AGMA polyplexes was degraded, compared with 100% of free DNA.

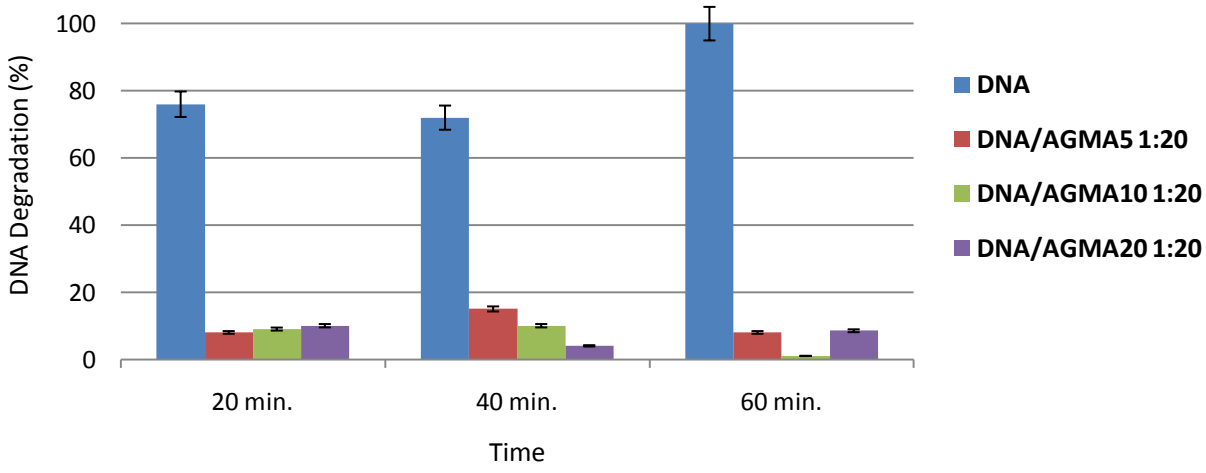

Figure 6.7. Enzymatic degradation of DNA and DNA/AGMA polyplexes with time.

In vitro gene transfection. To establish the relationship between the molecular weight of AGMA5, AGMA10 and AGMA20 and their gene ability to act as DNA carrier, we carried out transfection experiments in Hela cells using a plasmidic DNA carrying GFP protein. The gene delivery efficacy was examined by fluorescence microscopy and analyzing the percentage of fluorescent cells by flow cytometric analysis.

Only a very limited number of fluorescent cells were obtained by transfecting Hela cells with DNA/AGMA5 polyplexes even at a DNA/polymer ratio as of 1:100. By contrast, AGMA10 and AGMA20 showed good transfection ability with little difference between the two, and were already effective at a 1:5 DNA/polymer w/w ratio. In particular, AGMA10 transfected cells showed a higher fluorescent cells number and a well spread cell morphology compared to cell transfected with commercial JetPEI. The poor efficiency of AGMA5 as transfection promoter was related to incomplete DNA encapsulation, leading to large and unstable polyplexes.

Comparing the in vitro data obtained with the three AGMA samples studied in the present work with the data previously reported for AGMA1, we noticed a lack of significant improvement in transfection efficiency passing from AGMA10 to AGMA20, a little improvement passing from AGMA1 to AGMA10, but a dramatic improvement passing from AGMA5 to AGMA10.

Further experiments were carried out only on AGMA10 due to its ease preparation if compared to AGMA20 which involves much longer reaction times and reduced yields.

The transfection efficiency of AGMA10 was quantified using two different w/w DNA/polymer ratios (1:10 and 1:30) and determining the fluorescent cell number 24 or 48 hours after transfection. A good transfection efficiency was already obtained at 24 hours. The percentage of GFP positive cells was of 35% and 71% with DNA/AGMA10 ratios of 1:10 and 1:30, respectively (Figure 6.8).

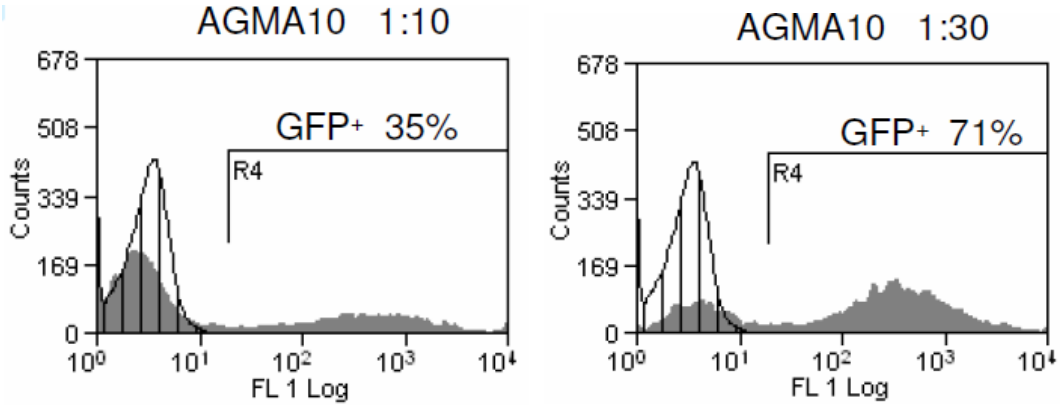

Figure 6.8. Cytofluorimetric analysis of Hela cells transfected with DNA/AGMA10 at 1:10 and 1:30 w/w ratio.

The DNA/AGMA10 polyplexes exhibited over JetPEI the advantage of a much lower cytotoxicity. To confirm this, the viability of the transfected cells was evaluated by measuring the activity of mitochondrial dehydrogenase with MTT substrate. DNA/AGMA10 complexes were non-toxic with 90% of cells viability compared to PEI/DNA complexes (60% of cells viability) (Figure 6.9-A). Cells transfected with PEI appeared rounded and partially floating, suggesting a toxic effect exerted by DNA/PEI complexes (Figure 6.9-B).

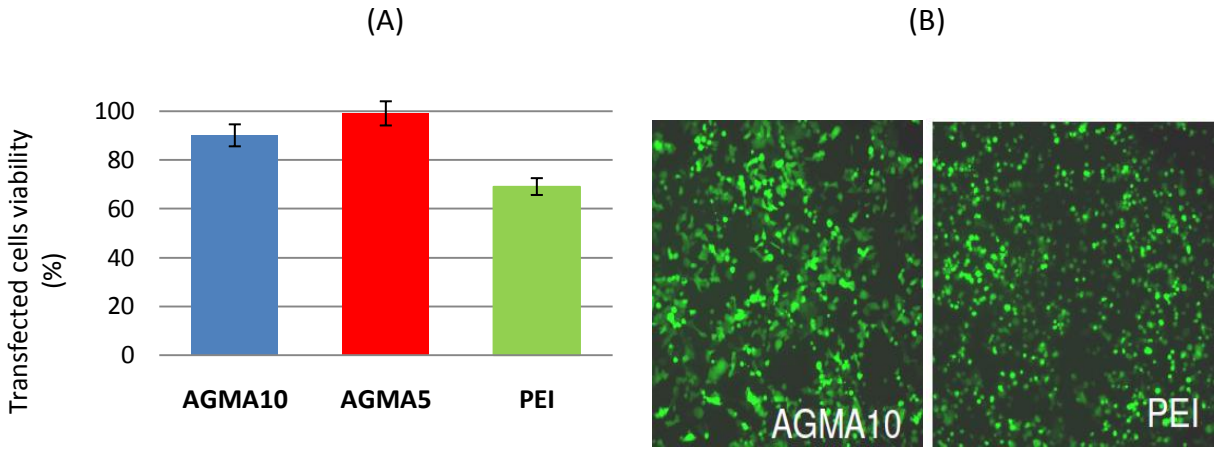

Figure 6.9. Viability of transfected cells evaluated by MTT (A) and fluorescent micrographs of Hela cells transfected with 1:30 w/w DNA/AGMA1 and DNA/PEI polyplexes.

Intracellular trafficking and nuclear localization. A sample of AGMA10 containing a small percentage (7%) of units carrying a primary amine group as side substituent, named AGMA10NH_2, was prepared by substituting a small percentage of mono-protected 1,2-diaminoethane for the same amount of agmatine in the polymerization recipe and subsequently removing the protecting group. AGMA10NH_2 was then labeled with FITC by a standard procedure (FITC-AGMA10)[44].

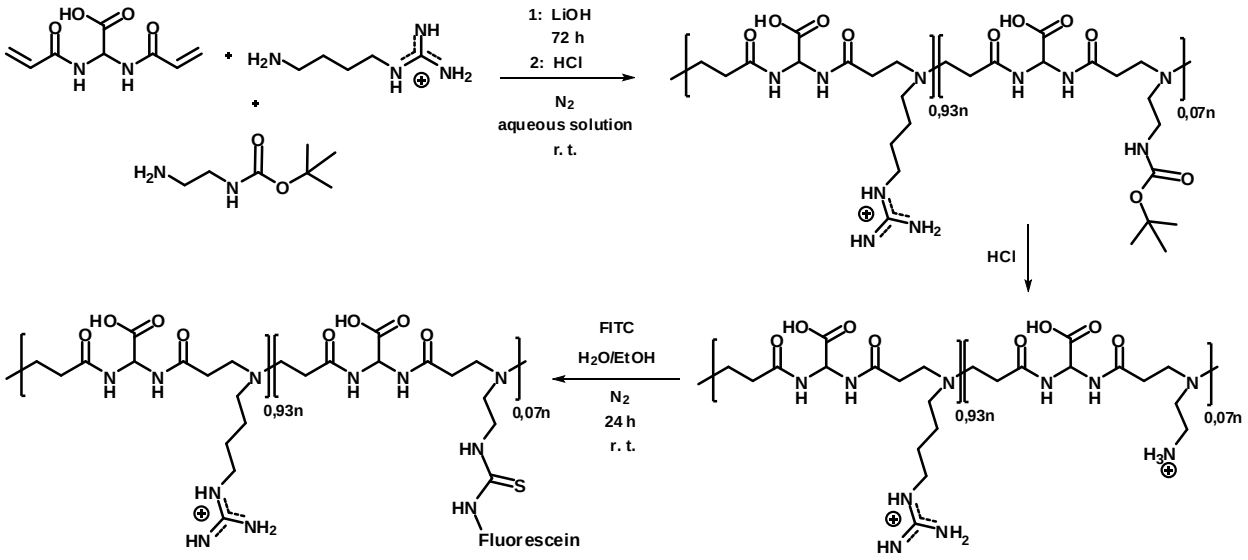

Scheme 6.2. Synthesis of FITC-AGMA10.

The resulting FITC-AGMA10 was used to study the intracelluar trafficking of the linear polymer and its polyplexes. The molecular weight values found for FITC-AGMA10 were very similar to those previously determined for AGMA10, showing that the labeling procedure did not induce any significant alteration of polymer properties.

FITC-AGMA10 was internalized into cells after 30 minutes of treatment and mainly localized in the perinuclear region (Figure 6.10-A). No specific localization of FITC-AGMA10 in endosomal vesicles and on plasma membranes was detectable. Interestingly, FITC-labelled AGMA10/DNA complexes were largely localized inside the nucleus, as clearly visualized by blue staining in Figure 6.10-B.

The different localization of labeled AGMA10 and DNA/AGMA10 is quantified in Figure 6.10-C.

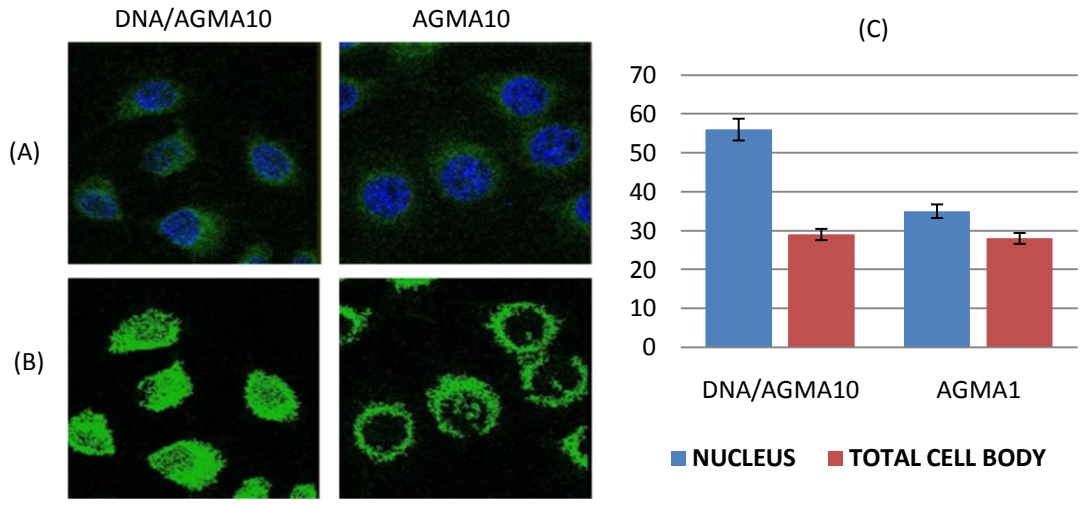

Figure 6.10: Intracellular trafficking and nuclear localization of FITC-AGMA10 and FITC-labeled DNA/AGMA10. (A) Nucleus is stained by DAPI (blue) whereas AGMA10 and DNA/AGMA10 are visualized in green. (B) The confocal images are rendered to enhance the nuclear localization and the main pixel intensity of different cell regions is quantified and reported in graph. (C) Quantification of the different localizations of labeled AGMA10 and DNA/AGMA10.

It seems that AGMA10 acts as an effective transfection promoters capable of transporting in the cytosol a DNA payload without exerting any measurable membranolytic activity in a pH interval including the pH values of both extracellular and intracellular liquid.

In vivo gene transfection. AGMA10 appeared to have all the qualifications required by a carrier for effective gene delivery. To confirm this assumption in vivo studies were also performed. In particular, a dose of 1:30 DNA/AGMA10 polyplexes nanoparticles, corresponding to 10 µg of DNA was injected in the tail vein of mice.

The Western blot results of the in-vivo gene expression in animals sacrificed 24 and 48 hours after treatment are reported in Figure 6.11.

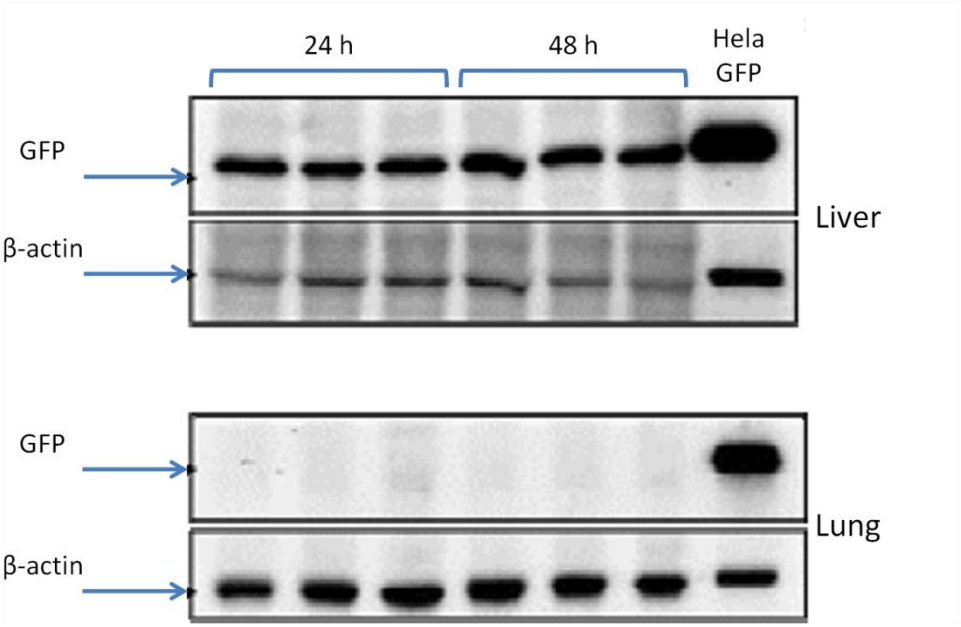

Figure 6.11: Western blot analysis of total lysate from livers and lungs of mice injected with DNA/AGMA10 polyplexes.

GFP was unequivocally expressed in the liver cells, whereas under the same conditions naked DNA was totally ineffective. No transfection evidence was found in all the other tissues examined, including lungs, suggesting that liver is the primary localization site of DNA/AGMA10 polyplexes. The intravenous administration of DNA/AGMA10 polyplexes to mice did not cause any detectable toxic effect and, not unexpectedly, the same was true for free AGMA10. The acute toxicity of free AGMA10 in mice is being determined by Intox Laboratories (Urawade, India) and although this study is not yet complete, the first results indicate that the maximum tolerated dose after intravenous administration is higher than 500 mg/kg that is a considerable low value for an effective DNA carrier.

6.4 CONCLUSIONS

In this work three samples of an amphoteric poly(amidoamine) bearing 4-aminobutylguanidine deriving units with different molecular weights, named AGMA5 ($\overline{M}_w$=5100), AGMA10 ($\overline{M}_w$ =10100) and AGMA20 ($\overline{M}_w$=20500) were investigated as gene carrier. In particular, the aim of this study was to evaluate the effect of the molecular weight of the polymers on their transfection efficacy. All samples condense DNA in spherical, positively charged nanoparticles which dimension depends on the w/w ratio between polymer and DNA and pH. The molecular weight of the polymeric samples had a significant influence on their efficiency as DNA carrier. AGMA10 and AGMA20 showed good transfection ability compared to AGMA5 which was almost ineffective even at a 1:100 w/w DNA/polymer ratio. The polyplex nanoparticles proved highly biocompatible and were easily internalized in cells escaping from the endosomal vesicles and mostly localizing in perinuclear region. DNA/AGMA10 polyplex intravenously administered to mice promoted gene expression in liver, but not in other organs, without detectable toxic side effects. It may be concluded that AGMA10 apparently satisfies the requirements of non-viral gene delivery carrier and holds a definite potential for in vivo application.

References:

1. Mulligan, R.C. *Science* **1993**, *260*, 926-932.
2. Lozier, J.N.; Brinkhous, K.M. *J. Am. Med. Assoc.* **1994**, *271*, 47-51.
3. Inui, K.; Okada, S.; Dickson, G. *Brain Dev.* **1996**, *18*, 357-361.
4. Hartigan-O'Connor, D.; Chamberlain, J.S. *Sem. Neurol.* **1999**, *19* (3), 323-332.
5. Hartigan-O'Connor, D.; Chamberlain, J.S. *Microsc. Res. Tech.* **2000**, *48*, 223-238.
6. Alton, E.W.F.W.; Geddes, D.M.; Gill, D.R.; Higgins, C.F.; Hyde, S.C.; Innes, J.A. *Gene Ther.* **1998**, *5*, 91-98.
7. Nabel, E.G. *J. Nucl. Cardiol.* **1999**, *6* (1), 69-75.
8. Dunnett, S.B.; Bjorklund, A. *Nature* **1999**, *399*, 263-267.
9. Alisky, J.M.; Davidson, B.L. *Hum. Gene Ther.* **2000**, *11* (17), 2315-2329.
10. Barkats, M.; Bilang-bleuel, A.; Buc-caron, M.H.; Castelbarthe, M.N.; Corti, O.; Finiels, F. *Prog. Neuorbiol.* **1998**, *55*, 333-341.
11. Chadwick, D.R.; Lever, A.M.L. *Exp. Opin. Ther. Patents.* **1998**, *8* (8), 983-990.
12. Bonadio, J.; Goldstein, S.A.; Levy, R.J. *Adv. Drug. Delivery Rev.* **1998**, *33*, 53-69.
13. Vile, R.G.; Russell, S.J.; Lemoine, N.R. *Gene Ther.* **2000**, *7*, 2-8.
14. Folkman, J. *Proc. Natl. Acad. Sci. USA* **1998**, *95*, 6367-6372.
15. Roth, J.A; Cristiano, R.J. *J. Natl. Cancer Inst.* **1997**, *89*, 21-39.
16. Shi, F.; Rakhmilevich, A.L.; Heise, C.P.; Oshikawa, K.; Sondel, P.M.; Yang, N.S. *Mol. Cancer Ther.* **2002**, *1* (11), 949-957.
17. Walther, W.; Stein, U.; Voss, C.; Schmidt, T.; Schleef, M.; Schlag, P.M. *Anal. Biochem.* 2003, *318* (2), 230-235.
18. Mansouri, S.; Lavigne, P.; Corsi, K.; Benderdour, M.; Beaumont, E.; Fernandes, J.C. *Eur. J. Pharm. Biopharm.* **2004**, *57*, 1-8.
19. El-Aneed, A. *J. Contr. Rel.* **2004**, *94*, 1-14.
20. Varmus, H. *Science* **1988**, *240*, 1427-1435.
21. Kim, K.H.; Yoon, D.J.; Moon, Y.A.; Kim, Y.S. *Yonsei Med. J.* **1994**, *35* (1), 25-33.
22. Muzyczka, N. *Curr. Top. Microbiol. Immunol.* **1992**, *158*, 67-95.
23. Marshall, E. *Science* **1999**, *286*, 444-447.

24. Marshall, E. *Science* **2000**, *287*, 1419-1421.
25. Marshall, E. *Science* **2002**, *298*, 510-511.
26. Kaiser, J. *Science* **2003**, *299*, 495.
27. Vaheri, A.; Pagano, J.S. *Virology* **1965**, *27* (3), 434-436.
28. Graham, F.L.; Eb, A.J.V.D. *Virology* **1973**, *52*, 456-467.
29. Boussif, O.; Lezoualch, F.; Zanta, M.A.; Mergny, M.D.; Scherman, D.; Demeneix, B.; Behr, J.P. *Proc. Natl. Acad. Sci. U. S. A.* **1995**, *92*, 7297-7301.
30. Zauner, W.; Ogris, M.; Wagner, E. *Adv. Drug Deliv. Rev.* **1998**, *30*, 199-204.
31. Behr, J.P. *Chimia* **1997**, *51*, 34-36.
32. Fischer, D.; Bieder, T.; Li, Y.; Elsasser, H.P.; Kissel, T. *Pharm. Res.* **1999**, *16*, 1273-1279.
33. Denning, j.; Duncan, R. *J. Biothecnol.* **2002**, *90*, 339-347.
34. Tanaka, S. *Cancer Gene Ther.* **2000**, *7*, 27-36.
35. Richardson, S.C.W.; Pattrick, N.G.; Stella Man, Y.K.; Ferruti, P.; Duncan, R. *Biomacromolecules* **2001**, *2* (3), 1023-1028.
36. Hill, I.R.; Garnett, M.C.; Bignotti, F.; Davis, S.S. *Biochim. Biophys. Acta* **1999**, *1427*, 161-174.
37. Jones, N.A.; Hill, I.R.; Stolnik, S.; Bignotti, F.; Davis, S.S.; Garnett, M.C. *Biochim. Biophys. Acta* **2000**, *1517*, 1-8.
38. Hill, I.R.; Garnett, M.C.; Bignotti, F.; Davis, S.S. *Anal. Biochem.* **2001**, *291* (1), 62-68.
39. Rackstraw, B.J.; Stolnik, S.; Bignotti, F.; Garnett, M.C. *Biochim. Biophys. Acta* **2002**, *1576*, 269-286.
40. Min, L; Chen, J.; Cheng, Y.P.; Xue, Y.N.; Zhuo, R.X.; Huang, S.W. *Macromol. Biosci.* **2010**, *10*, 384-392.
41. Christensen, V.; Chang, C.W.; Kim, W.J.; Kim, S.W.; Zhong, Z.; Lin, C.; Engbersen, J.; Feijen, J. *Bioconjugate Chem.* **2006**, *17* (5), 1233-1240.
42. Garnett, M.C.; Ferruti, P.; Ranucci, E.; Suardi, M.; Heyde, M.; Sleat, R. *Biochem. Soc. Trans.* **2009**, *37*, 713-716.
43. Franchini, J.; Ranucci, E.; Ferruti, P.; Rossi, M.; Cavalli, R. *Biomacromolecules* **2006**, *7* (4), 1215-1222.

44. Ferruti, P.; Franchini, J.; Bencini, M.; Ranucci, E.; Zara, G.P.; Serpe, L.; Primo, L.; Cavalli, R. *Biomacromolecules* **2007**, *8* (5), 51-58.

45. Ferruti, P.; Ranucci, E.; Trotta, F.; Gianasi, E.; Evagorou, G.E.; Wasil, M.; Wilson, G.; Duncan, R. *Macromol. Chem. Phys.* **1999**, *200*, 1644-1654.

46. Sze, A.; Erickson, D.; Ren, L.; Li, D.J. *J. Colloid Interface Sci.* **2003**, *261*, 402-410.

47. Pack, D.W.; Hoffman, A.S.; Pun, S.; Stayton, P.S. *Nature Review Drug Discovery* **2005**, *4*, 581-593.

- ✓ **Tricarbonyl-Rhenium Complexes of a Thiol-Functionalized Amphoteric Poly(amidoamine).**

  Daniela Donghi, Daniela Maggioni, Giuseppe D'Alfonso, Federica Amigoni, Elisabetta Ranucci, Paolo Ferruti, Amedea Manfredi, Fabio Fenili, Agnese Bisazza and Roberta Cavalli. Biomacromolecules, 2009, 10 (12).

- ✓ **Direct microfabrication of topographical and chemical cues for the guided growth of neural cell networks on polyamidoamine hydrogels.**

  Gabriel Dos Reis, Fabio Fenili, Antonella Gianfelice, Gero Bongiorno, Davide Marchesi, Pasquale Emanuele Scopelliti, Antonio Borgonovo, Alessandro Podesta`, Marco Indrieri, Elisabetta Ranucci, Paolo Ferruti, Cristina Lenardi, Paolo Milani. Macromol. Biosci., 2010, 10.

- ✓ **Synthesis of polymers containing regularly distributed tetrathia-[7]-elicene units along the backbone.**

  Fabio Fenili, Alberto Bossi, Paolo Ferruti, Amedea Manfredi, Stefano Maiorana, Clara Baldoli, Silvia Cauteruccio, Emanuela Licandro, Elisabetta Ranucci. Journal of Polymer Science, Part A, 2010, 48 (21).

- ✓ **A novel biodegradable polyamidoamine hydrogels as guide for peripheral nerve regeneration.**

  Valerio Magnaghi, Vincenzo Conte, Patrizia Procacci, Giorgio Pivato, Paolo Cortese, Erika Cavalli, Giorgio Pajardi, Elisabetta Ranucci, Fabio Fenili, Amedea Manfredi, Paolo Ferruti. Submitted to Journal of Biomedical Material Research, Part A.

- ✓ **Amphoteric agmatine containing polyamidoamines as carriers for plasmid DNA in vitro and in vivo Delivery.**

  Roberta Cavalli, Agnese Bisazza, Roberto Sessa, Luca Primo, Fabio Fenili, Amedea Manfredi, Elisabetta Ranucci, Paolo Ferruti. Biomacromolecules, 2010, 11 (10).

- ✓ **7th International Symposium on Polymer Therapeutics: From Laboratori to Clinic Practice.** Valencia, may 24-28th 2008.

  Poster: BIOREDUCIBLE POLY(AMIDOAMINE) HYDROGELS WITH TUNABLE DEGRADATION PROPERTIES.

- ✓ **15th CIRMIB Biomaterials School NoE Expertissues School. Strategies and Materials for Regenerative Medicine: Focus on Bone and Cartilage.** Ischia, July 7-11th 2008

  Poster: NOVEL POLY(AMIDOAMINE)-BASED HYDROGELS AS SCAFFOLD FOR TISSUE ENGINEERING.

- ✓ **II° Forum Nazionale dei Giovani Ricercatori su Materiali Polimerici e Biomateriali.** Genova, July 4-5th 2008

  Poster: NOVEL POLY(AMIDOAMINE)-BASED HYDROGELS AS SCAFFOLD FOR TISSUE ENGINEERING.

- ✓ **II° Congresso Nazionale di Chimica e Tecnologia delle Ciclodestrine.** Asti, 3-5 May 2009.

  Oral presentation: β-CYCLODEXTRIN-POLY(4-ACRYLOYLMORPHOLINE) AND POLY(AMIDOAMINE) CONJUGATES AS ANTICANCER AND ANTIVIRAL DRUG CARRIERS.

- ✓ **VII° Convegno Nazionale INSTM sulla Scienza e Tecnologia dei Materiali.** Tirrenia, 9-12 june 2009.

  Poster: MICROFABRICATION OF BIOMIMETIC POLY(AMIDOAMINE) BASED HYDROGELS FOR BIOMEDICAL APPLICATIONS.

- ✓ **Nanomedicine 2009, 2nd European Summer School in Nanomedicine.** Lisbon, 12-16 june 2009.

  Poster: NEW NANOPARTICLES BASED ON CHOLESTEROL-POLY(AMIDOAMINE) AND β-CYCLODEXTRIN-POLY(ACRYLOYLMORPHOLINE) CONJUGATES AS DRUG CARRIERS.

- ✓ **2nd International Congress on Biohydrogels.** Viareggio, 10-15 november 2009.

  Oral presentation: NOVEL POLY(AMIDOAMINE)-BASED HYDROGELS AS SUBSTRATES FOR TISSUE ENGINEERING.

- ✓ **Workshop of the 24M Nanother project.** Bordeaux, 4-5 October 2010.

  Oral presentation: POLYAMIDOAMINES BASED NPs: SYNTHETIC APPROACH.